HYDRAULIC SOLENOID VALVE RELIABILITY AND MODELING STUDY

Except where reference is made to the work of others, the work described in this thesis is my own or was done in collaboration with my advisory committee. This thesis does not include propriety or classified information.

_____

Santosh Vishwanath Angadi

Certificate of Approval:

_____	_____
Jeffrey C. Suhling Quina Distinguished Professor Mechanical Engineering	Robert L. Jackson, Chair Assistant Professor Mechanical Engineering
_____	_____
Song-yul Choe Associate Professor Mechanical Engineering	George T. Flowers Dean Graduate School

HYDRAULIC SOLENOID VALVE RELIABILITY AND MODELING STUDY

Santosh Vishwanath Angadi

A Thesis

Submitted to

the Graduate Faculty of

Auburn University

in Partial Fulfillment of the

Requirements for the

Degree of

Master of Science

Auburn, Alabama
December 19, 2008

HYDRAULIC SOLENOID VALVE RELIABILITY AND MODELING STUDY

Santosh Vishwanath Angadi

Permission is granted to Auburn University to make copies of this thesis at its discretion, upon request of individuals or institutions and at their expense. The author reserves all publication rights.

_____
Signature of Author

_____
Date of Graduation

VITA

Santosh V. Angadi, son of Mr. Vishwanath V. Angadi and Mrs. Nirmala V. Angadi, was born on July 26, 1982, in Gadag, Karnataka, India. He graduated with Bachelor of Technology degree in Metallurgical Engineering from National Institute of Technology, Karnataka, Surathkal, in 2004. In order to enhance his academic qualifications, he joined the Masters program in the department of Mechanical Engineering at Auburn University in Fall 2006.

THESIS ABSTRACT

HYDRAULIC SOLENOID VALVE RELIABILITY AND MODELING STUDY

Santosh Vishwanath Angadi

Master of Science, December 19, 2008
(B.Tech., National Institute of Technology, Karnataka, Surathkal, India, 2004)

111 Typed Pages

Directed by Robert L. Jackson

The current work has studied the reliability of a solenoid valve (SV) used in automobile transmissions through a joint theoretical and experimental approach. Based on an extensive literature search, the most common failures seen in solenoid valves appear to be due to either overpowering and eventual overheating of the valves, or wearing out of the valve components. The goal of this work is to use accelerated tests to characterize SV failure and correlate the results to new comprehensive finite element models.

A custom test apparatus has been designed and built to simultaneously monitor and actuate up to four SVs using the LabView™ programming language environment and a National Instruments™ Data Acquisition device. The test apparatus is capable of applying a controlled duty cycle, applied voltage and actuation frequency. The SVs are also placed in a thermal chamber so that the ambient temperature can be controlled

precisely. The apparatus measures in real-time the temperature, current, and voltage of each SV. A multimeter is used to measure the electrical resistance across each SV. A series of tests have been conducted to produce repeated failures of the SVs. The failure of the SV appears to be caused by overheating and failure of the insulation used in the solenoid coil. The current tests are run at a 100ºC ambient temperature, 16.8V of average peak voltage, 50% duty cycle, and 60 Hz actuation frequency. Upon failure, the solenoid electrical resistance drops to a significantly lower value due to shorting of the solenoid coil. This drop in resistance causes a measurable and noticeable increase in the average current. The insulation also melts and exits the SV. Hence, increasing ambient temperature and current is believed to cause a decrease in SV reliability.

In addition, a comprehensive multiphysics theoretical model of the SV is constructed using the commercial finite element software ANSYS™. The multiphysics model includes the coupled effects of electromagnetic, thermodynamics and solid mechanics. The resulting finite element model of the SV provides useful information on the temperature distribution, mechanical and thermal deformations, and stresses. The model is also correlated to the experimental results and can be used as a predictive tool in future solenoid design. Finally, a proposed solution to improve SV reliability is to increase heat conduction and convection away from the SV, or by decreasing the ambient temperature or find an insulation material resistant to high temperatures.

ACKNOWLEDGEMENTS

I wish to acknowledge my sincere gratitude to my advisor, Dr. Robert L. Jackson, for his great motivation, support and encouragement during the course of this study. I would like to thank my committee members, Dr. Song yul-Choe and Dr. Jeffrey C. Suhling, for their continuous support in this study. I deeply acknowledge and extend gratitude for financial support from the NSF Center for Advanced Vehicle Electronics (CAVE).

I would like to express deep gratitude and gratefulness to my parents and sister for their enduring love, immense moral support and encouragement in my life. I wish to thank all my colleagues and friends at Auburn for their friendship and help.

Style manual or journal used: Guide to Preparation and Submission of Theses and Dissertations

Computer software used: Microsoft Office 2003, Ansys 11.0, Matlab 7.0.4

TABLE OF CONTENTS

LIST OF FIGURES x

LIST OF TABLES xiv

1. INTRODUCTION 1
   1.1 Detailed list of applications of solenoid valves 3

2. MOTIVATION AND OBJECTIVES 5

3. LITERATURE REVIEW 7
   3.1 Common failures of solenoid valves 11

4. EXPERIMENTAL METHODOLOGY 13
   4.1 Preliminary Tests 22

5. MODELING METHODOLOGY 27

6. RESULTS AND DISCUSSION 38
   6.1 Modeling Results 38
      6.1.1 Local Wire Model 48
      6.1.2 Theoretical Design of Reliability Test 51
   6.2 Experimental Results 57
      6.2.1 Direct Solenoid Coil Temperature Measurement 63
      6.2.2 Categorization of Results 65
      6.2.3 Analysis of Results 66
      6.2.4 Visual Analysis of Failure Mechanism 76

7. CONCLUSIONS 90

8. RECOMMENDATIONS FOR FUTURE WORK 92

BIBLIOGRAPHY 94

APPENDIX 97

LIST OF FIGURES

Figure 1.1: Schematic of a typical cross-section of a solenoid valve [1] 3

Figure 4.1: Schematic diagram of solenoid valve experimental test rig.....14

Figure 4.2: Delta Design 9039 thermal chamber used to control the ambient temperature around the solenoid valves.....16

Figure 4.3: Photograph of the solenoid test fixture that is inserted into the thermal chamber.....17

Figure 4.4: Photograph of an SC5 solenoid controller board 18

Figure 4.5: Photograph showing solenoid valve test fixture and thermocouple.....19

Figure 4.6: A schematic of the solenoid valve test fixture and thermocouple mount 19

Figure 4.7: Measured actuation voltage applied to the solenoid valve (peak voltage: 11.4 V, duty cycle: 50%, actuation frequency: 60 Hz).....23

Figure 4.8: Measured actuation current applied to the solenoid valve (peak voltage: 11.4 V, duty cycle: 50%, actuation frequency: 60 Hz).....25

Figure 4.9: The measured average, RMS and peak current measured as a function of the applied voltage.....26

Figure 5.1: A plot of the finite element mesh used to model the solenoid valve.....28

Figure 5.2: Schematic of solenoid valve and portion considered in model.....31

Figure 5.3: Schematics of the solenoid valve core used for modeling (supplied by KTL, dimensions in mm).....32

Figure 5.4: Schematics of the solenoid valve plunger used for modeling (supplied by KTL, dimensions in mm).....32

Figure 5.5: Schematic of the FEM model of the Solenoid Valve, including Boundary Conditions 34

Figure 5.6: Finite element prediction of the temperature for various convection coefficients 37

Figure 6.1: The predicted temperature distribution in the solenoid cross section for 0.86 Amps of current 39

Figure 6.2: The predicted von Mises stress distribution in the solenoid cross section for 0.86 Amps of current 40

Figure 6.3: The finite element prediction of the Joule heating within the solenoid coil ... 42

Figure 6.4: Distribution of the Joule heat generation for 1 Amps of RMS current applied evenly over the cross-section of the solenoid coil 43

Figure 6.5: The finite element model predictions of the deflections in the *x* direction within the solenoid valve resulting from thermal expansion (for 1 Amps) 44

Figure 6.6: The finite element model predictions of the deflections in the *y* direction within the solenoid valve resulting from thermal expansion (for 1 Amps) 45

Figure 6.7: Comparison of the theoretically predicted and experimentally measured solenoid temperature 46

Figure 6.8: The maximum stresses predicted by the finite element model 47

Figure 6.9: Schematic of the hexagonally symmetric local solenoid wire model 48

Figure 6.10: The finite element mesh of the local solenoid wire cross-section 49

Figure 6.11: Finite element predicted local solenoid coil wire temperature distribution .. 50

Figure 6.12: The finite element model predictions of the local deflections within the solenoid coil resulting from thermal expansion (for 1 Amps) 51

Figure 6.13: The FEM predicted temperature in the coil and on the external surface of the solenoid valve 52

Figure 6.14: The maximum stresses predicted by the finite element model 53

Figure 6.15: The predicted temperature distribution in the solenoid cross section for 1 Amps of current and 80°C ambient temperature 55

Figure 6.16: The predicted von Mises stress distribution in the solenoid cross section for 1 Amps of current and 80°C ambient temperature 56

Figure 6.17: Variation of actuation voltage with time for a solenoid valve in operation ..57

Figure 6.18: Variation of actuation current with time for a solenoid valve in operation ..58

Figure 6.19: Variation of applied current and running average for current as a function of time for 2 completely failed solenoid valves 60

Figure 6.20: Variation of applied current and running average for current as a function of time and also showing one completely failed solenoid and one solenoid that did not fail.... 61

Figure 6.21: Variation of temperature with time for 2 completely failed solenoid valves.... 62

Figure 6.22: Variation of temperature with time for one completely failed solenoid and one solenoid that did not fail.....63

Figure 6.23: Variation of resistance with temperature.....65

Figure 6.24: The calculated experimental cumulative density function for failure of the solenoid valves.....66

Figure 6.25: Variation of change in resistance in relation to the maximum temperature for the tested solenoid valves.....70

Figure 6.26: Variation of change in resistance Vs number of cycles for the tested SVs...71

Figure 6.27: Variation of peak current as a function of maximum temperature for the tested SVs.....73

Figure 6.28: Variation of number of cycles as a function of the maximum temperature for the tested solenoid valves.....75

Figure 6.29: A macroscale photograph of a SV belonging to (a) case (the solenoid valve was run for 24 hours without failure) 77

Figure 6.30: A macroscale photograph of a solenoid valve belonging to (b) case (partially failed but still run for 24 hours) 78

Figure 6.31: Macroscale photograph of a solenoid valve belonging to the (c) case (completely failed) 79

Figure 6.32: Macroscale photograph of a solenoid valve belonging to the (c) case (completely failed).....80

Figure 6.33: Cross section of a (a) type tested solenoid valve.....81

Figure 6.34: Cross section of a (b) type tested solenoid valve 82

Figure 6.35: Cross section of a (c) type solenoid valve.....83

Figure 6.36: Microscale photographs of the case (a) solenoid valve cross-section.....86

Figure 6.37: Microscale photographs of the type (b) solenoid valve cross-section.....87

Figure 6.38: Microscale photographs of the type (c) solenoid valve cross-sections (part 1).....88

Figure 6.39: Microscale photographs of the type (c) solenoid valve cross-sections (part 2).....89

LIST OF TABLES

Table 4.1: Tested solenoid valve rated operating parameters.....14

Table 5.1: Material Properties used in FEM model.....33

Table 5.2: Material Properties for Air.....36

Table 6.1: Solenoid valve recorded and calculated/measured data for 100°C ambient temperature, 50% duty cycle, 60 Hz actuation frequency, 16.8 V actuation voltage.....68

CHAPTER 1
INTRODUCTION

A solenoid valve (SV) is an electromechanical device used to control the flow of gas or liquid by passing an electric current through a coiled wire, thereby altering the valve position (see Fig. 1.1). SVs are used in various applications ranging from automobiles (as in transmission control, hydraulic power brake system, anti-lock brakes, traction control, etc.), aerospace and nuclear power plants to irrigation and water treatment, boom control in an agricultural vehicle. They also are widely used for domestic purposes, namely, washing machines, gardening, commercial dishwashers, etc. Due to the extensive use of the solenoid valve it is very important to fully understand its behavior and the mechanisms which govern its reliability. Unfortunately, the available literature on solenoid valve reliability is relatively scarce (see Literature Review in Chapter 3).

The chief components of solenoid valves (especially, the ones used in automobiles) are the plunger, coil, spring, needle, and the seals. The valve part of the assembly is actuated by a plunger that is forced to move from an electromagnetic coil. The electromagnetic coil must provide a large enough force to overcome a spring which opens or closes the solenoid valve when the coil is not powered. The general cross section of a solenoid (not a complete solenoid valve) with the various parts is shown in Fig.1.1. For solenoid valves, the solenoid is then used to regulate flow of fluid by opening and closing a channel.

A solenoid in a solenoid valve is an actuator and consists of a coil. When an electric current flows through the coil, a magnetic field is produced. Lorentz force is created perpendicularly to both the directions of magnetic field and current. Lorentz's force law (Eq. 1.1) relates this magnetic force (F) to the vector cross product of the current flowing through the conductor (I) and the magnetic field (B):

$$\vec{F} = \vec{I} \times \vec{B} \tag{1.1}$$

The primary operating parameters influencing solenoid valve performance are

1) Operating temperature
2) Operating voltage
3) Maximum current
4) Coil resistance
5) Cycling frequency
6) Duty cycle (DC)
7) Valve construction materials

The current work will focus primarily on the effect that items 1, 2 and 3 have on solenoid performance.

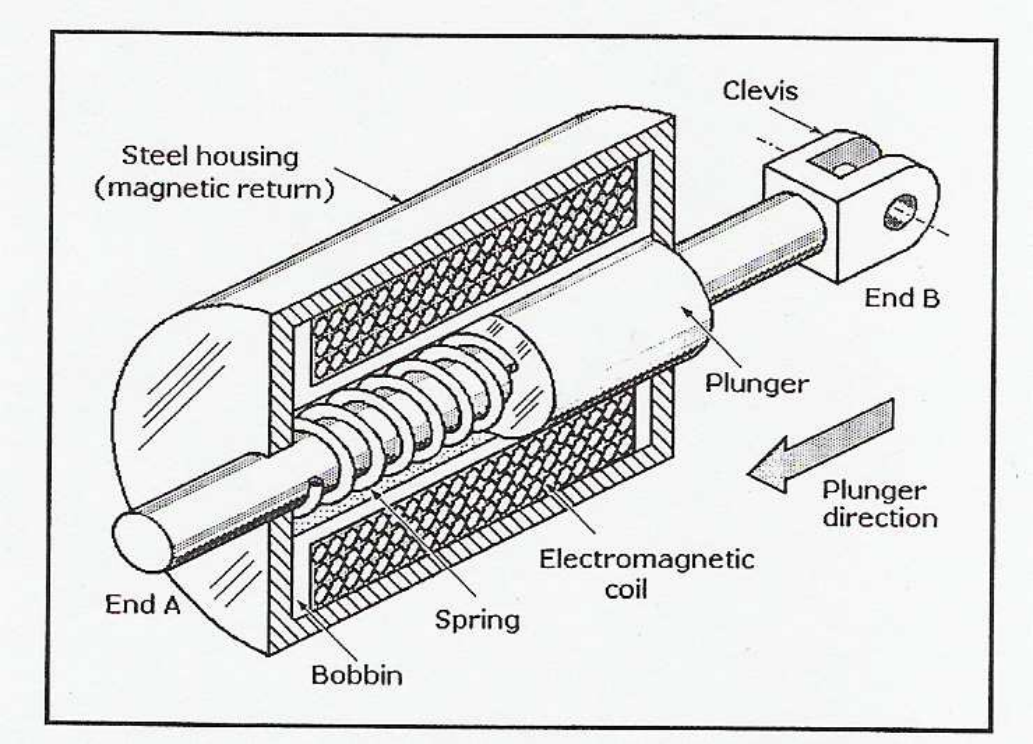

Figure 1.1: Schematic of a typical cross-section of a solenoid valve [1]

In the present work, solenoid valves used in control of automobiles transmission are being investigated to characterize their performance and reliability through both experimental and theoretical modeling approaches. The following section will outline the motivation and objectives for the problem. Later sections will discuss the experimental and theoretical methodology. Finally, the results will be discussed and conclusions (and recommendations) will be made based on these results.

1.1 Detailed list of applications of solenoid valves

In nuclear engineering applications, the valves are often situated in extreme conditions [4]. Two way solenoid valves are sometimes used for the 'post accident

containment atmosphere sampling' and so due to this application there can be heat traced lines into the solenoid valve that are held to nearly 172°C. Solenoid valves are also used in 'reactor head vent service' which is a yet another application with an extreme duty cycle.

In the automotive field, the solenoid valves are used as actuators and to control fluid pressure. The types of solenoid valves that are used are 'idle speed control valves, shift control valves of automatic transmissions and torque converter looked-up control valves' [5]. A high speed oil hydraulic on-off three way solenoid valve is used tremendously in applications involving hydraulic pressure as well as position control. Hydraulic circuits are controlled by solenoid valves through drain opening and closing for high pressure hydraulic fluid. A few examples of automotive applications include the automatic power transmission, the automobile brake system, the boom control in an agricultural vehicle, and the hydraulic pump swash plate position control [6]. Solenoid valves are found in the hydraulic compact unit (HCU) of hydraulic power brake (HPB) systems and anti-lock brakes (ABS) [7-11]. An automatic transmission is often controlled by the transmission control module (TCM) which employs solenoid valves to control the transmission fluid flow to clutches [12-17].

Solenoid valves are also used in a wide variety of other commercial, domestic and military applications which require controlled motion. Some of these additional applications are: Commercial laundry equipment and facilities, commercial dishwashers, car and truck wash facilities, irrigation systems, humidification, water treatment, poultry incubators/watering equipment, and industrial maintenance, repair, and operation [1].

CHAPTER 2
MOTIVATION AND OBJECTIVES

Motivation:

Two primary motivating factors for the present investigation on SVs are

1) Although it is well known that SVs are used in many applications, as mentioned in the previous section, the published literature on reliability, life and failure data and information on theoretical models and experimental testing of SVs is limited.
2) SV operation can generate large amounts of heat as a result of high duty cycles and electrical resistance (that is, high applied currents) thereby causing it to fail due to thermal effects and the accompanying wear of its parts.

Objectives:

Based on these above two factors, the chief objectives of the current investigation are defined as to

1) Provide a comprehensive technical literature review on SV performance and reliability.
2) Design and fabricate an experimental setup based on the actual operating conditions of a SV.
3) Develop an electromagnetic, thermo-mechanical SV numerical model that would be able to simulate the structural and thermal deformations (due to thermal

expansion) and understand the effects of electrical resistance on reliability, failure and performance of a SV.

4) Characterize and improve the overall performance (involving electromagnetic, mechanical and thermal fields) of a SV.

CHAPTER 3
LITERATURE REVIEW

The following are the results of an extensive literature search on solenoid valve performance, especially with respect to reliability and failure. Based on this search, it appears that the published literature on solenoid valves' modeling and experiments is surprisingly scarce. However, the existing literature does provide guidance as to common problems seen in SVs and the environmental and operating parameters which influence them. This information can then be used to design an experiment which can be used to map the failure and reliability of the SV researched in the current study.

Probably the most extensive work on solenoid valve reliability is provided by Mercer [2]. According to Mercer [2], manufacturing plant reliability is a critical issue. A plant can bear a sufficiently high amount of capital and throughput. Therefore, when the plant is shutdown due to failure of components, a large amount of time and money can be lost. Solenoid valves are often an integral part of these plants and therefore reliability of a solenoid valve always needs to be higher than that of the total (complete) plant. The proper functioning of SVs is important, because a SV failure can lead to complete shut down of an automatic plant and generation of substantial amounts of unusable products prior to detection of the failure. Due to large variations of solenoid valve designs, lack of clear user reliability requirements, and generally expected low production cost, the evaluation of SV reliability has not been given sufficient attention. The 'life test data' for the SVs run under standard rated conditions have been gathered but not for conditions

outside these ratings. Therefore, the reliability cannot be easily predicted for SVs which are exposed to harsh or sudden changes in operating conditions and parameters.

Several critical factors that affect the reliability or failure of a ‘two-way, direct acting, normally closed, packless solenoid valve’ [2] are structural collapse related to material strength, fluid flow rate, component misalignment, etc, broken spring related to fatigue strength, stroke, component misalignment, etc, coil burnout related to mains voltage and frequency, stroke, spring force, frequency of operation, fluid temperature, aging of insulation, etc [2]. Failure of solenoid valves can also occur gradually due to wear, leakage, noise, loss of speed as well as pressure rating.

Solenoid valves are known to exist commercially now for about 70 years and only with a higher expenditure and investment in characterizing solenoid performance can enhanced reliability be achieved. One of the major problems associated with the reliability of SVs is over-design whose effect can be just as strong as under-design of a solenoid valve. The function of a core spring in a solenoid valve is to shut the SV with respect to the pressure of the fluid. However, when a solenoid is over-designed, a highly powerful solenoid is required to overpower a spring that is designed to be too stiff. This requires the use of a larger coil which will generate larger amounts of heat via Joule heating, thereby decreasing the insulation’s expected working life [2].

The ‘residual magnetism level’ has to be at a minimum in parts such as the core and the plug-nut upon their incorporation into the SV to avoid ‘intermittent failures’. Yet another major contribution for reduced reliability of SVs comes from presence of stress concentration points, the appearance of which is generally attributed to the residual stresses generated during operations such as ‘machining or pressing’. Thus, in order to

produce SVs with enhanced reliability consistently, the manufacturer must show considerable care to detect the above mentioned types and causes of failures of SVs and other similar failures [2]. This often only is found in manufacturers with considerable experience, since the transfer of design and reliability information in industry is very limited.

Coming to the SV life expectancy issue, the regulated air (or fluid) is often obtained from an ordinary compressor in SV applications. A mist of oil vapor in a very minimal quantity is often mixed into the air to serve the purpose of lubrication for solenoid valves' interior parts. Unlike this, if air is obtained from an oil free compressor then this leads to wearing out of the SV very quickly. It is been stated that the SV life expectancy is enhanced ten-fold if it is used on air that has oil vapor in small amounts than on dry air that is free of oil [2]. Of course this is not that important to the current application since lubrication should be adequately applied from the regulated transmission fluid.

Baker [3] also provides some practical advice on installing and using solenoids effectively. He points out that a very common problem is solenoid burnout and it is usually the result of a valve being used for conditions it was not designed for. Providing too little or too much voltage to a solenoid valve can both result in overheating of the solenoid valve. In addition, heat can be generated due to higher cycling rates and duty cycles. Sometimes a blocked or stuck armature can overheat since power is continuously applied in attempt to free it.

Slightly more recently, Rustagi and Heilman [4] also gave suggestions on how to achieve longer and more reliable solenoid valve operation, especially for application in nuclear energy facilities. In this critical application, reliability becomes much more

important. In addition, it can be very difficult to replace or repair solenoid valves due to their location in contaminated areas. Similar to the other works, Rustagi and Heliman state that overheating of the coil can be a cause of failure. Therefore, in long-term continuous cycles the voltage is often reduced to prevent excess heat generation. In addition, seal failure and rupture were also seen as a potential problem.

Most theoretical models of solenoid valves are designed to consider their dynamic characteristics so that a control scheme can be designed and optimized [6, 18-25]. Most of these previous works do not consider the coupled thermo-mechanical behavior of the solenoid valve. However, there are a few past works that have modeled the pseudo-static performance of the solenoid valve using finite elements and other computational methods [26, 27]. The current work will develop a new multiphysics model of the solenoid valve which will consider the true coupled nature of the mechanisms that govern solenoid performance and reliability.

The current work focuses mostly on the thermo-mechanical failure mechanisms of the solenoid valve. It should also be noticed that in many cases these various failure mechanisms do not occur independently. Several mechanisms may be initiated or progressed due to the occurrence of another mechanism. For instance, the Joule heating could cause the solenoid temperature to rise significantly. The seals in the solenoid could then degrade due to the elevated temperatures, then causing the solenoid to leak and perhaps fail.

3.1 Common failures of solenoid valves

As previously discussed, solenoid valves may fail for a number of different reasons such as manufacturing defects, improper design, and improper selection for application. The specific mode of failure depends greatly on the original cause and the operating conditions. The following is a collected list of the various failures seen in solenoid valves:

1. 'Sticking' problem as a result of residual magnetism [2].
2. Structural collapse, coil burnout and broken spring [2, 3].
3. Solenoid's coil efficiency and thus the flux density and torque output are lowered owing to heat buildup due to application of constant voltage to the solenoid [1].
4. The valve fails to open when solenoid is energized due to low voltage at solenoid [3], solenoid failure, worn rings, and pressure drop [1].
5. The valve fails to close when solenoid is de-energized due to bending of piston ring, foreign matter lodged on body seat and preventing plunger from seating, plunger tip is severely worn [1].
6. High duty cycle will cause the solenoid to use more power which will lead to temperature rise [1, 3].
7. Due to the SV being run for longer periods at high temperature, there is thermal expansion and accompanying thermal deformations [3].
8. Wear and friction of SV components cause degradation of performance and finally failure [18]. Friction can also cause more power to be used (high temperature) [1]
9. Elevated temperatures and wear can also cause the seals to leak [1].
10. Effect of varying (that is, increasing) duty cycle and frequency on SV operation.

11. If the SV is operated at a higher than rated current, the Joule heating can cause the operating temperature to increase, which then can cause other problems in the SV.
12. Thermal cycling effects can age the materials of the SV [2].

CHAPTER 4
EXPERIMENTAL METHODOLOGY

In order to monitor and evaluate solenoid valve failure, a solenoid valve experimental test rig or apparatus was designed and fabricated. The apparatus is capable of testing four SVs simultaneously. The solenoid valves are also placed in a thermal chamber to control the ambient temperature. The solenoids are powered and actuated in a controlled manner while the current, voltage and temperature are being measured. Both before and after the test on each solenoid valve, the electrical resistance is measured directly by making use of a multimeter across the solenoid valve at room temperature. The goal of the apparatus is to be able to apply sufficient loadings on the SV to cause failure similar to that seen in application. When the SVs do fail, a significant change in the measured temperature and electrical resistance is expected. An accelerated testing procedure will be used to create tests which cause SV failure in a reasonable amount of time. The chosen tests are also based on the results of the multi-physics finite element model of the solenoid valve that is discussed in Chapters 5 and 6.

Parameter	Value
Operating Current	1.8 A
(Cycling) Frequency	61.2 Hz
Coil Resistance	3.4 ohm
Operating Voltage	12 V
Operating Temperature	-30 to 130 deg C

Table 4.1: Tested solenoid valve rated operating parameters

The tested solenoid valve is a three way valve and of normally open type. The operating conditions are given in Table 4.1. To accelerate the tests and reduce the time to failure, these operating conditions may be slightly exceeded to induce solenoid failure. In application, the solenoid valve may also fail due to the designed operating parameters being exceeded.

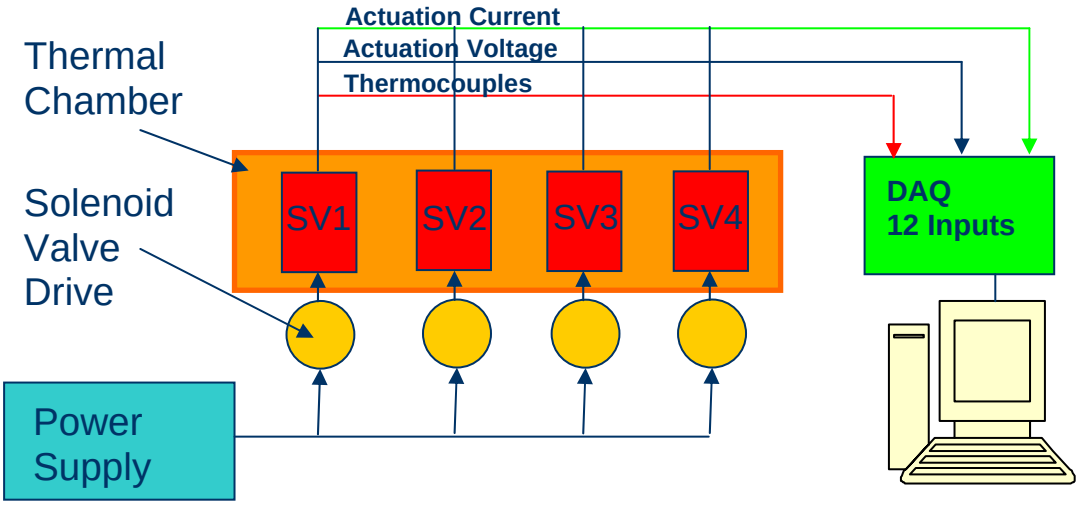

Figure 4.1: Schematic diagram of solenoid valve experimental test rig

A schematic diagram of the experimental test rig fabricated for the current work is shown in Fig. 4.1. It depicts the basic wiring connections among the various instruments used for testing of the solenoid valves and to record the resulting test data. The instruments used are two power supply systems, an SC5 solenoid controller board (manufactured by RW Automation), current transformers (CTs), E type thermocouples, a National Instrument SC2345 signal conditioning block with modules and a National Instruments data acquisition (DAQ) board. A detailed list of these items is provided in Appendix. Three types of modules, namely, an analog voltage input module (0-42V range, 10kHz data acquisition rate), an analog voltage input module (0-5V range, 10kHz data acquisition rate) and a thermocouple input module are used in the SC2345 signal conditioning block to condition the raw signals. The LabView™ (LV) graphical programming software is used extensively to gather voltage, current, and temperature data of the solenoid valves that are being tested.

The solenoid valves are placed in Delta Design 9039 thermal chamber (see Fig. 4.2). After preliminary testing, it was found that the thermal chamber was actually too effective at controlling the temperature of the solenoid valve. When the solenoid valves were inside the chamber, the measured increases in temperature from the ambient temperature were actually less than when the solenoid valves were outside the chamber. This is because the thermal chamber has a fan which circulates the air so that the temperature is uniform throughout the chamber. This unfortunately also causes forced convection which tends to hold the solenoid valve at the same temperature as the chamber. In contrast, when the solenoid valve is outside the chamber, the air is mostly still and the much less effective mechanism of free convection is dominant. In addition,

free convection was used in the modeling section to consider the heat dissipation from the solenoid valve (see Chapter 5). To reduce the effect of the forced convection, metal boxes were placed over the valves in the chamber (see Fig. 4.3). This practice was very successful at increasing the rise in temperature in the solenoid valves due to Joule heating. This in turn allowed for more control over failure of the solenoid valve.

Figure 4.2: Delta Design 9039 thermal chamber used to control the ambient temperature around the solenoid valves

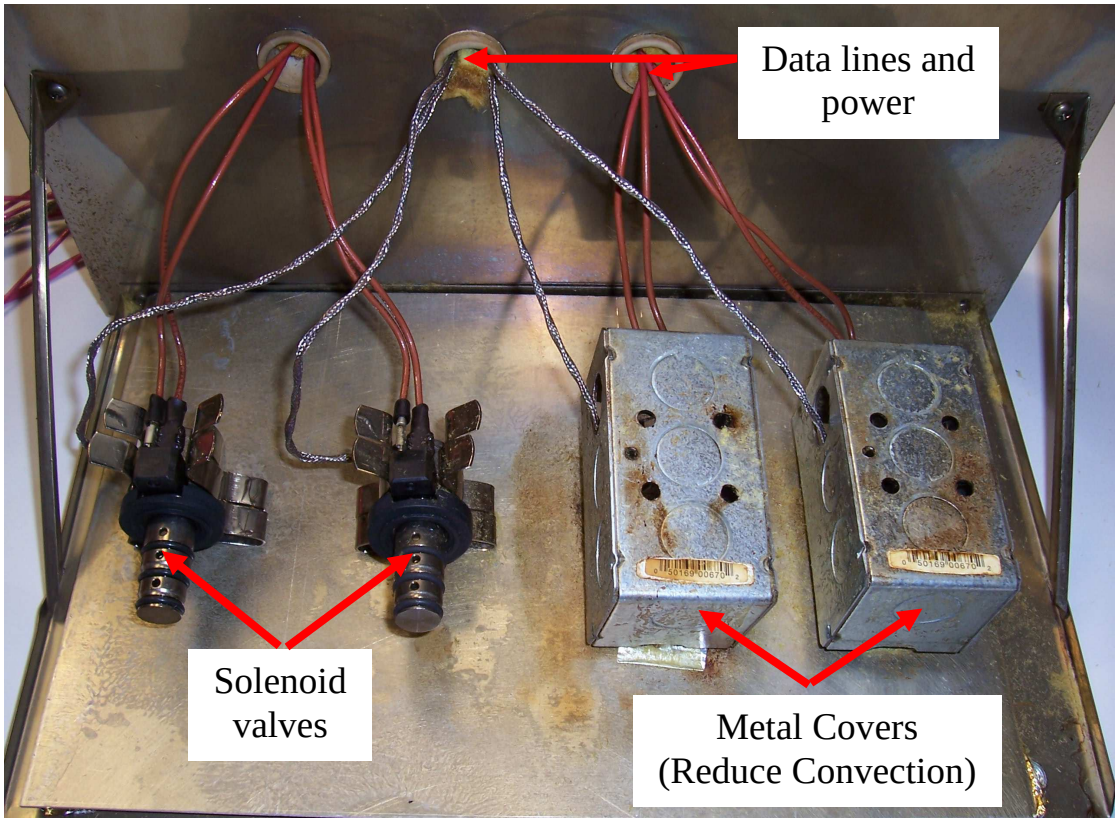

Figure 4.3: Photograph of the solenoid test fixture that is inserted into the thermal chamber

An SC5 solenoid controller board is used to control the solenoids simultaneously at a specified peak current, sustained current, voltage, actuation rate and duty cycle (see Fig. 4.4). A duty cycle is defined as the ratio of 'on' time (that is, the time for which the solenoid valve is under actuation) to the total period of actuation. The higher this ratio, the more load the solenoid valve is under. By increasing the duty cycle, the solenoid valve can be stressed and caused to fail.

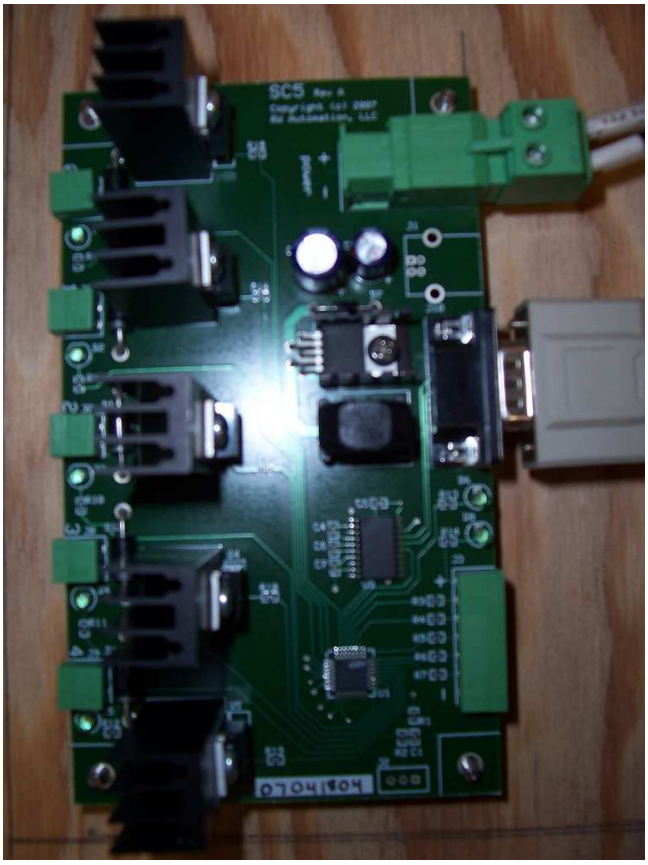

Figure 4.4: Photograph of an SC5 solenoid controller board

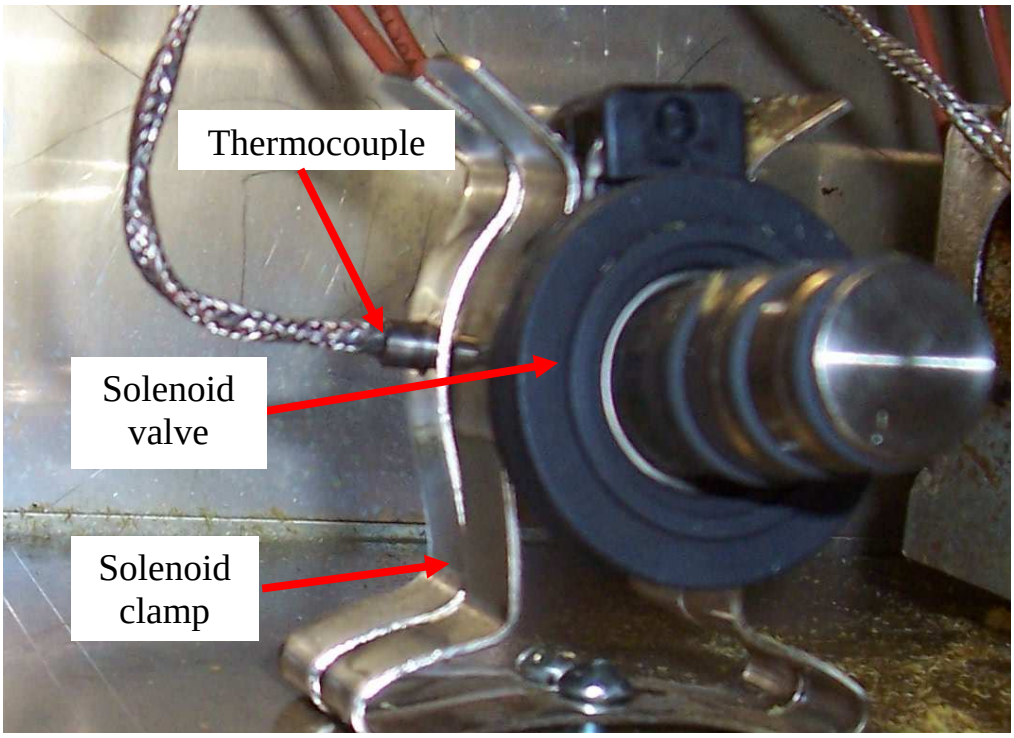

Figure 4.5: Photograph showing solenoid valve test fixture and thermocouple

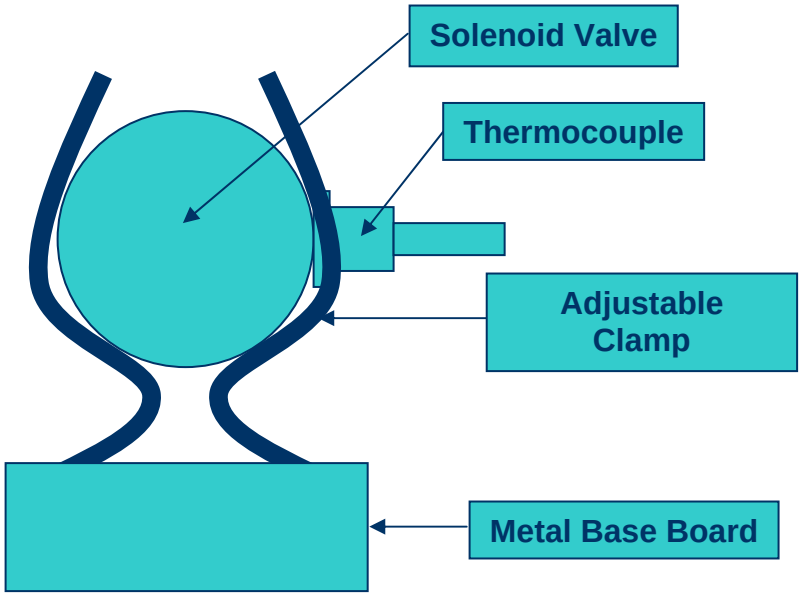

Figure 4.6: A schematic of the solenoid valve test fixture and thermocouple mount

One of the two power supply systems is used to supply a voltage of 20 V to an SC5 solenoid controller board used to actuate the SVs and the other supplies 5 V for current transformers (CTs). The CT for each SV measures the current that is passing though each SV. An SC5 board supplied by RW Automation, LLC Company is used to drive or actuate the SVs, each with operating voltage of 16.8 V.

E type thermocouples are used to measure the operating temperature of the SVs during their cycling process. As shown in Figs. 4.5 and 4.6, the thermocouples are placed to come into contact with the side of the SV's metal casing. Although the thermocouple is not measuring the temperature of the SV coil directly, the measured temperature should be proportional to the coil temperature. It is also shown later by experiment and theory that there is only a few degrees difference between the coil temperature and the measured external temperature. The temperature range for the E type thermocouple is -200ºC to 900ºC. It is expected that when the solenoid valves fail, their measured temperature will rise and their measured electrical resistance will change.

To convert the voltages (mV) read by the thermocouples into temperatures (ºC) for E type thermocouple, a NIST standard voltage to temperature conversion formula is used which is shown below.

$$\begin{aligned} T = {} & X_1 \cdot 1.7057035 \cdot 10^{1} - X_1^{2} \cdot 2.3301759 \cdot 10^{-1} + X_1^{3} \cdot 6.5435585 \cdot 10^{-3} \\ & - X_1^{4} \cdot 7.3562749 \cdot 10^{-5} - X_1^{5} \cdot 1.7896001 \cdot 10^{-6} + X_1^{6} \cdot 8.4036165 \cdot 10^{-8} \\ & - X_1^{7} \cdot 1.3735879 \cdot 10^{-9} + X_1^{8} \cdot 1.0629823 \cdot 10^{-11} - X_1^{9} \cdot 3.2447087 \cdot 10^{-14} \end{aligned} \tag{4.1}$$

where T = temperature of SV in ºC

X_1 = thermocouple voltage in mV

The voltage across each solenoid is measured directly in volts and is conditioned through the analog input voltage modules (42V, 10kHz).

The output of the current transformers (CTs) is a voltage which is proportional to the current powering the SV. The input voltage signal from current transformer (CT) is also first conditioned through another analog voltage input module (5V, 10kHz). It is then converted to current (for each SV). This type of module is chosen specifically based on CT specifications. For each of the SV in operation, an independent CT is used. To convert voltages (V) read by the analog voltage input modules from the current transformers (CTs) into current, the conversion formula shown below is used

$$I = 4.8 \cdot V_2 - 12 \tag{4.2}$$

where I = current through the SV

V_2 = voltage measured from the current transformer

A separate CT is used to measure the current powering each solenoid valve. Using Eq. (4.2), the current flowing through each solenoid valve is calculated.

To measure the electrical resistance of each solenoid valve, a multimeter is used. For a completely failed or a partially solenoid valve, the resistance is measured when its temperature reduces to room temperature. Similarly, for a solenoid valve that is run for a specified test duration of 24 hours but has not undergone failure, its resistance is measured when it cools down to room temperature.

Thus, through experimental testing of the SVs, we obtain the resistance of the SV, the applied current flowing through the SV, the applied voltage across the SV and the

temperature of the SV. This data is then used to characterize and analyze solenoid valve failure. The results of the theoretical model will also be correlated to the results of experimental measurements.

It was also found that when the solenoid valves do fail, the wires in the coils short and cause the resistance to drop. Due to shorting between copper coil wires, the effective length of the wire (L) decreases and the area of cross-section of the wire (A) increases, which leads to a drop in resistance of the copper wire (R), as can be noticed from the equation for resistance through a wire:

$$R = \frac{\rho L}{A} \tag{4.3}$$

where ρ is the material electrical resistivity.

This causes the current to increase significantly since the power source is held at a constant voltage. This actually caused failures of the control board channels. To alleviate this problem, type BAF-3 fuses (fast acting 3 Amp rating) were inserted in the power lines to the solenoid valves. Therefore, if the current applied to solenoid valve increased past 3 Amps, the fuse would blow and cut-off the power. This practice also reduced the risk of fire due to a failed solenoid valve.

4.1 Preliminary Tests

Preliminary tests on the solenoid valves were completed to determine their regular operating conditions, such as steady-state temperature for various inputs, and the shape of the actual actuation voltage and current waves. These results are then used in

conjunction with the finite element predictions of solenoid valve operation to design tests which will provide controllable and repeatable failures of the solenoid valves.

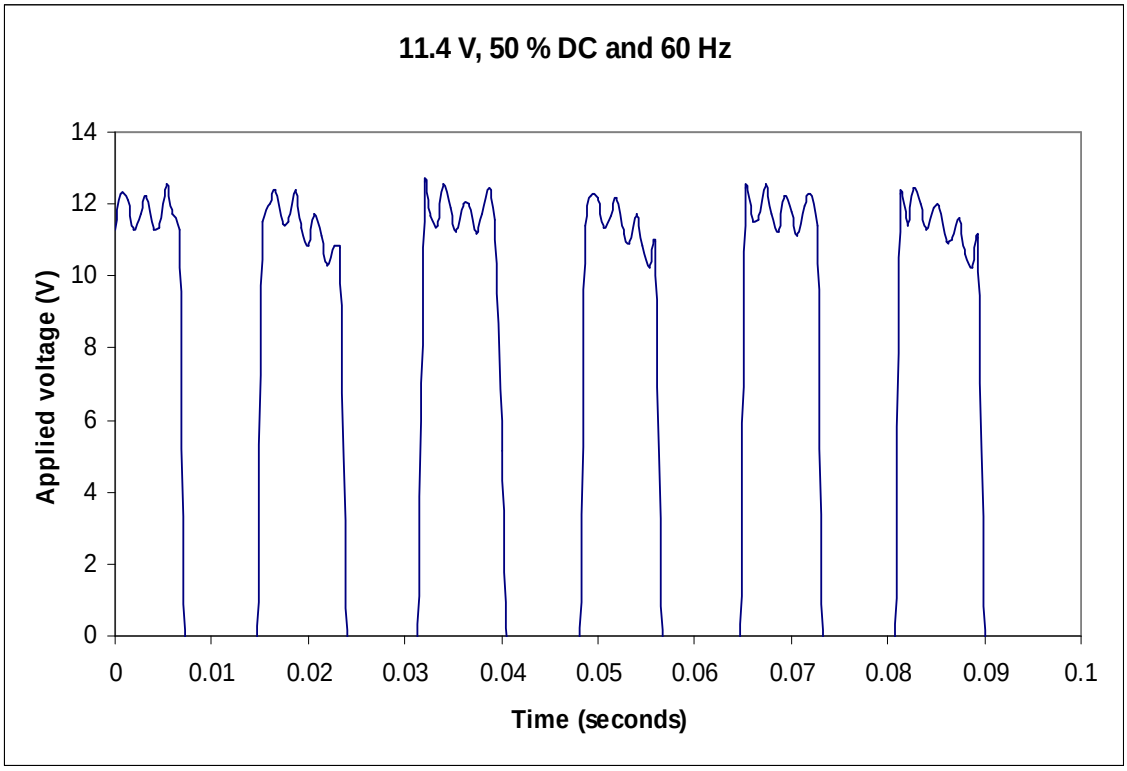

Figure 4.7: Measured actuation voltage applied to the solenoid valve (peak voltage: 11.4 V, duty cycle: 50%, actuation frequency: 60 Hz)

Firstly, the real time voltage and current actuating a solenoid valve is measured (see Figs. 4.7 and 4.8). As expected, the measured voltage shows a clear square wave that is actuated 50% of the time (see Fig. 4.7). The peaks of the square waves are not precisely flat due to limitations of the control module. This is similar to what a solenoid valve would experience in an actual application.

Next, the measured actuation current is shown in Fig. 4.8. This plot shows a more interesting trend. Since the electrical actuation of the solenoid valve is a dynamic event, it experiences some electrical impedance. This causes the current to lag the voltage

during actuation as shown in Fig. 4.8. Once the voltage across the solenoid is actuated, the current responds, but not instantaneously. Rather, the current increases toward the expected peak current of voltage/resistance, in an asymptotic fashion. Then, once the voltage is cutoff, the current also decreases in a similar manner, but never reaches a zero value (see Fig. 4.8). This results in the peak and minimum current to never be reached, and for the average current to not be exactly equal to designed peak current divided by two. For this reason the average current for various actuation voltages was measured (see Fig. 4.9). The average current was measured by simply averaging the actuation current over many cycles, as shown in Fig. 4.8.

The measured average, RMS and maximum currents are shown in Fig. 4.9 as a function of the applied voltage. In each of 7 cases, average current is calculated by taking an average of all current values recorded during SV operation. The average peak current is calculated by taking the average of highest current value in each cycle of a waveform. These values are very important for modeling and prediction of solenoid valve behavior. In the finite element model which will be discussed in Chapter 5, a RMS current is applied to the solenoid coil, since it is modeled in a pseudo-steady-state condition (independent of time). This RMS current is the same that is measured experimentally. The steady-state temperatures for each one of the applied voltages and currents are also recorded. Those results are shown in comparison to the finite element predicted results in Chapter 6 (see Fig. 6.7). The results show that the temperature increases as the current increases, which is predicted by the law of Joule heating.

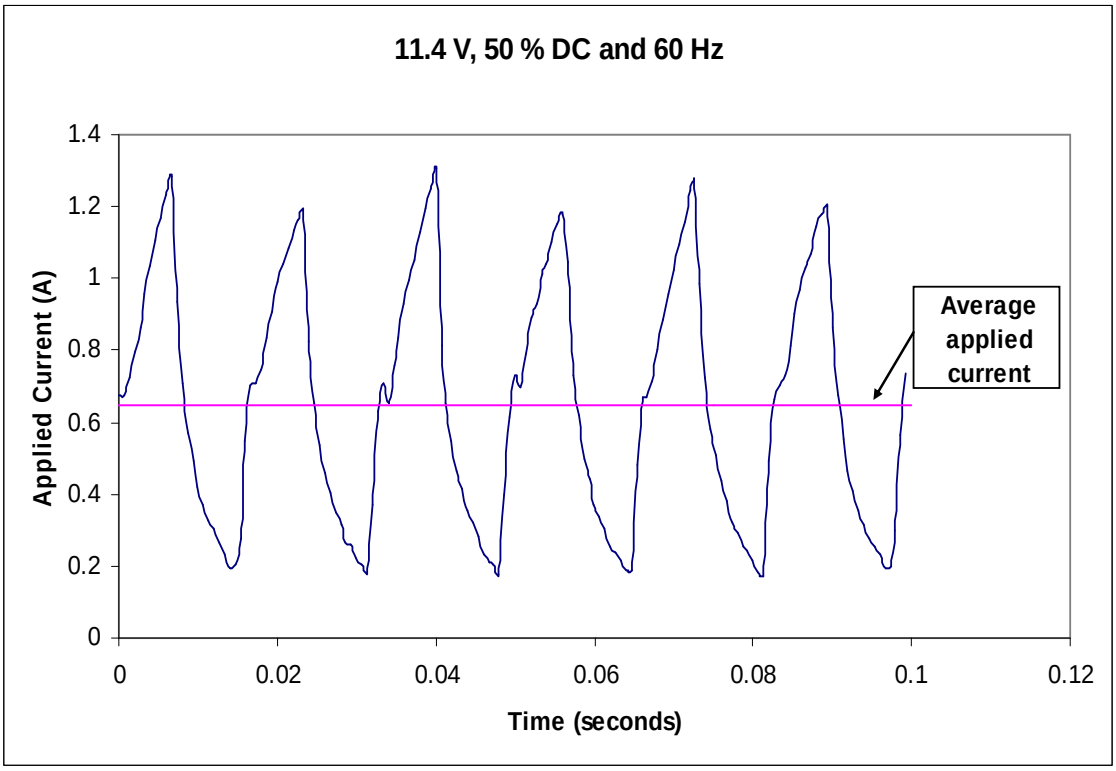

Figure 4.8: Measured actuation current applied to the solenoid valve (peak voltage: 11.4 V, duty cycle: 50%, actuation frequency: 60 Hz)

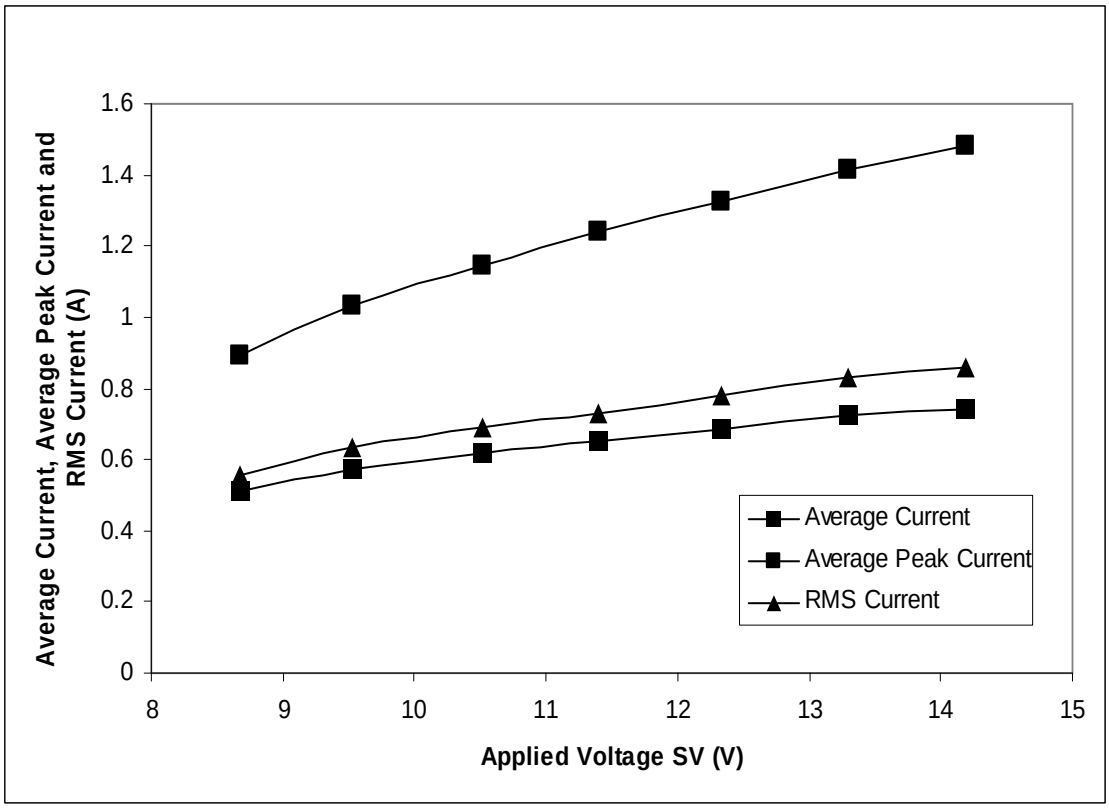

Figure 4.9: The measured average, RMS and peak current measured as a function of the applied voltage

Based on these preliminary test results and the numerical results, the test conditions were decided upon. For each test of the solenoid valve, the power supply is set to 20 V, however the actual voltage actuating the solenoid valve is then 16.8 V. The solenoid valve is then run at 50% duty cycle and at 60 Hz. During a test, the ambient temperature in the thermal chamber is set to 100ºC. The tests were usually run for 24 hours or until the solenoid valves failed. The failure criterion is defined by the moment when the solenoid valve ceases to actuate and is usually marked by a sudden increase in the measured current and temperature. The failure criterion will be discussed further in Chapter 6.

CHAPTER 5
MODELING METHODOLOGY

A multiphysics (thermal, mechanical and electro-magnetic) model of the solenoid valve (SV) is developed in Ansys™ (see Fig. 5.1), a finite element analysis package, the results of which are discussed in the following section. The model solves the coupled fields of equations and thus captures effects not normally considered by conventional uncoupled finite element models. For instance, the heat generated by the solenoid coil will be due to Joule heating. This heating will increase the temperature which will cause thermal expansion and stresses in the coil and the surrounding parts. Therefore, these different fields are coupled together and for improved accuracy, should be solved simultaneously. This results in a very powerful tool that can be used to characterize solenoid valve performance.

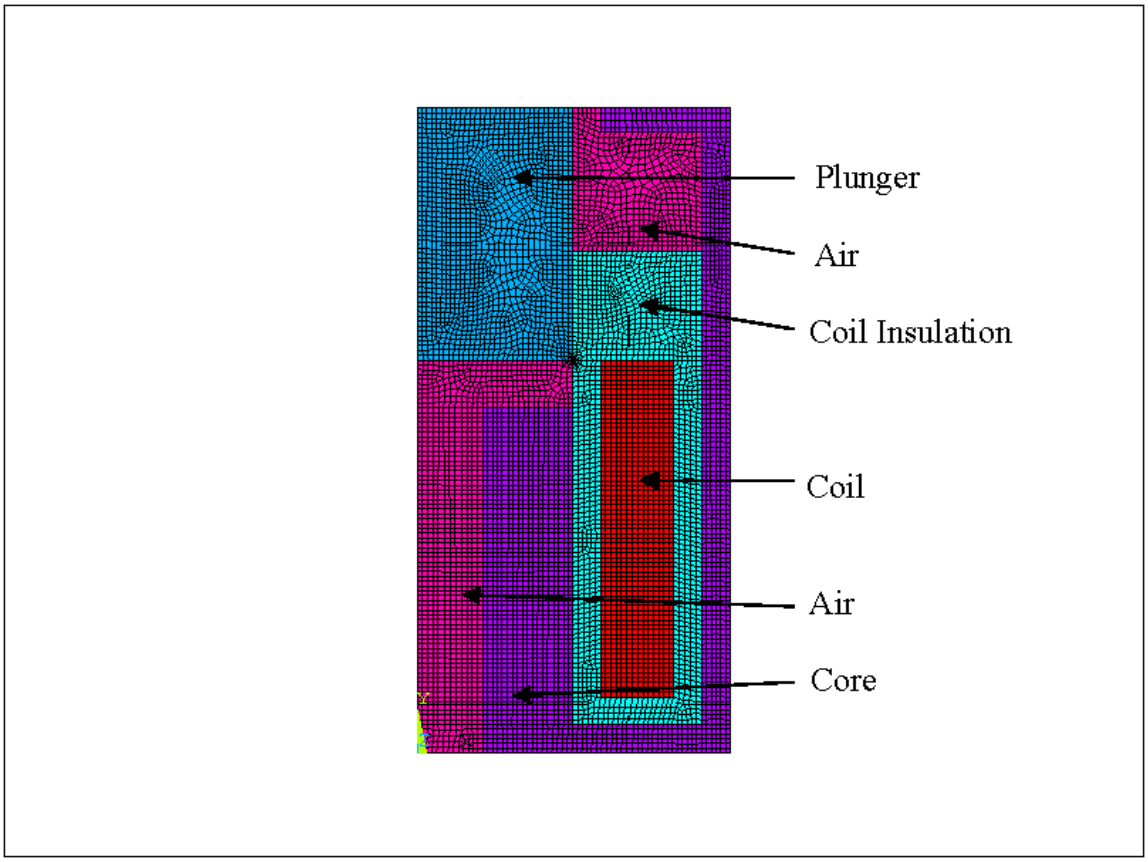

Figure 5.1: A plot of the finite element mesh used to model the solenoid valve

The mechanical field of the problem considers the stresses and strains of the material, and how it will deform and possibly fail due to over stressing. The theory of elasticity is used to model the deformations in the material. Then, three dimensional Hooke's law, which relates the stresses and strains, is given in cylindrical coordinates (r,θ,z) as:

$$\varepsilon_r = \frac{1}{E}[[\sigma_r - \nu(\sigma_\theta + \sigma_z)] + \alpha\Delta T] \tag{5.1}$$

$$\varepsilon_\theta = \frac{1}{E}[\sigma_\theta - \nu(\sigma_r + \sigma_z)] + \alpha\Delta T \tag{5.2}$$

$$\varepsilon_z = \frac{1}{E}\left[\sigma_z - \nu\left(\sigma_r + \sigma_\theta\right)\right] + \alpha\Delta T \tag{5.3}$$

$$\gamma_{r\theta} = \frac{2\left(1+\nu\right)}{E}\tau_{r\theta} \tag{5.4}$$

$$\gamma_{rz} = \frac{2\left(1+\nu\right)}{E}\tau_{rz} \tag{5.5}$$

$$\gamma_{\theta z} = \frac{2\left(1+\nu\right)}{E}\tau_{\theta z} \tag{5.6}$$

where E is the elastic modulus, ν is Poisson's Ratio, σ is the normal stress, τ is the shear stress, ε is the normal strain, γ is the shear strain, α is the thermal expansion coefficient, and ΔT is the change in temperature of the material. In the current analysis, the solenoid valve will be modeled as being axisymmetric in geometry and loading. For axisymmetric cases, the displacement/strain relations are

$$\gamma_{r\theta} = \gamma_{\theta z} = \tau_{r\theta} = \tau_{\theta z} = u_\theta = 0 \tag{5.7}$$

$$\varepsilon_r = \frac{\partial u_r}{\partial r} \tag{5.8}$$

$$\varepsilon_\theta = \frac{u_r}{r} \tag{5.9}$$

$$\varepsilon_z = \frac{\partial u_z}{\partial z} \tag{5.10}$$

$$\gamma_{rz} = \frac{\partial u_r}{\partial z} + \frac{\partial u_z}{\partial r} \tag{5.11}$$

where u is the normal displacement. The equations for continuity are also satisfied in the FEM software. Notice that in Eqs. (5.1 to 5.3) the strains are also dependant on the temperature of the material. Since the temperature in the solenoid valve will not be uniform, the thermal field must also be solved to obtain temperature.

The two-dimensional steady-state heat transfer equation using cylindrical coordinates r and θ is:

$$\frac{\partial^2 T}{\partial r^2}+\frac{1}{r}\frac{\partial T}{\partial r}+\frac{1}{r^2}\frac{\partial^2 T}{\partial \theta^2}=\frac{1}{k}Q(r,\theta) \tag{5.12}$$

where $Q(r,\theta)$ is volumetric heat generation, T is the temperature distribution, which must be periodic or constant around the circumference. In the solenoid valve problem, there will be several sources of heat such as Joule heating and friction. Since the contact force on the plunger surfaces should be small, the friction force should be small and the frictional heating should be negligible. Probably the most significant source of heating will be from the Joule heating of the coil. Joule heating is described by

$$Q_{joule}=I^2\rho \tag{5.13}$$

where I is the electrical current and ρ is the electrical resistivity. Therefore the thermal and electrical fields are coupled, and the mechanical and thermal fields are coupled. The electrical and thermal fields may also be affected by the deformations of the solenoid, as it may affect the flow of current and heat.

In addition, heat may be convected away from the solenoid valve through the air. This will be modeled as free convection. A more complete description of the convection modeling is given later.

The electromagnetic, thermal and structural (that is, the directly coupled multiphysics) modeling of the SV under investigation is being performed with the measured dimensions of the actual SV product, the known applied current density, and the expected material properties of the various parts. However, to improve computational time only a portion of the SV will be modeled in the FEM software (see Fig. 5.2). Dimensions of the SV parts in mm are given in Figs. 5.3 and 5.4 as they were supplied by KTL. The resulting finite element mesh is shown in Fig. 5.1. The mesh was refined to satisfy mesh convergence.

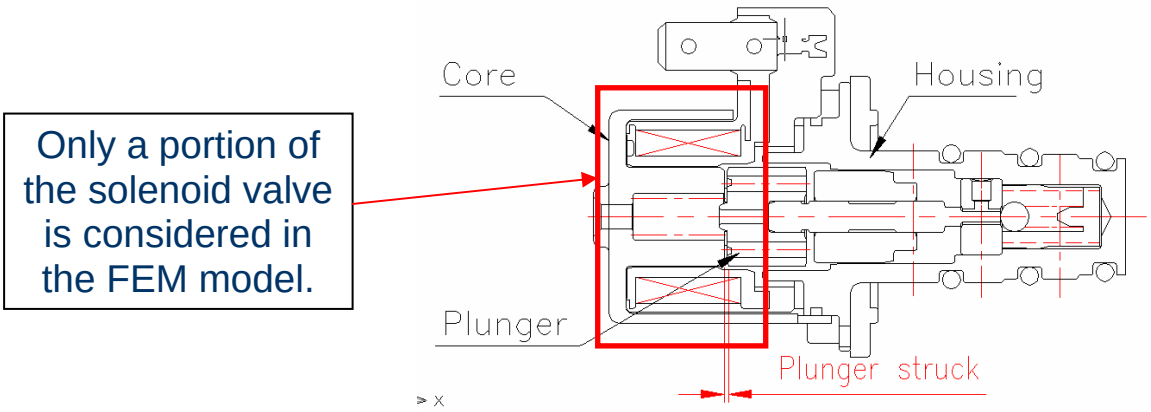

Figure 5.2: Schematic of solenoid valve and portion considered in model

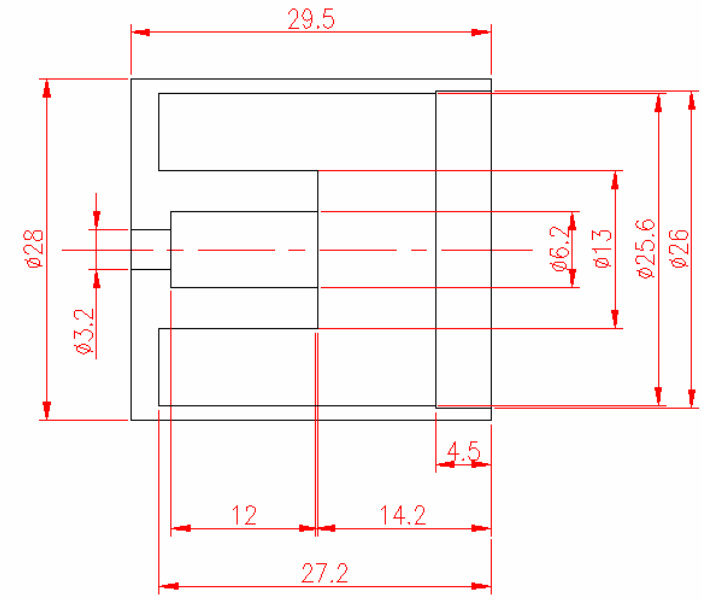

Figure 5.3: Schematics of the solenoid valve core used for modeling (supplied by KTL, dimensions in mm)

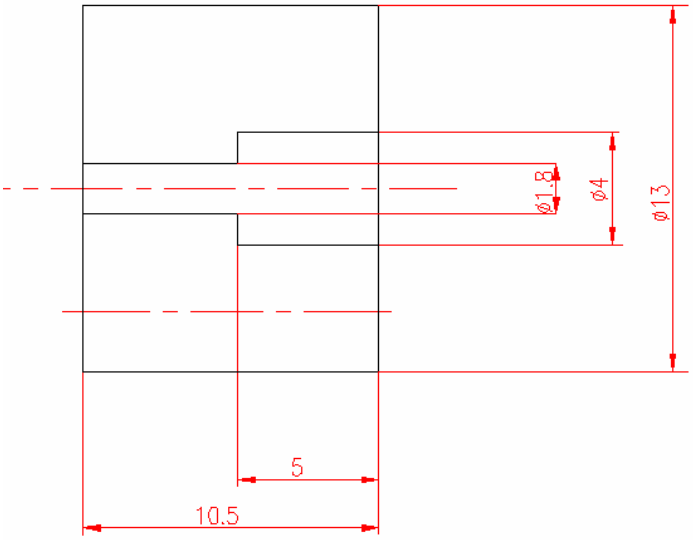

Figure 5.4: Schematics of the solenoid valve plunger used for modeling (supplied by KTL, dimensions in mm)

Multiphysics modeling of a SV using Ansys™ gives insight into the temperature distribution and the location of the highest temperature in the SV. It will also make predictions for the mechanical and thermal deformations and stresses due to high temperatures in the SV, and thus the resulting mechanical stresses and deformations on parts of the SV. The model calculates the magnetic flux distribution in the SV, the magnetic flux lines and the magnetic force on the plunger due to the applied current as well.

Most of the necessary material properties are readily available. The properties used for the materials of the solenoid valve in the current study are shown in Table 5.1.

Property	1AIW Insulation Polyamide-imide	1AIW Copper Wire	SMF1010 Plunger Iron Powder	SM15C Core Carbon Steel	Air
E (GPa)	6.32	110	200	205	0
v	0.38	0.343	0.29	0.29	0.5
k (W/mK)	0.363	385	76.2	44.5	0.0313
ρ (Ωm)	$1 \cdot 10^{15}$	$1.7 \cdot 10^{-8}$	$8.9 \cdot 10^{-7}$	$2.49 \cdot 10^{-7}$	$1 \cdot 10^{14}$
α (μm/mK)	25	16.4	12.2	11	0
μ_r	1	1	100000	1500	1

Table 5.1: Material Properties used in FEM model

It is also important to apply realistic boundary conditions to the finite element model. Since the model considers many different fields (thermal, mechanical and electromagnetic), several different sets of boundary conditions must be applied (see Fig. 5.5). As shown, the deflections in the Y-direction are held constant on the top surfaces. One point is used to keep the model from translating in the X-direction. Free convection

is assumed on all the outer boundaries of the solid materials, except on the line of symmetry, where axisymmetric boundary conditions are assumed. Zero normal magnetic flux is also assumed on all the outer boundaries.

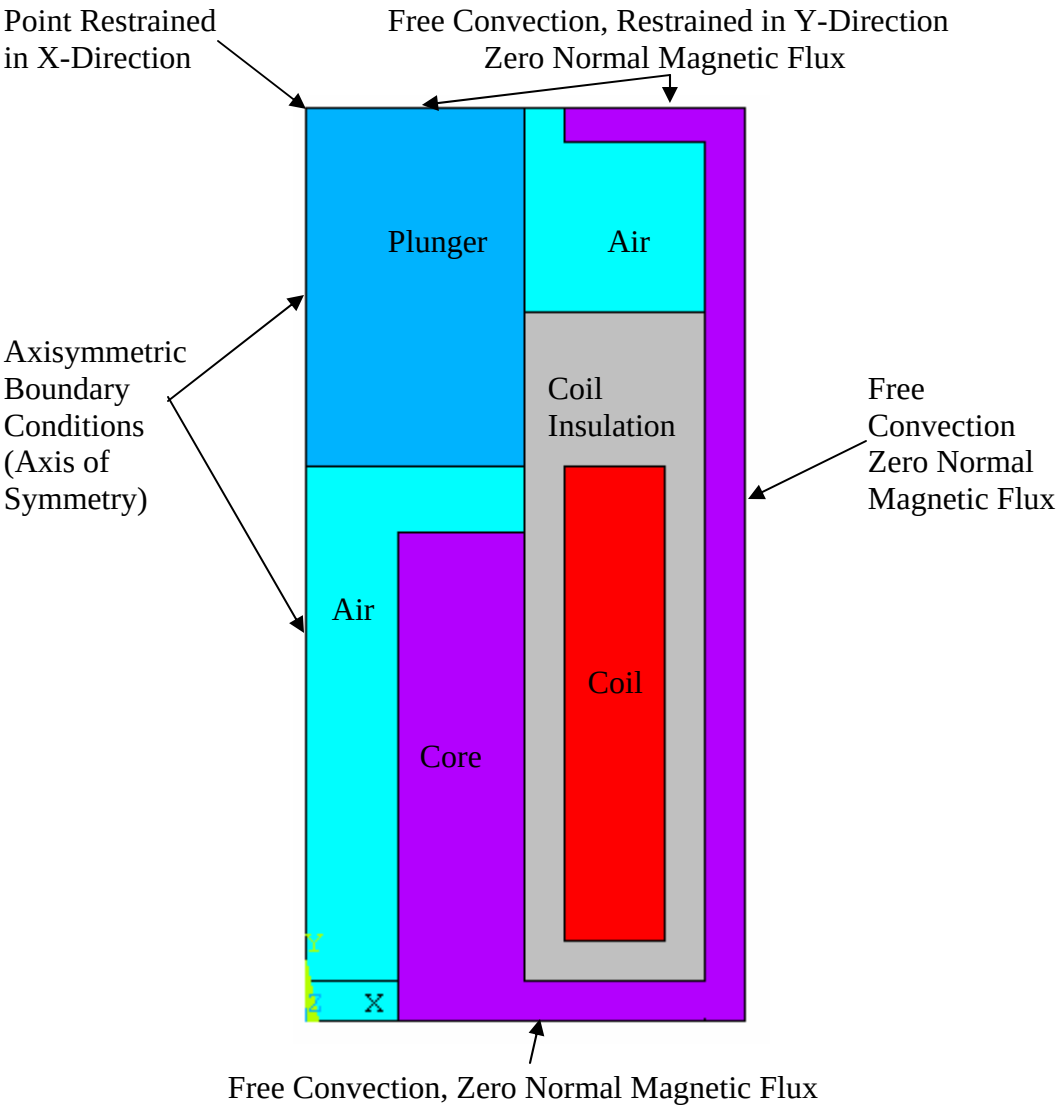

Figure 5.5: Schematic of the FEM model of the Solenoid Valve, including Boundary Conditions

To model the convection of heat away from the surfaces of the solenoid valve, the finite element model uses *Newton's law of cooling* (the following equation) to predict the heat loss due to convection (q):

$$q = hA\Delta T \tag{5.14}$$

where A is the surface area, ΔT is the difference in temperature between the surface and the ambient air, and h is known as the convection coefficient, or film coefficient. It can be very difficult to analytically predict h for a given geometry. Empirical correlations are therefore often used. For an infinitely long cylinder geometry, Churchill and Chu [28] related h to the Nusselt number, Nu, by the equation

$$h = \frac{k \cdot Nu}{D} = \frac{k}{D}\left\{0.60 + \frac{0.387Ra^{1/6}}{\left[1+\left(\frac{0.559}{\mathrm{Pr}}\right)^{9/16}\right]^{8/27}}\right\}^2 \tag{5.15}$$

where k is the thermal conductivity, D is the diameter of the cylinder, Ra is the Rayleigh number and Pr is the Prandtl number. For this case of a long cylinder, the Rayleigh number is given by

$$Ra = \frac{g\beta(\Delta T)D^3}{\eta\delta} \tag{5.16}$$

where g is the gravitational constant (9.81 m/s^2), β is the volumetric thermal expansion coefficient, η is the kinematic viscosity, and δ is the thermal diffusivity. For air, some of these properties are given in Table 5.1, and the rest are given in Table 5.2. Pr is also

taken to be 0.697. For these properties, and diameter of the solenoid (28 mm), the value of *Ra* calculates to be 78469. Then, the predicted value for *h* is 8.14 W/m^{2}K.

Property	Air
β (K^{-1})	$2.725 \cdot 10^{-3}$
η (m^2/s)	$22.8 \cdot 10^{-6}$
δ (m^2/s)	$32.8 \cdot 10^{-6}$

Table 5.2: Material Properties for Air

In addition, a suitable value for *h* can be found by fitting the external temperature of the solenoid valve predicted by the FEM model to that measured using the test apparatus. The external temperature extracted from the FEM model was from the same location that the thermocouple contacts the solenoid valve in the test rig (it is about 0.5 cm from the end of the solenoid casing). As shown in Fig. 5.6, the fit results in a value of 7.15 W/m^{2}K, which is a very similar value that which was calculated from the empirical prediction above (Eq. (5.15)). This fit was performed for the case of a solenoid valve running at 13.2 V, 0.86 Amp (RMS), 50% Duty Cycle, and 60 Hz.

Using the fit value of h=7.15 W/m^{2}K, the predicted external temperature can be compared to a wide range of experimental results for various excitation voltages. The results are used in the current work to design and select the conditions used to test the solenoid valves. This and other results of the numerical model are discussed in Chapter 6.

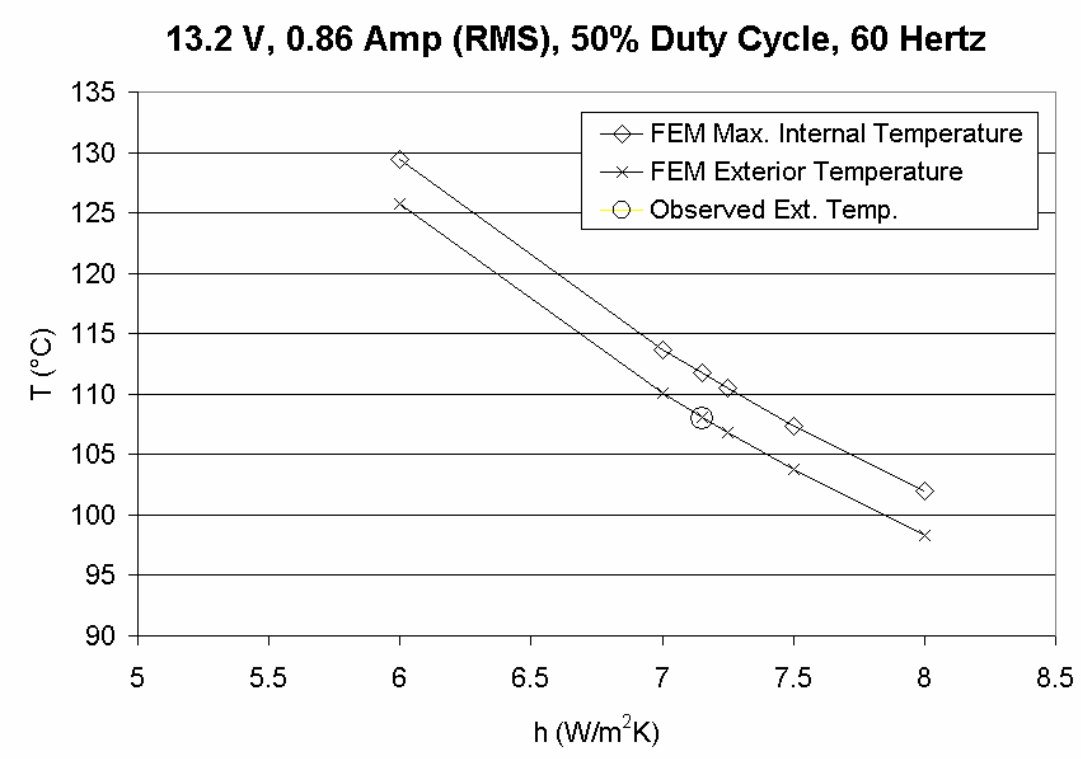

Figure 5.6: Finite element prediction of the temperature for various convection coefficients

CHAPTER 6
RESULTS AND DISCUSSION

6.1 Modeling Results

An electromagnetic analysis of the solenoid valve using the Ansys™ finite element package has been performed and the results are presented below. The FEM model solves the coupled mechanical, thermal and electromagnetic physics of the problem. The results shown below are for the same solenoid valves tested in the experimental portion of this work and the physical properties used to model this case are given in Tables 5.1 and 5.2.

The multiphysics model of the solenoid valve can produce predictions for a wide range of quantities, such as temperature, strain, stress, Joule heat, etc. Some of these results are presented below for conditions similar to those expected in the solenoid valve application and during testing. One will also find that they produce the expected trends that would result from simple approximations and predictions of solenoid behavior.

The finite element predicted temperature distribution of the solenoid valve coil is shown in Fig. 6.1. As expected, the highest temperatures are found within and around the coil. The plastic encapsulating the coil is a poor conductor and so it causes the heat to build up near the coil. As will be shown in the experimental work, this build up of heat can cause the wire insulation to fail and the plastic to melt, causing failure of the solenoid valve. It can also be observed that the minimum temperatures are located near the top of the solenoid coil, as that is where much of the heat is conducted into the valve portion of the part and convected away. Since an averaged model is used to consider the solenoid

coil, the local temperature distributions in each wire of the solenoid coil are not seen (individual wires are not modeled). Therefore, the local temperatures in the wire might be larger than the 'averaged' temperatures predicted by the finite element model and shown in Fig. 6.1. However, later in this section, a localized model of the coil wires will also be presented.

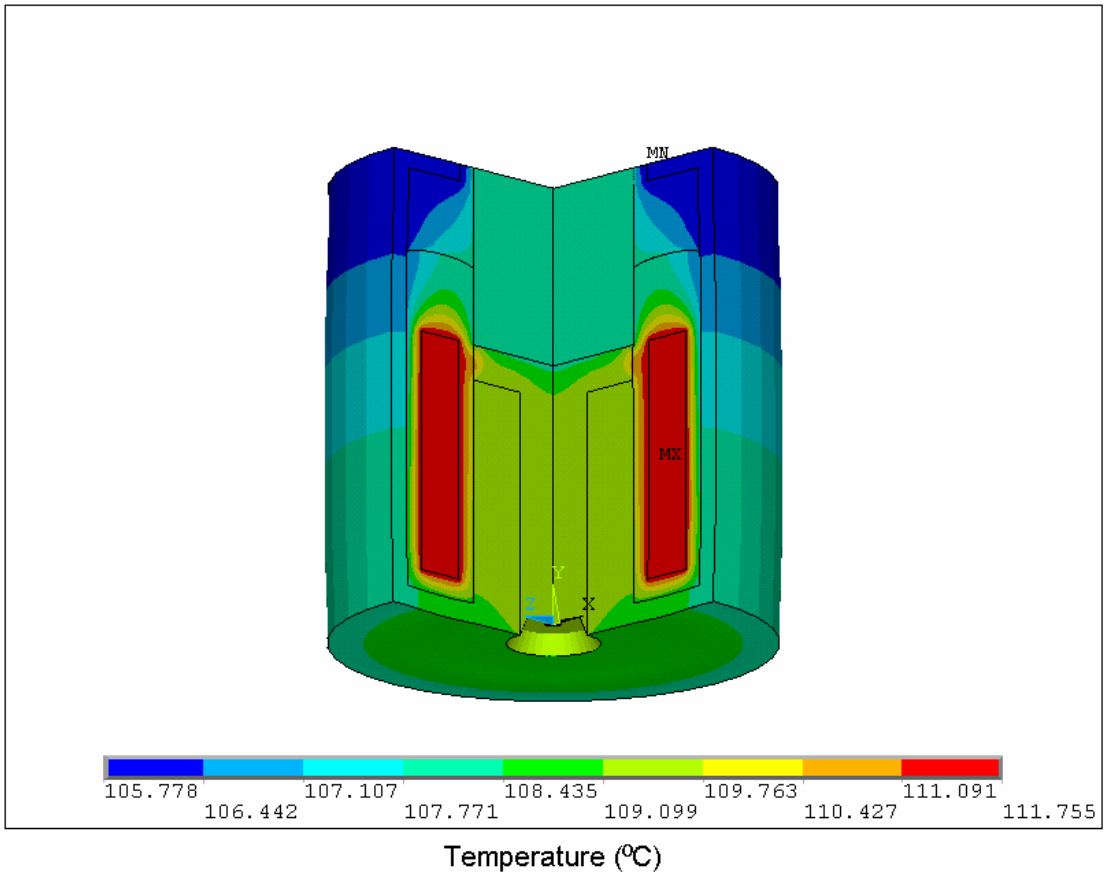

Figure 6.1: The predicted temperature distribution in the solenoid cross section for 0.86 Amps of current

The temperature distribution shown in Fig. 6.1 will of course cause thermal expansion in the materials. The expansion and strain will not match between the various materials and parts which will then cause stresses to form (see Fig. 6.2). These stresses

could be substantial and could also influence the failure and reliability of the solenoid valve. It appears that the highest stresses occur within the casing of the solenoid. However, there are also significant compressive stresses within the solenoid coil that will cause the wire and insulation to press against each other. Combined with high temperatures, this could cause the insulation to squeeze out from between the wires and result in shorting and failure.

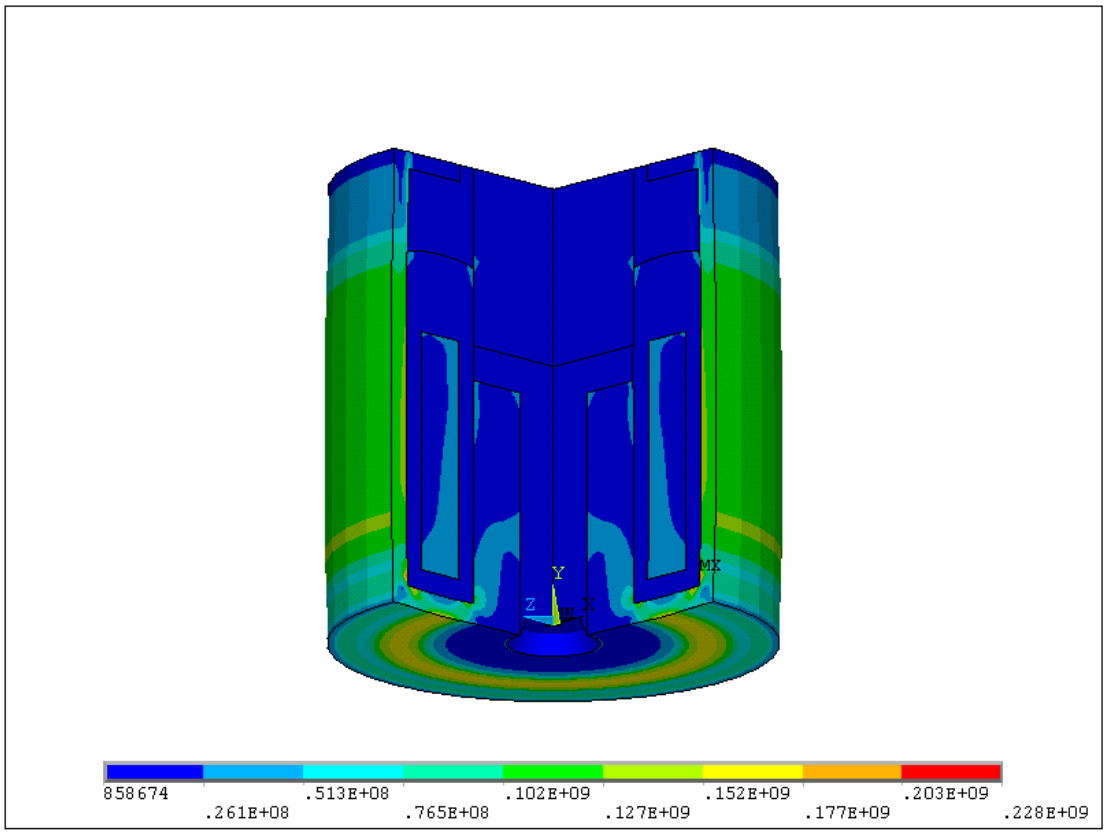

Figure 6.2: The predicted von Mises stress distribution in the solenoid cross section for 0.86 Amps of current

It should be noted that the manufacturing tolerances of the solenoid valve could greatly affect the stresses resulting from thermal expansion. For instance, stresses from thermal expansion often result when a part is confined by another part from expanding. The confinement results in forces between the parts that produce stresses. If even a gap is in between the parts due a mismatch in machine tolerances, the stresses could be lower, because the parts have more room to expand. Therefore, these machine tolerances which may statistically vary from part to part could also cause statistical variation in the experimental results. These variations are not considered in the finite element model.

The finite element model is a multiphysics model and so it automatically calculates the Joule heating occurring locally within the solenoid coil when electrical current is applied. The Joule heat generated is calculated from the equation:

$$q' = \frac{Q}{V} = \frac{I^2 R}{V} = \frac{I^2 \rho L}{A^2 L} = \frac{I^2 \rho}{A^2} \tag{6.1}$$

where Q is the power of the heat generated, q' is the volumetric heat generated, V is the volume, A is the cross-sectional area of the wire, L is the length of the wire, I is the current, and ρ is the electrical resistivity. As expected, the total heat generated increases with the current squared (see Fig. 6.3). The heat generated can reach 1 W or more. The Joule heat generation is calculated over the entire surface of the solenoid. It is assumed in the current analysis that the current is distributed evenly through the cross-section of the solenoid coil. This results in the uniform heat generation as shown in Fig. 6.4 for the case of a 1 Amp RMS current applied to the solenoid coil. Although the heat generation

is uniform, the temperature distribution will not be. Also, the geometry of the solenoid cross-section is deformed in Fig. 6.4 due to the thermal expansion.

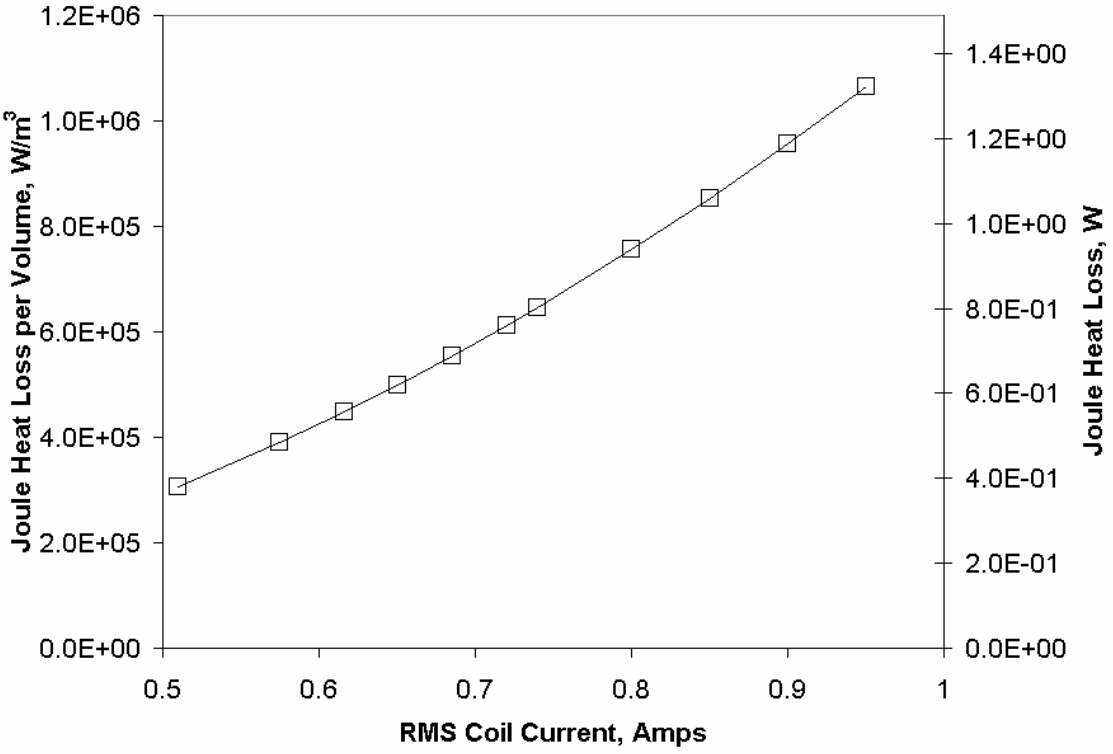

Figure 6.3: The finite element prediction of the Joule heating within the solenoid coil

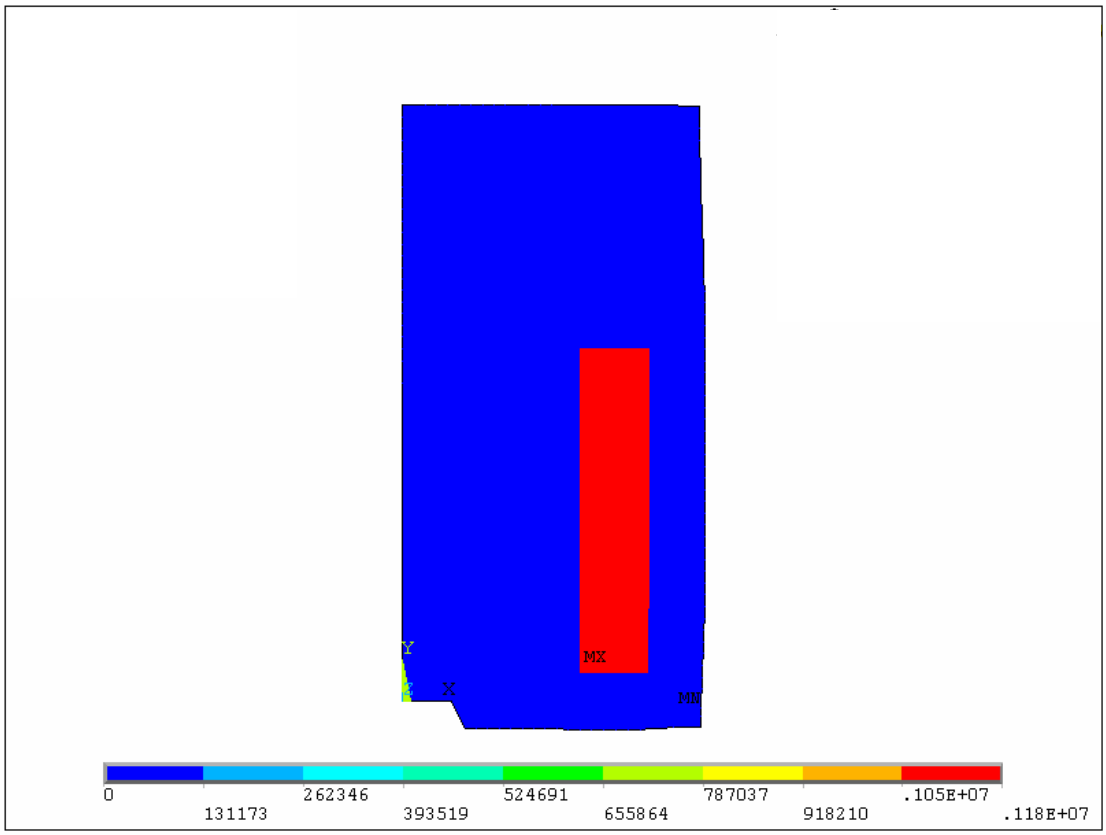

Figure 6.4: Distribution of the Joule heat generation for 1 Amps of RMS current applied evenly over the cross-section of the solenoid coil

As mentioned previously, the heat generated and the temperature distributions will result in thermal deflections and stresses. The finite element predicted deflections in the cross-section are shown in Figs. 6.5 and 6.6. The deflections in the *x* direction are maximum near the outer radius of the solenoid valve casing and appear to reach a value of almost 0.05 mm (see Fig. 6.5). The deflections in the *y* direction are smaller than the deflections in the *x* direction and also appear to maximize at different locations as shown in Fig. 6.6. Of course, these deflections are relative since they depend on which points were fixed in the model. As discussed in Chapter 5 on the modeling methodology, the

axis of symmetry restricts the deflection in the *x* direction, while the cross section is fixed in the y-direction along the top surface.

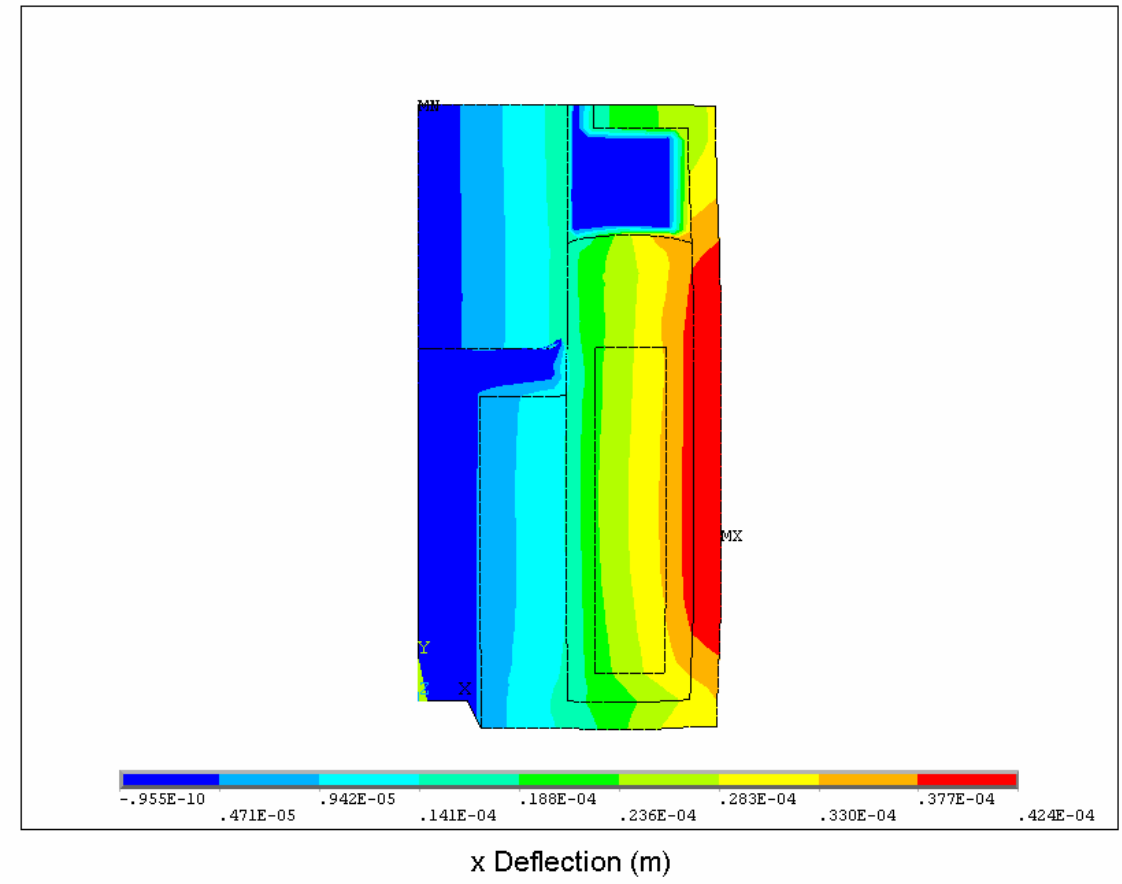

Figure 6.5: The finite element model predictions of the deflections in the *x* direction within the solenoid valve resulting from thermal expansion (for 1 Amps)

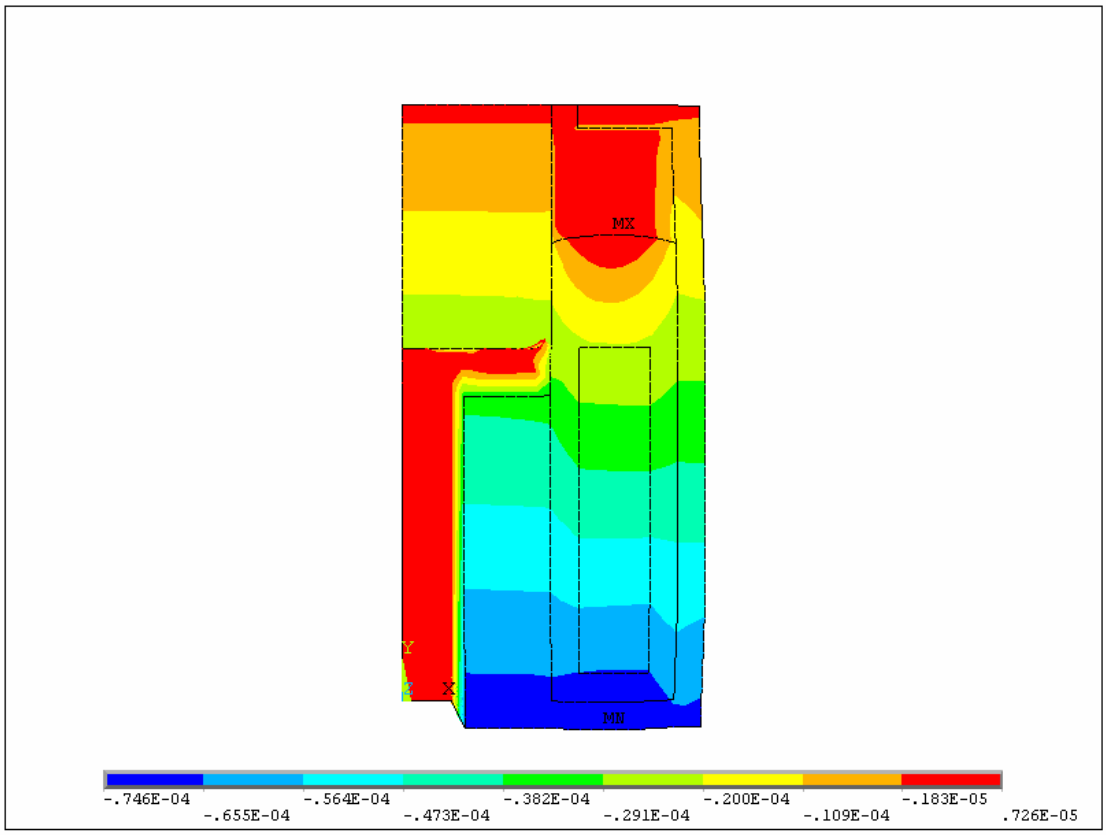

Figure 6.6: The finite element model predictions of the deflections in the *y* direction within the solenoid valve resulting from thermal expansion (for 1 Amps)

Preliminary tests of the solenoid valves were then run to verify the effectiveness of the finite element model in predicting the solenoid valve operation. The solenoid valve was run at 60 Hz, under a constant duty cycle, a constant peak voltage, a constant peak current, and in ambient air. The tests were run until the solenoid valve reached a 'steady-state' temperature as measured by the external thermocouples (see Chapter 4 on experimental methodology). For various values of applied current, the 'steady-state' temperature was recorded (see Fig. 6.7). Note that these temperatures are for the thermocouple touching the external surface of the solenoid valve and therefore to make a

consistent comparison, the temperature from the finite element model located at nodes corresponding to the location of the thermocouple must be used. As shown in Fig. 6.7, the experimentally measured and finite element predicted temperatures agree very well. It can also be observed that the maximum temperature predicted by the finite element model is not significantly higher than the external temperatures. This suggests that the externally measured temperature is sufficient for evaluating solenoid valve performance. This will also be confirmed through a localized finite element model of the solenoid valve wires (see later section) and by measuring the temperature directly from the solenoid coil (see experimental results section).

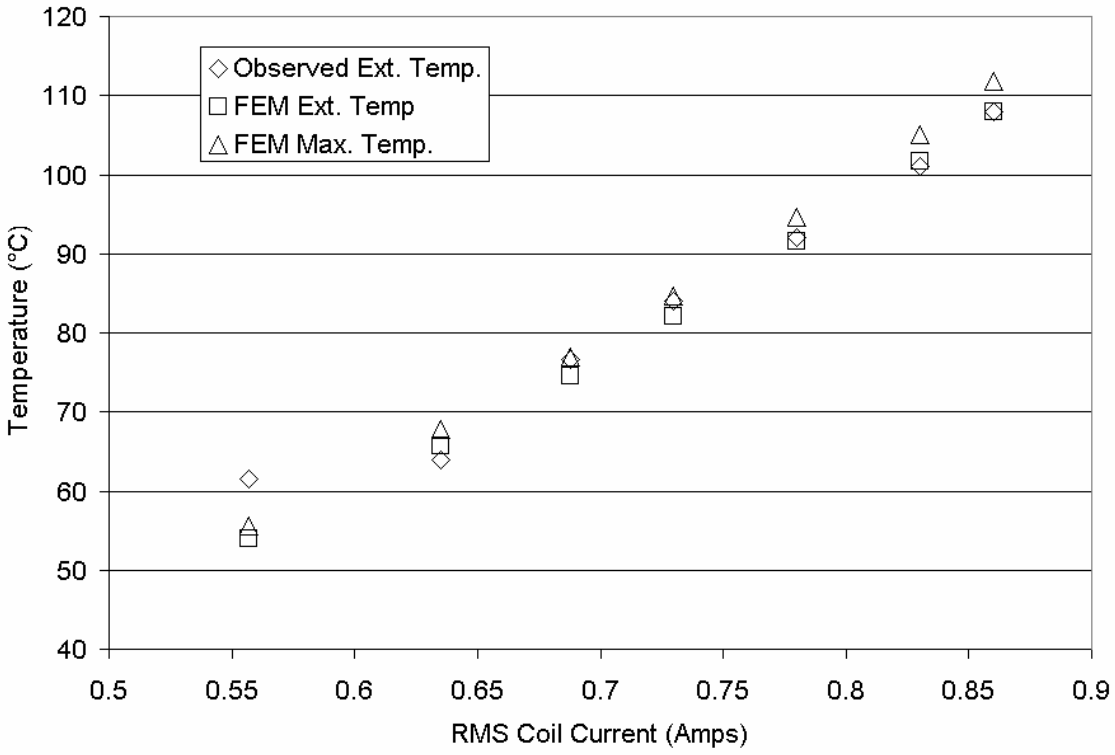

Figure 6.7: Comparison of the theoretically predicted and experimentally measured solenoid temperature

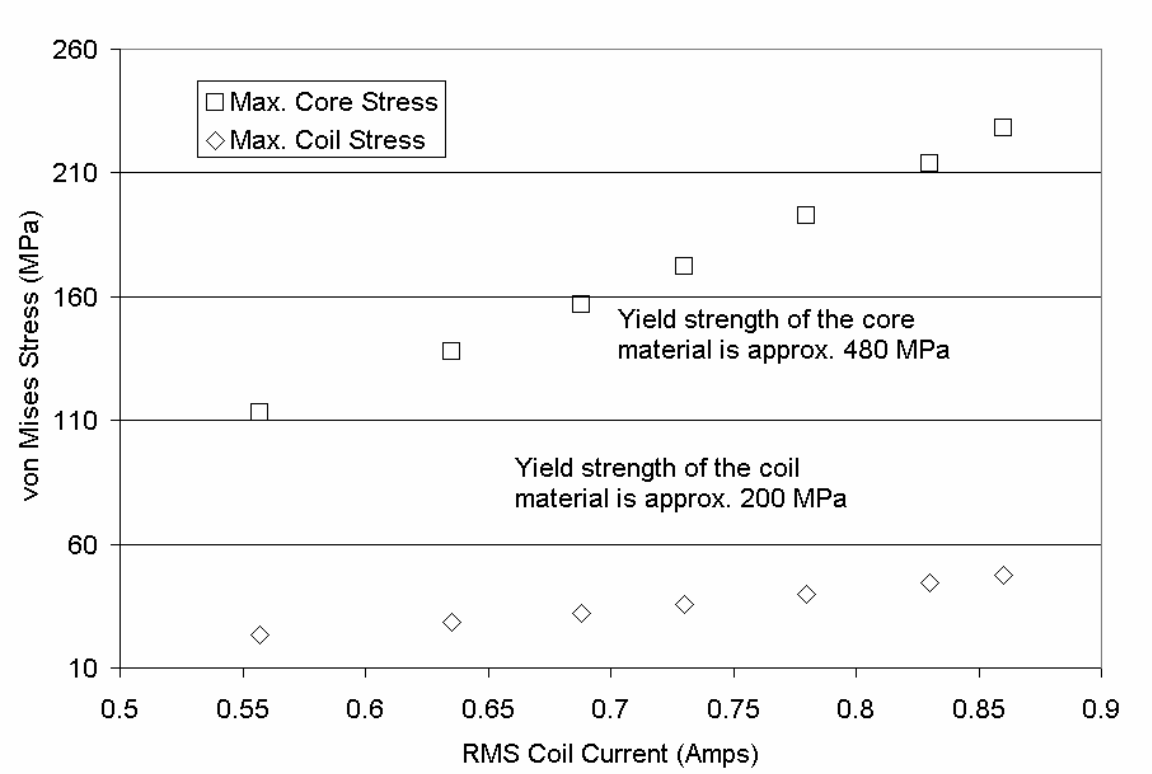

Figure 6.8: The maximum stresses predicted by the finite element model

Since the finite element model appears to be able to make good predictions of the solenoid valve performance, we can now use it to generate results over a wide range of operating conditions. As shown in Fig. 6.8, the maximum von Mises stress in the solenoid core and coil for various applied currents were recorded. The stresses in the core are significantly higher than the coil, but the steel material of the core is also much stronger. The yield strength of the copper wire making up most of the solenoid coil is approximately 200 MPa and the yield strength of the core steel is approximately 480 MPa. As the current is increased, the stress does increase, but for the conditions shown the stresses do not reach the yield strengths. It is therefore believed that the failure of the solenoid valves is not sourced only from thermally induced stresses. However, the

stresses are high enough that, in combination with high temperatures, they could cause damage to the wire insulation.

6.1.1 Local Wire Model

A finite element model of the local wires within the solenoid coil is also constructed. The purpose of this localized model is to determine if the local temperature of the wires is significantly higher than the average temperature predicted by the larger scale solenoid valve model. To create a local wire model, the hexagonal symmetry of the wire coil structure is employed (see Fig. 6.9). This cross-section is then meshed as shown in Fig. 6.10. It is assumed that all the boundaries follow the laws of symmetry, so that they have zero normal deflections and zero heat conduction. However, the temperature of the locations where the insulation contacts the edges is held constant. Then a current is applied to each of the wires and the temperature distribution and deflections of the cross-section can be predicted.

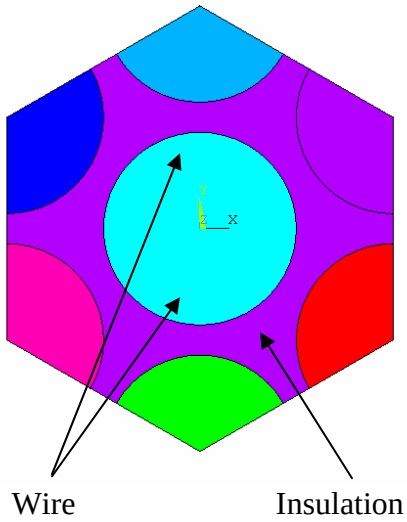

Figure 6.9: Schematic of the hexagonally symmetric local solenoid wire model

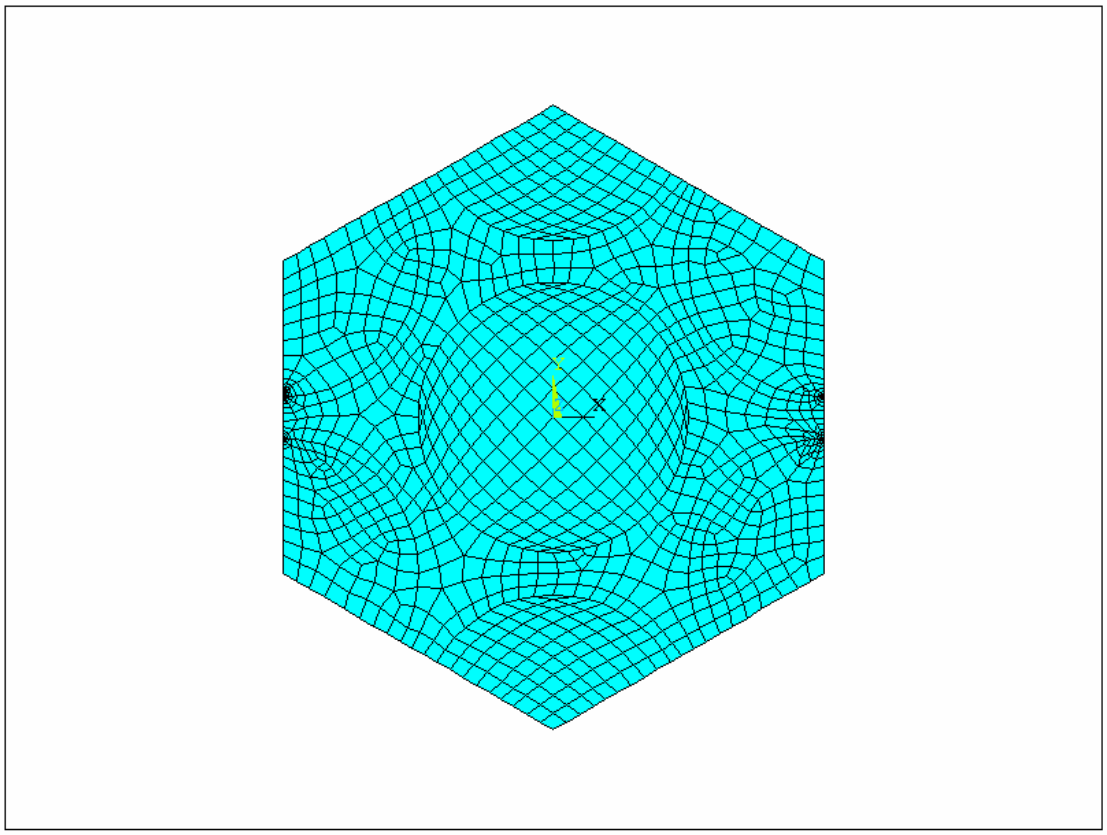

Figure 6.10: The finite element mesh of the local solenoid wire cross-section

The local solenoid wire model is then used to predict the local temperatures for the case of solenoid valve powered with a RMS current of 1 Amps and 80°C ambient temperature, which as will be shown in the following section, results in a peak temperature of 210.8°C. The resulting temperature distribution is shown in Fig. 6.11. The predicted rise in the local temperature is only 1.5°C. Therefore, it appears that local temperature rise should not be an important effect when considering solenoid valve performance and reliability. However, as will be shown next, that does not appear to be the case for the predicted deflections.

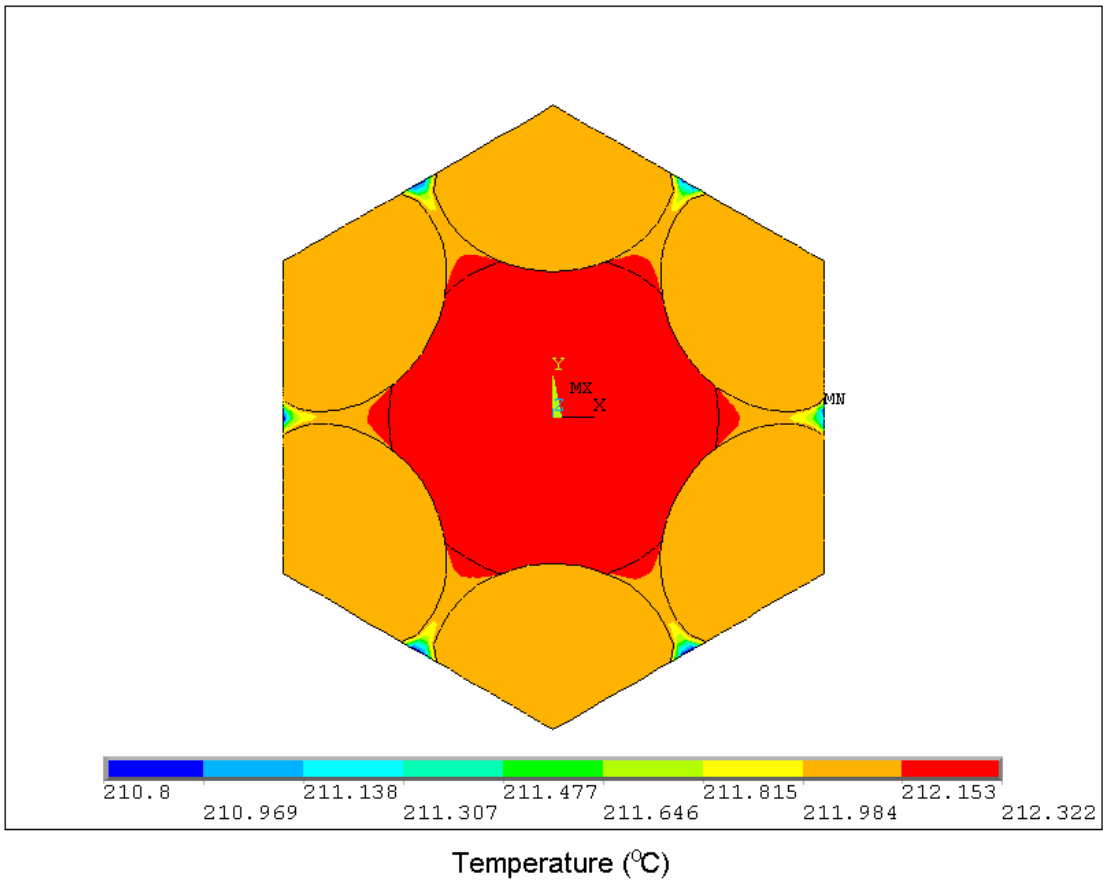

Figure 6.11: Finite element predicted local solenoid coil wire temperature distribution

The rise in temperature of the wire and insulation from room temperature will cause a significant amount of thermal expansion and deflection as shown in Fig. 6.12. Although the wires appear to be overlapping due to the deflection shown in Fig. 6.12, they are not, it is just because the deflections are exaggerated for clarity. Nonetheless, the deflections are large (as much as 0.44 mm). These deflections should compress the relatively weak polyamide-imide insulation very easily, especially since the temperatures are also very high. This will result in the possible failure of the insulation and shorting

between the solenoid coil wires. This mechanism is believed to be one of the failure mechanisms occurring in our current tests of the solenoid valves.

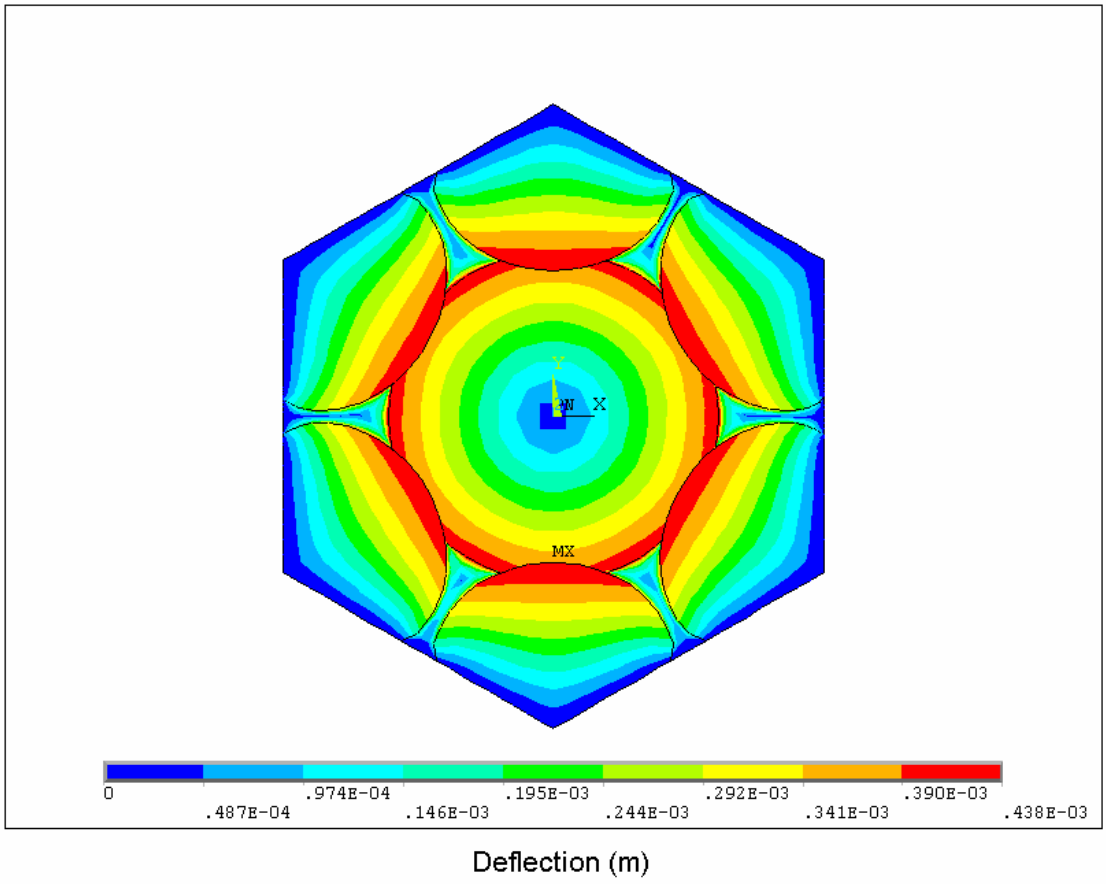

Figure 6.12: The finite element model predictions of the local deflections within the solenoid coil resulting from thermal expansion (for 1 Amps)

6.1.2 Theoretical Design of Reliability Test

The finite element model can now be used to make theoretical predictions of solenoid valve operational parameters which affect reliability, such as temperature, stress and strain. These predictions are useful to then design the test loads and conditions which may cause failure in the solenoid valve. First, to increase the severity of the test

and to model realistic temperatures seen in the transmission, the air temperature in the model is increased to 80°C. It was observed that when the solenoids were run at room temperature it was difficult to obtain failure. Changing the ambient temperature to 80°C can be accommodated by making a simple change in the model boundary conditions.

The finite element model is then used to generate results over a wide range of applied currents (see Figs. 6.13 and 6.14). Based on the FEM predictions, a test procedure can be designed to bring the temperature of the solenoid valve coil near to the critical operating temperature of the polyamide-imide insulation (approximately 200°C [29]).

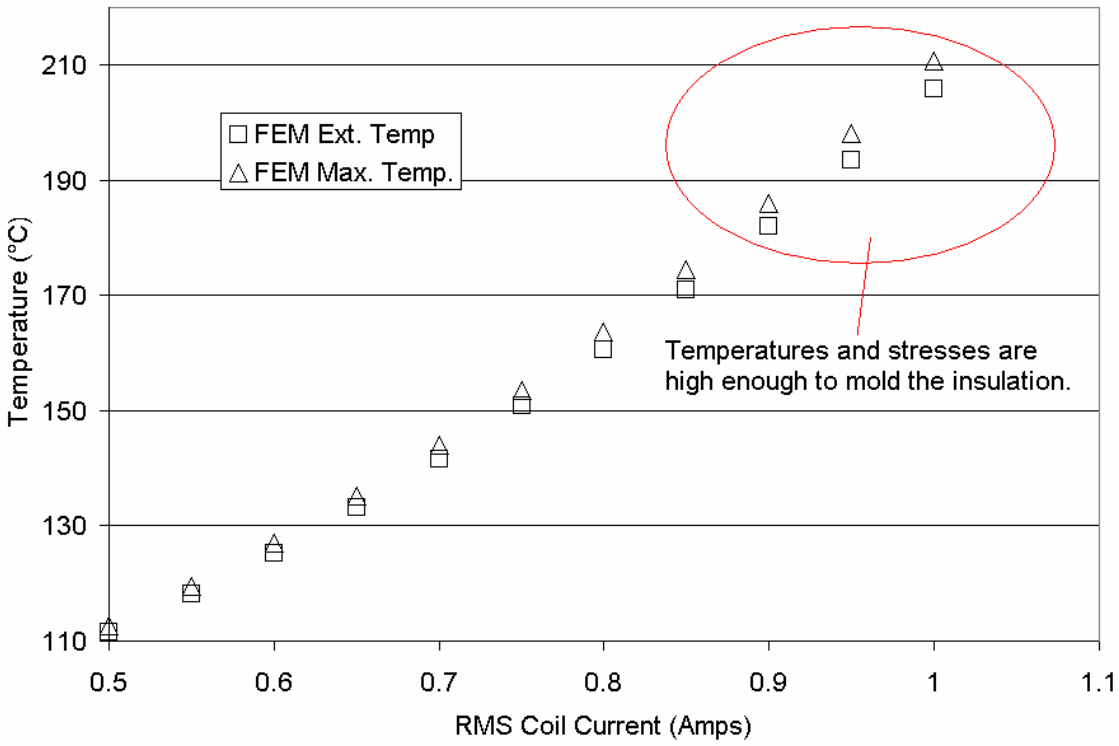

Figure 6.13: The FEM predicted temperature in the coil and on the external surface of the solenoid valve

The applied RMS current was varied between approximately 0.5 Amps and 1 Amps and the external and maximum temperatures were recorded (see Fig. 6.13). Once again the temperature increasing with current was expected. Also, the difference between the maximum temperature and the external temperature that would be measured by the thermocouple is very small. Based on these predictions, the temperatures in the coil can rise to values that are above what is recommended for the insulation. In addition, at these temperatures, it is expected that the stresses within the solenoid coil wire should be very high due to thermal expansion (see earlier section on the local wire model).

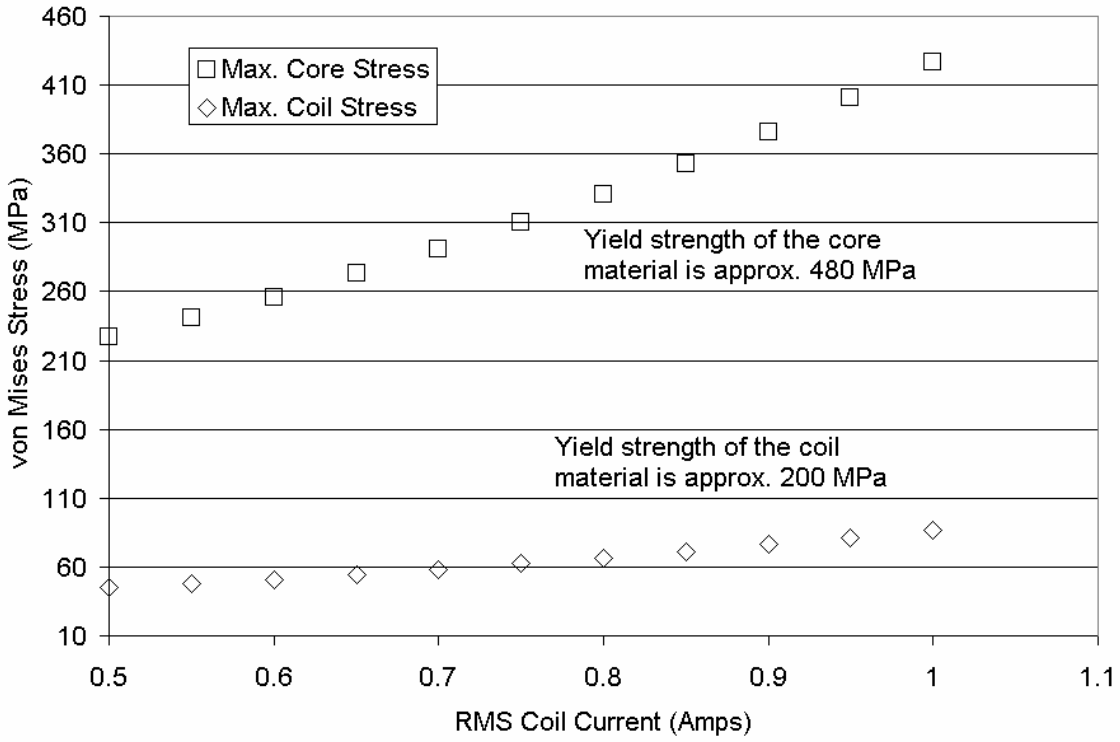

Figure 6.14: The maximum stresses predicted by the finite element model

The stresses under these elevated conditions (80°C ambient temperature) are predicted to be significantly higher than the room temperature case (see Figs. 6.8 and

6.14). However, it should be remembered that these predicted stresses are expected to be heavily influenced by the machining tolerances of the parts. Still, these high stresses, especially within the coil, are expected to influence and assist the failure of the solenoid valve. These stresses in combination with the elevated temperatures will essentially form and mold the insulation present in between the wires. Signs of these high compressive stresses have been seen in all the run solenoid valves, even the ones that did not fail (see Figs. 6.36-6.39). The wires in the solenoid coil appear to change from a round cross section to a hexagonal shape due to the high compressive stresses (see Experimental Results section).

The experimental test procedure used in the current analysis was devised based on the elevated temperatures and stresses seen at certain applied currents when the ambient temperature is raised. To further evaluate solenoid performance under these conditions, the finite element predicted temperature and stress distribution for the most severe case modeled (1 Amps) are presented (see Figs. 6.15 and 6.16).

In Fig. 6.15, the predicted temperature distribution for 1 Amps and 80°C ambient temperature is shown. Note that the temperature is only about 5°C higher in the coil than on the outer surface where the thermocouples are located in the test apparatus. The maximum temperature is located in the coil where the Joule heating is present. The plastic material around the coil is also heated considerably, which is also noticed in the experimental results. During an experiment, the plastic material surrounding the coil actually melts and exits the solenoid valve when failure occurs.

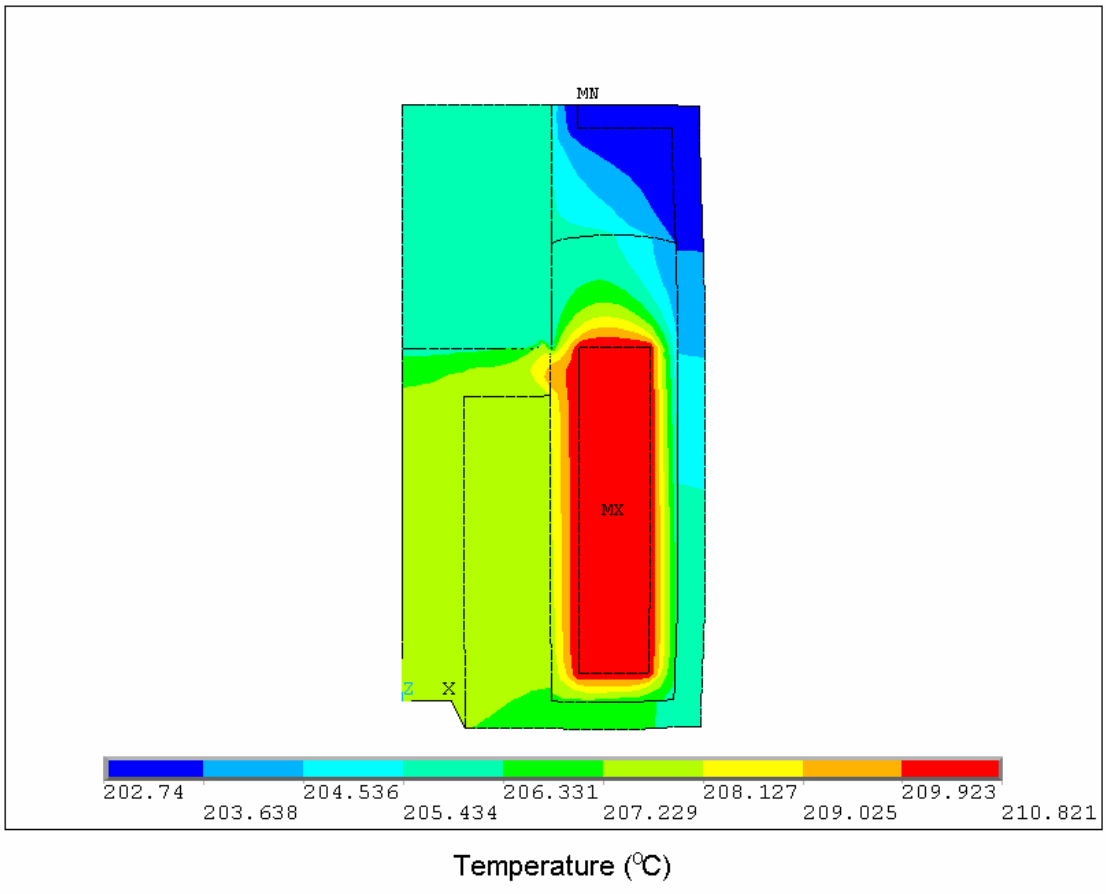

Figure 6.15: The predicted temperature distribution in the solenoid cross section for 1 Amps of current and 80°C ambient temperature

The predicted von Mises stress distribution for this same extreme case is shown in Fig. 6.16. The stresses are greatest in the steel core and outer casing of the solenoid valve. However, the stresses within the coil are still elevated and could cause the insulation to fail under compression.

In summary, the finite element model results suggest that the solenoid valve will fail due to a thermal-mechanical failure of the insulation between the solenoid coil wires. It is expected that if a high enough ambient temperature and RMS coil current is applied then the temperatures and compressive stresses will be sufficient to soften or melt the

insulation enough to move it from between the copper wires. The copper wires would then short out and cause the resistance in the coil to drop. This would result in the solenoid coil magnetic force being reduced and perhaps fail to actuate the valve. These theoretical predictions will be experimentally confirmed in the following section.

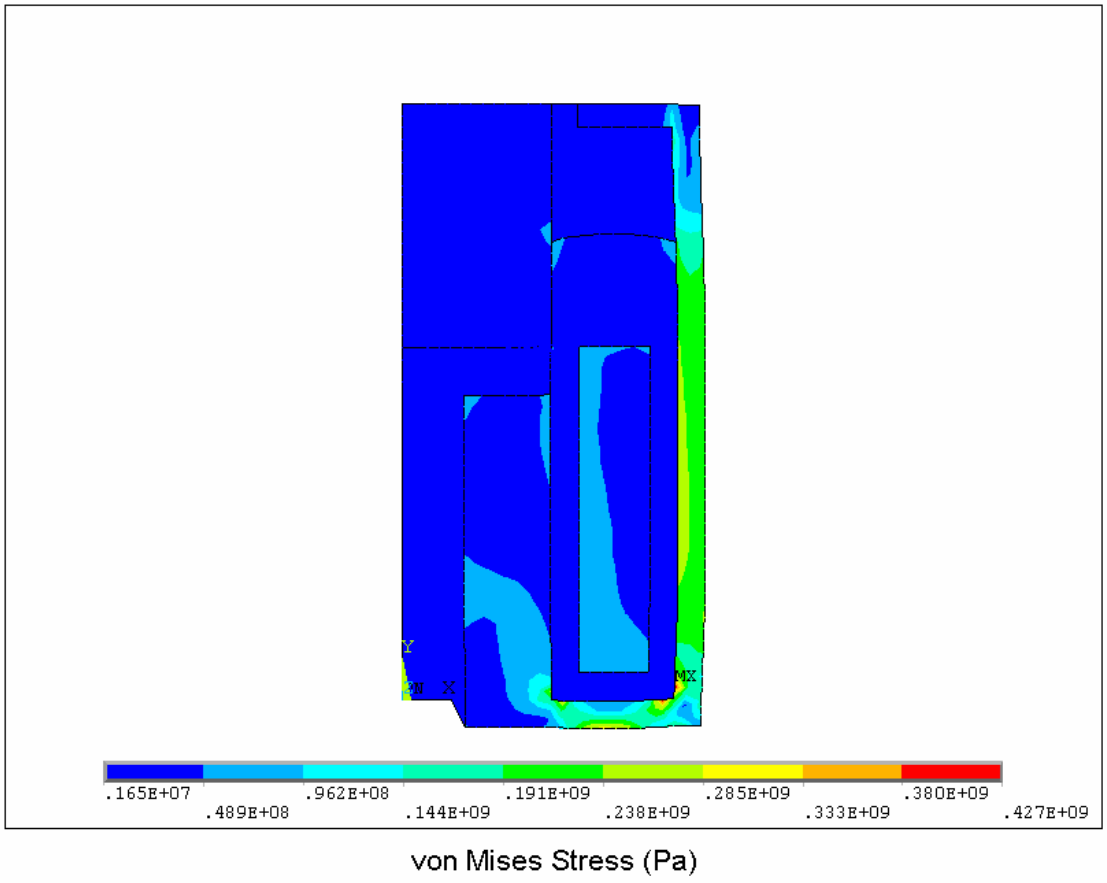

Figure 6.16: The predicted von Mises stress distribution in the solenoid cross section for 1 Amps of current and 80°C ambient temperature

6.2 Experimental Results

A total of 22 solenoid valves are tested for a maximum period of 24 hours at a temperature of 100°C in a thermal chamber, 16.8 V of average peak voltage, 50% duty cycle (DC) and 60 Hz of cycling frequency. Originally the tests were run at a 80°C ambient temperature but failure was not occurring at a sufficient rate so the ambient temperature was increased to 100°C. A 24 hour test implies that the solenoid valves are scheduled to run for 5,184,000 (approximately five million) cycles in 24 hours with no failure.

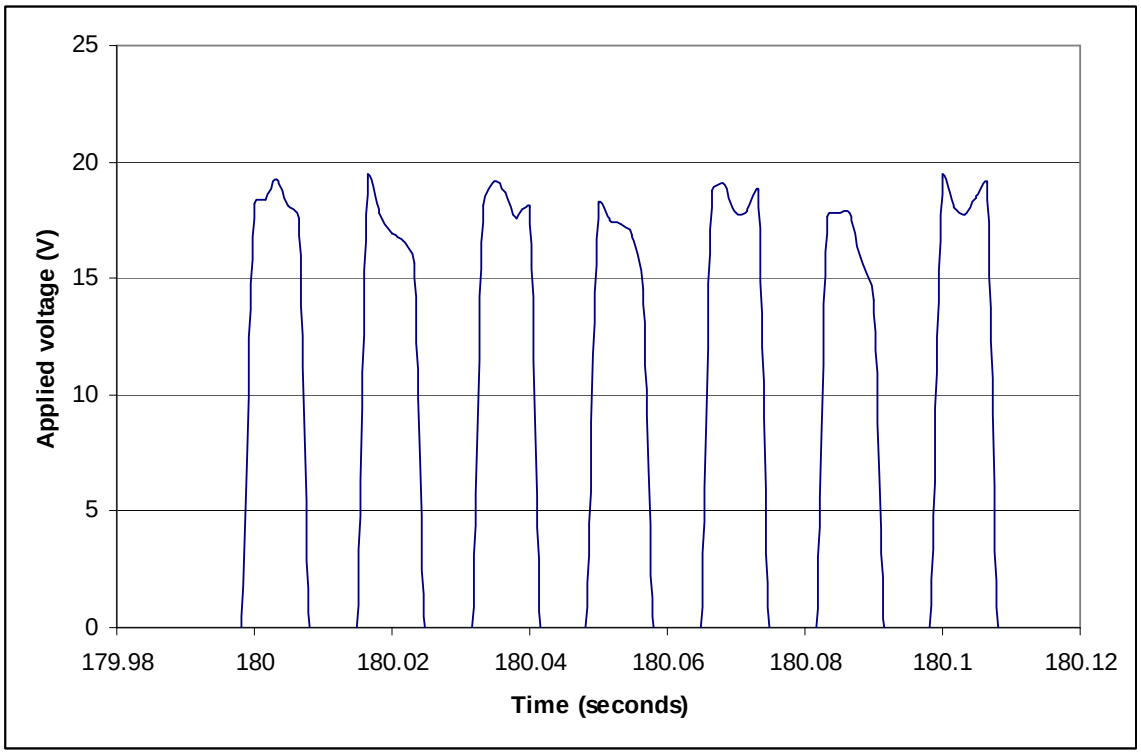

Figure 6.17: Variation of actuation voltage with time for a solenoid valve in operation

A sample of the voltage and current waveforms (providing the applied voltage and current for all the solenoid valves) generated during testing of the solenoid valves are displayed in Figs. 6.17 and 6.18. From Fig. 6.17, it can be noticed that the applied average peak voltage during the tests is 16.8 V. In addition, the waveforms are not perfect square waves, but are similar to what the solenoid valves would bear in an actual application.

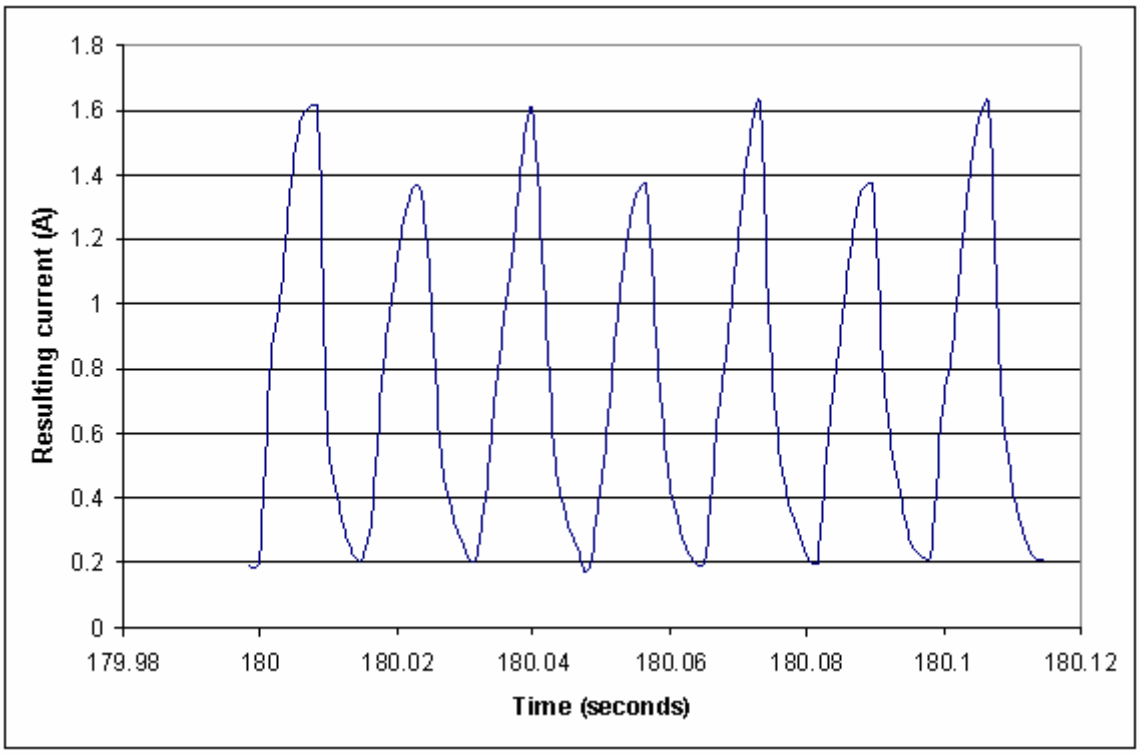

Figure 6.18: Variation of actuation current with time for a solenoid valve in operation

The recorded actuation current is also shown in Fig. 6.18. As was also shown for lower actuation voltages in Chapter 4, the actuation current lags the actuation voltage. Once the voltage is actuated, the current increases at a reduced rate to the expected

current which is equal to the voltage divided by the resistance. This is due to electrical inductance in the solenoid valve and power lines.

Although a total of 22 solenoid valves are tested, Figs. 6.19-6.22 show the current, the calculated running average of the current, and the measured temperature as a function of time for 4 of the solenoid valves. Figs. 6.19 and 6.21 show peak current and maximum temperature values at which complete failure has occurred for 2 valves, whereas Figs. 6.20 and 6.22 show the current, running average and temperature data for a completely failed valve and for a valve where no failure has occurred. It is clearly evident that solenoid failure is marked by a sudden increase in temperature and current. Once failure occurs the solenoid valve ceases to actuate and the protective fuse blows causing the applied current and voltage to reduce to zero. These clear failure points are used to extract the time to failure for each solenoid valve. A detailed set of the extracted results and observations on all solenoid valves tested in this work is included in the following sections (see Table 6.1).

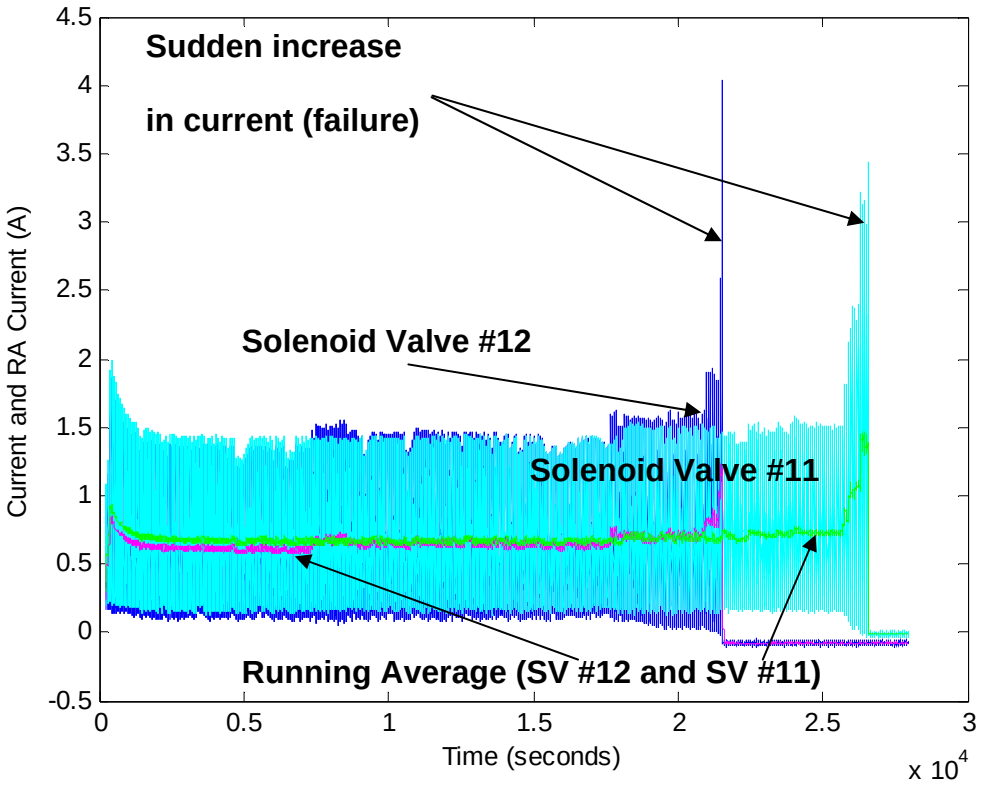

Figure 6.19: Variation of applied current and running average for current as a function of time for 2 completely failed solenoid valves

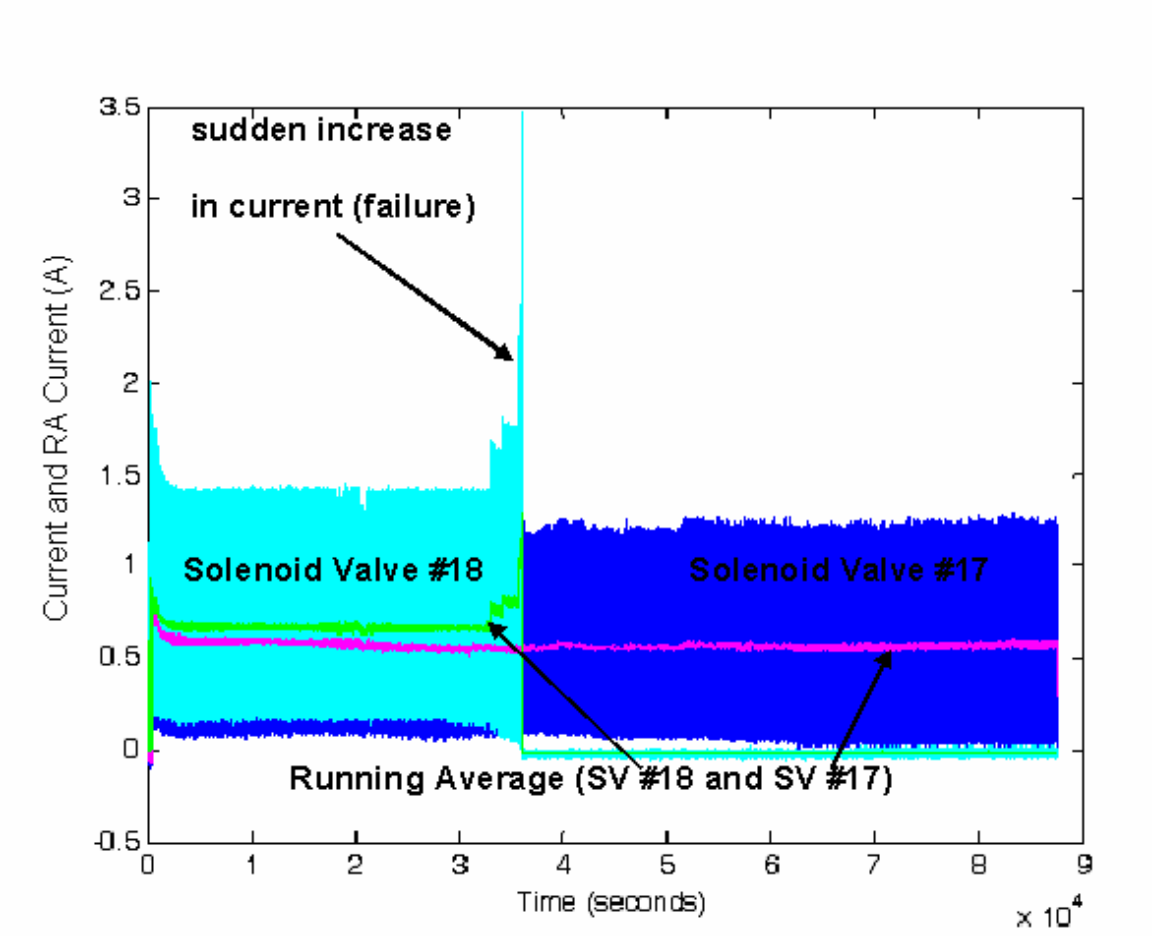

Figure 6.20: Variation of applied current and running average for current as a function of time and also showing one completely failed solenoid and one solenoid that did not fail

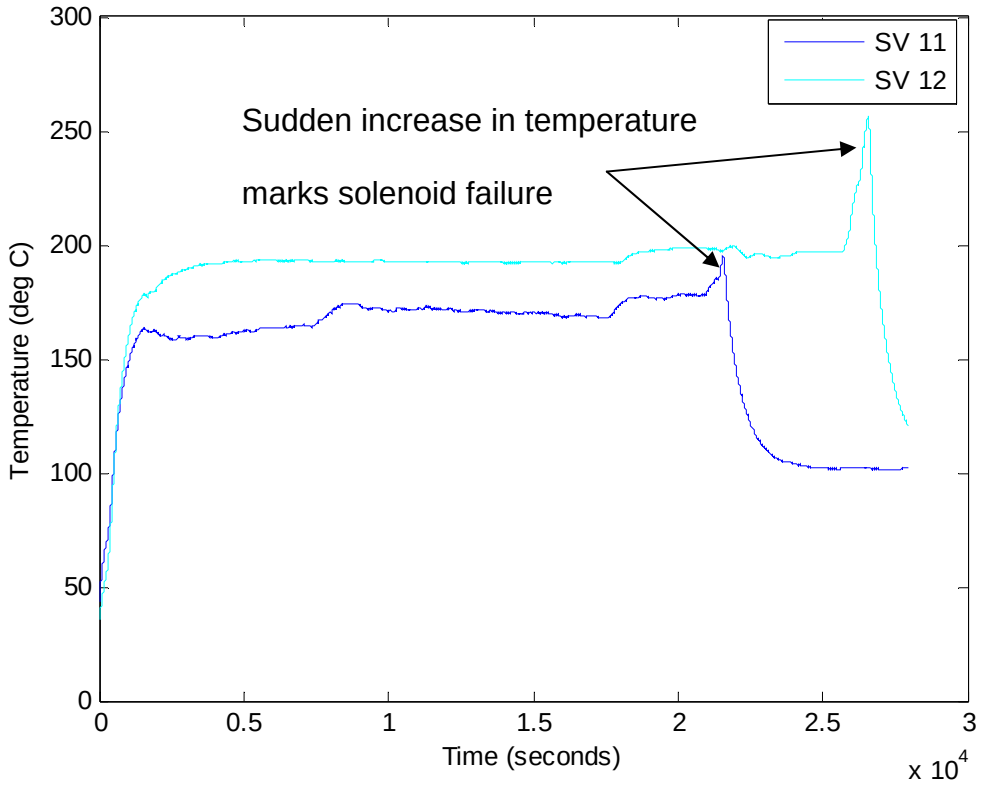

Figure 6.21: Variation of temperature with time for 2 completely failed solenoid valves

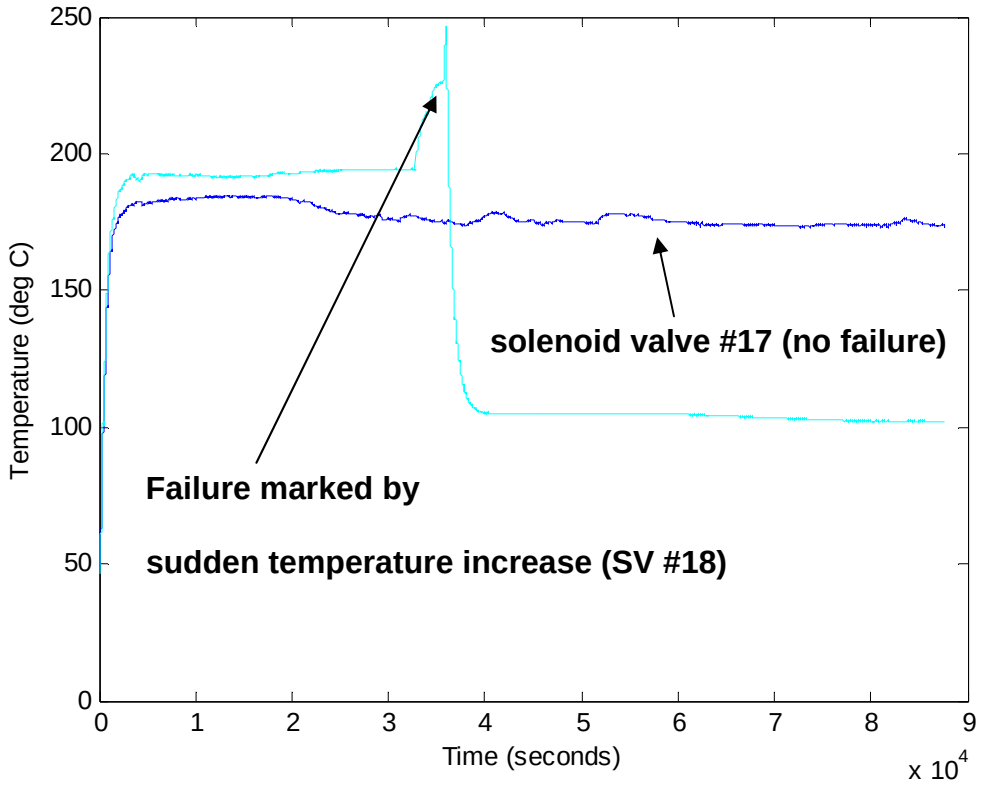

Figure 6.22: Variation of temperature with time for one completely failed solenoid and one solenoid that did not fail

6.2.1 Direct Solenoid Coil Temperature Measurement

As discussed in the Experimental Methodology, the temperature is measured during a test using thermocouples that are pressed against the outside of the metal casing of the solenoid valve near the coil. Based on the reported finite element results, it is believed that these external temperatures are very close to the coil temperature. To confirm this, the solenoid coil can be used as a thermistor to measure temperature. As the temperature increases, the coil wire will expand and lengthen, thus causing a measurable increase in the electrical resistance. However, this measurement cannot be made easily while the solenoid valve is in operation. In the current work, the resistance of the

solenoid valve was measured before and immediately following a test. These resistances were then used to confirm the coil temperature. The dependence of resistance on temperature is given by the following equation [30] :

$$R = R_{ref}(1+\alpha(\Delta T)) \tag{6.2}$$

where

R = Resistance (Ω) at a given temperature, (T) ($^{\circ}$C)

R_{ref} = Resistance (Ω) at reference temperature, T_{ref} ($^{\circ}$C) (generally 20 $^{\circ}$C), that is, 3.4 Ω

α = Temperature coefficient of resistance for a given material (For copper, the material used as conductor in solenoid coil, the value of α is 0.004041 /$^{\circ}$C)

ΔT – Difference between T and T_{ref}

A plot of resistance versus the temperature is thus shown in Fig. 6.23. The trend confirms that the method is very effective at measuring the coil temperature and that the coil temperature is nearly the same as the external temperature of the thermocouple. It is seen that in this work for a particular value of temperature (for example, 80 $^{\circ}$C) the measured experimental value of resistance through E type thermocouple using a multimeter is 4.2 Ω. The theoretical and experimental values match precisely when the above equation is used to find resistance at 80 $^{\circ}$C and for α = 0.004041 /$^{\circ}$C. Similarly, for various temperatures, the resistance measured by the thermocouple and that calculated from the above equation match very closely.

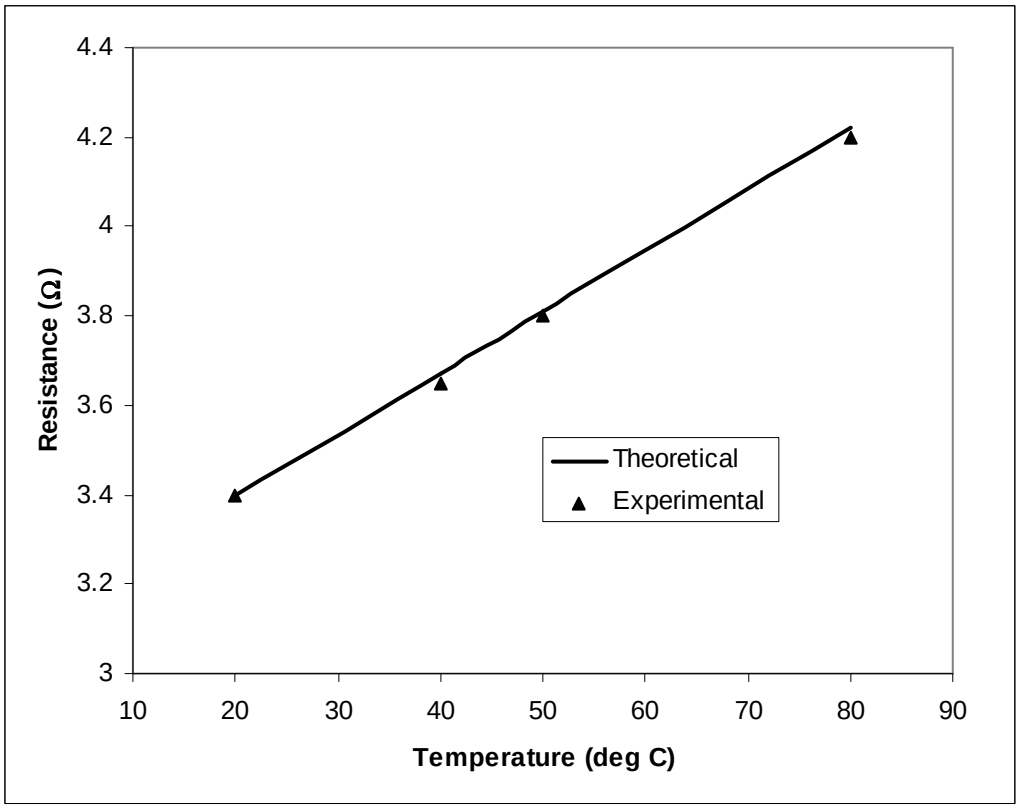

Figure 6.23: Variation of resistance with temperature

6.2.2 Categorization of Results

As shown in the previous sections, the tests in this work have succeeded at producing a controlled failure of the solenoid valve. However, due to manufacturing tolerances and experimental inconsistencies, the solenoid valves do not fail at precisely the same moment and for the same conditions. It has been observed that the tested solenoid valves can be categorized into three types:

a. Solenoid valve run for 24 hours (no failure)

b. Partial failed solenoid valve but still actuating for 24 hours

c. Completely failed solenoid valve

These three categories are also represented in many of the following plots of the data. In addition, differences in the solenoid wire cross-section after a solenoid has failed can be observed. This is shown in sections 6.2.3 and 6.2.4.

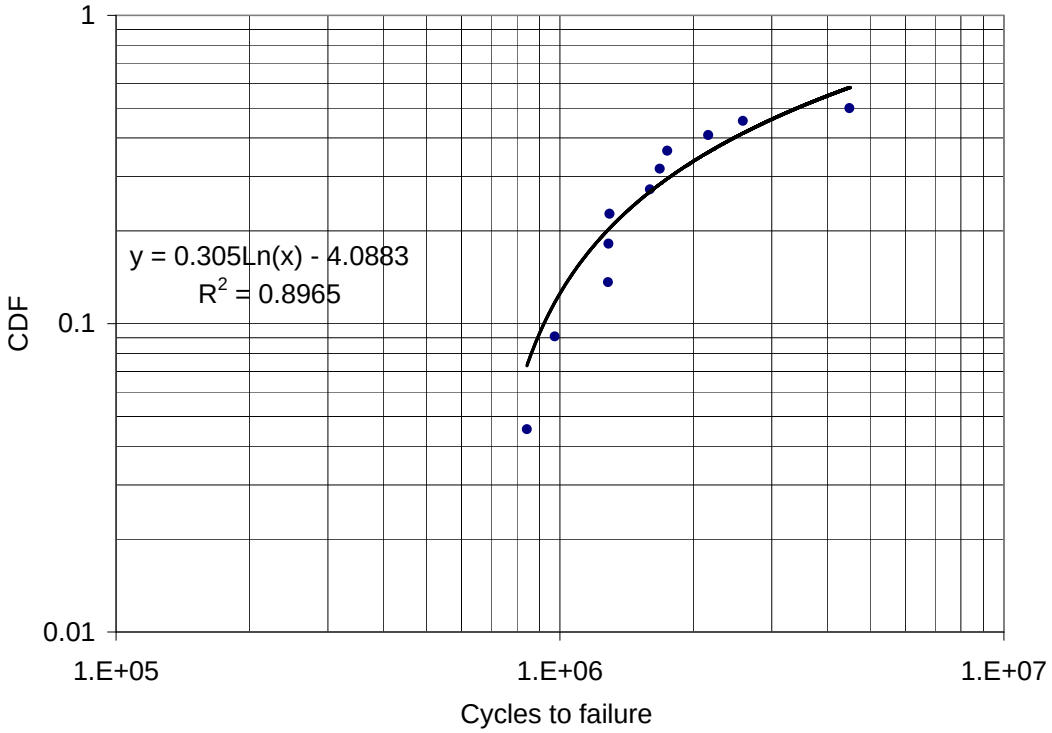

Figure 6.24: The calculated experimental cumulative density function for failure of the solenoid valves

6.2.3 Analysis of Results

The cumulative density function (CDF) is used extensively to test or study the reliability of components and thereby predict life of components. Essentially, a CDF will show the percentage of solenoid valves which have failed for a given number of cycles. Fig. 6.24 shows the calculated experimental CDF and the cycles to failure for the solenoid valves. In this plot, only the data for the solenoid valves that have either

partially or completely failed have been considered. Fig. 6.24 signifies that the probability for failure of SVs increases as the cycles to failure increase.

The calculated CDF appears to show that the failure rate does not follow a Weibull distribution**.** Rather, the failure rate appears to level-off as the number of cycles is increased. A logarithmic function is fit to the CDF data that might be used to make rough approximations for solenoid reliability. Many studies find that a Weibull equation provides a good fit, but that is not the case here. This suggests that failure may not be due to a fatigue mechanism. The current analysis actually finds that the failure of the tested solenoid valve is correlated better with the maximum temperature. This confirms the theory that the failure mechanism is a thermo-mechanical one that occurs when the temperature and stress are large enough to cause the insulation to fail and the coil wires to short.

The tests on all the tested SVs (a total of 22 SVs) are conducted for 24 hours. However, SV 15, 23, 29 were prematurely stopped before the full 24 hours. This might be because other solenoid valves in the same test (SV 16, 24, 30) failed quickly (in the range of 6-10 hours) and so unexpectedly the power supply became switched off. 19 solenoid valves are either run for full 24 hours with no failure or run until they exhibit either partial or complete failure.

Solenoid Valve	Maximum Temperature (deg C)	Number of cycles (N)	Δ Resistance (Ω)	Peak Current (A)	Status
9	178	4487400	0.6	1.58	Partial Failure
10	181	5248800	0	1.46	No Failure
11	197	1292820	1.7	4.04	Failure
12	256	1594080	1.7	3.43	Failure
13	172	5184000	0	1.26	No Failure
14	269	2582400	2.1	2.97	Failure
15	176	1744320	0	1.36	Incomplete
16	223	1744320	0.5	1.7	Partial Failure
17	176	5257500	0.1	1.23	No Failure
18	246	2157660	1.8	3.47	Failure
19	173	5342280	0.1	1.27	No Failure
20	197	5342280	0.1	1.39	No Failure
21	171	5235600	0.1	1.21	No Failure
22	301	1678440	1.7	2.94	Failure
23	161	1283100	0.1	1.21	Incomplete
24	265	1283100	0.8	5.44	Failure
25	171	5197740	0	1.29	No Failure
26	274	1286520	1.5	3.43	Failure
27	153	5244540	0	1.27	No Failure
28	255	972960	1.9	3.48	Failure
29	174	842460	0	1.27	Incomplete
30	227	842460	2.1	2.88	Failure

Table 6.1: Solenoid valve recorded and calculated/measured data for 100°C ambient temperature, 50% duty cycle, 60 Hz actuation frequency, 16.8 V actuation voltage

From the solenoid tests, four key outputs are extracted for all valves (see Table 6.1). These key outputs are the maximum temperature reached during tests, the number of cycles run, the Δ Resistance (the change in resistance) and the peak current observed at failure or at the end of a 24 hour test. The key parameters are taken into account in analyzing the performance of solenoid valves and to study their reliability, and thus to predict and find ways to improve the reliability and the life of SVs tested in this investigation.

In each of the following 4 plots (see Figs. 6.25 to 6.28), the tested SVs are categorized into (a), (b) and (c) types. All the plots clearly exhibit a common trend that illuminates our fundamental understanding about the solenoid valve reliability, performance, and behavior when they are subjected to accelerated operating conditions and temperatures. As will be discussed further, this common trend also indicates and defines the failure mechanism of the solenoid valves This will then help in prediction of life (defined as how many cycles they run without failure) of solenoid valves and methods to further improve reliability and performance of solenoid valves. To understand the failure mechanism even further, a visual inspection of the tested solenoid valves is also presented later in this work (see section 6.2.4).

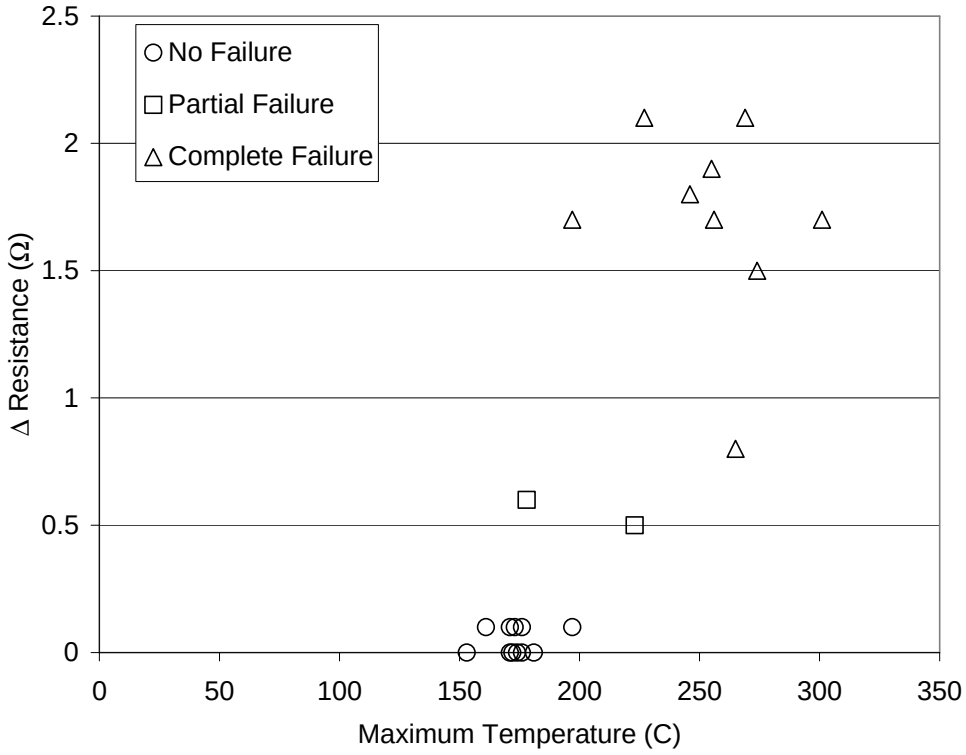

Figure 6.25: Variation of change in resistance in relation to the maximum temperature for the tested solenoid valves

Fig. 6.25 shows a clear change in the electrical resistance of solenoid valve with respect to the maximum temperature reached during each test. The resistance of each new SV measured before testing is 3.4Ω and each wire of a solenoid coil is insulated from all nearby wires by a thin polyamide-imide insulation. The melting point of the insulation material (polyamide-imide) used in the solenoid coil is approximately 200°C [29]. Therefore it is believed that if the temperature and stresses in the coil are high enough, then the solenoid insulation will fail. The drop in resistance means that the solenoid valve coil wire has shorted so that the current can bypass significant portions of the coiled wire. For most of the valves that belong to the (c) case (complete failure), the

change in resistance is high (there is a drop in resistance from the original 3.4 or 3.5 ohms for a new solenoid valve to a very low value varying in the range 1.2 to 2.5 ohms).

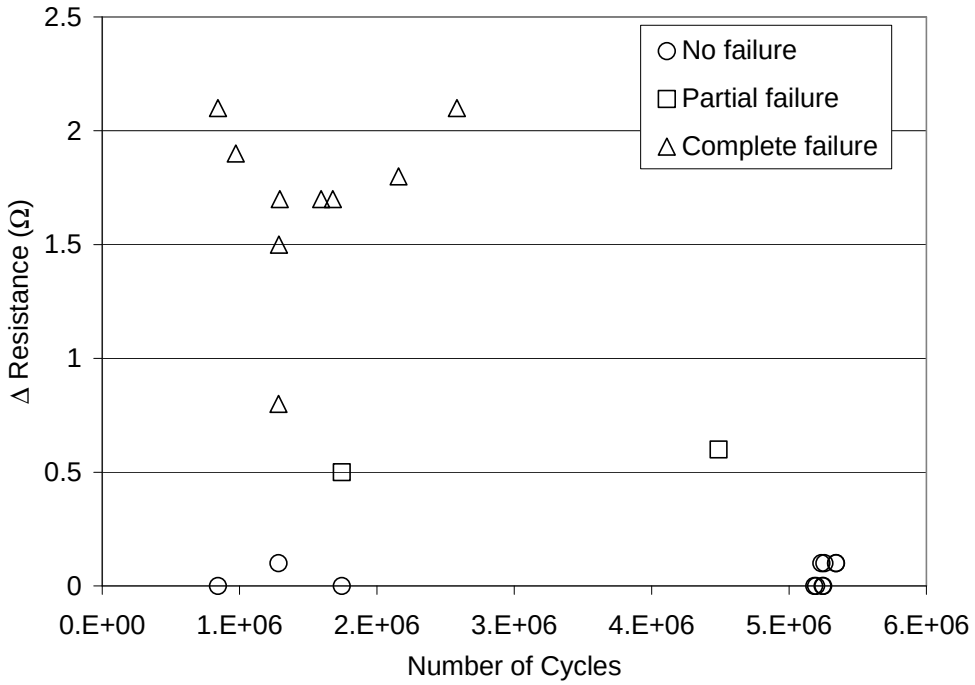

Figure 6.26: Variation of change in resistance Vs number of cycles for the tested SVs

The change in resistance is also shown as a function of the number of cycles in Fig. 6.26. The results show that for the failed solenoid valves almost a million cycles or more were still required for failure to occur. This suggests that the failure may also be a cyclic process as the wire insulation is slowly degraded over many cycles of operation. However, it also appears that many solenoid valves survive for many millions of cycles without reaching failure. Surprisingly, in this work for all the valves tested for more than 5 million cycles ((a) case valves), there were no signs of failure which is validated by

extremely small changes in resistance of the order of 0 to 0.2 ohms, even after the valves were cycled for 24 hours. It could be that there are differences in the manufacturing tolerances of the solenoid valves that allow some valves to operate for longer before failure. The performance of (a) type of valves clearly proves the well established fact that many SVs run for very long durations to the order of many years without failure when operated at the rated operating conditions. In contrast, the current tested SVs are subjected to more severe operating conditions (16.8 V average peak voltage, 100 deg C, 50 % DC, etc.) and are made to run in these conditions for atleast a period of 24 hours (that is, approximately 5 million cycles). Despite this, many of them run well even after 5 million cycles while being exposed to these operating conditions (the accelerated test conditions). The problem is some of them do fail, and it appears to be significant portion.

An interesting observation is that the sound level or tone of actuation emitted by the solenoid valves was lowered to a good extent during their testing, even for those that did not fail. All the 22 SVs tested in this work (note that these valves are tested at 60 Hz cycling frequency) produced a very distinct well heard clear actuation sound at the start of each test. Perhaps, there is a run-in period where the sound level is higher, but with additional wearing in, the parts start operating more efficiently. It is often observed in the testing of mechanical components that during this wear-in period many components will fail, but those that survive then have very long lives. This could explain what is being observed in the current tests of solenoid valves.

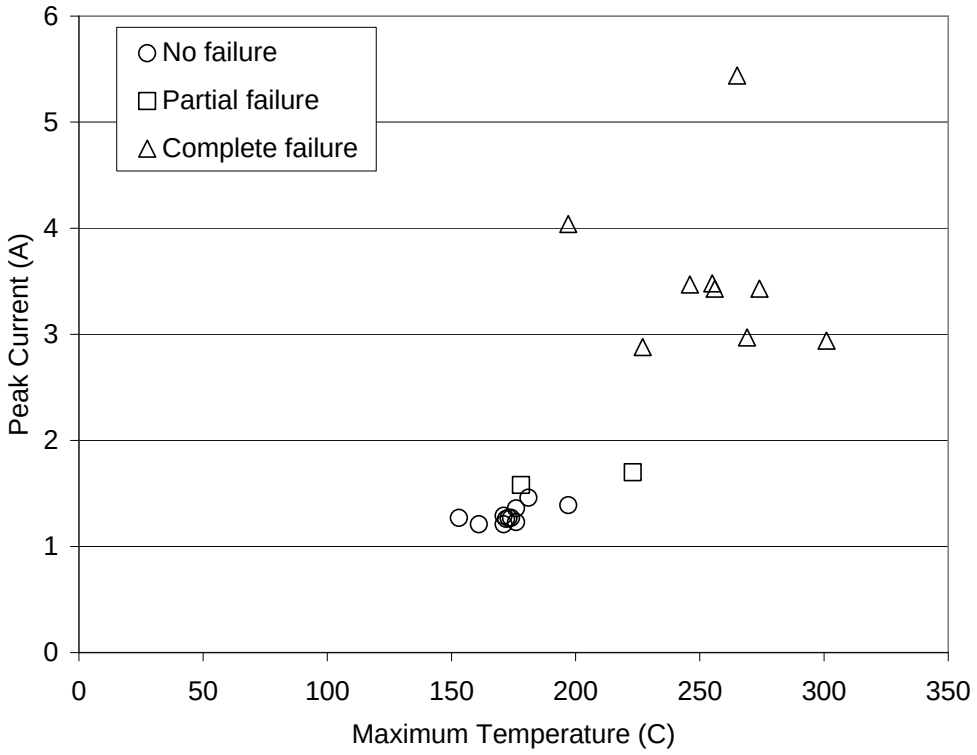

Figure 6.27: Variation of peak current as a function of maximum temperature for the tested SVs

From Figs. 6.25 and 6.27, for the reasonable ambient temperatures of 100°C and applied electrical loads, it is observed that these valves are subjected to high temperature (in the range of 200 to 300°C) which is well above the melting point of the coil insulation. Figure 6.27 also presents perhaps the best correlation of data and the clearest indicator of failure. The peak current of the completely failed solenoid valves are all above a value of approximately 2.8 Amps and there also appears to be a separation of the data at approximately 200°C. Initially, for each of the valves when it begins to operate, the applied peak current is approximately 1.3 to 1.4 Amps, but this applied peak current increases in gradual steps until point of complete failure occurs due to a corresponding

gradual drop in the resistance of SV to a very low value (Table 6.1). The valves have then been exposed to extreme temperatures that eventually cause complete failure as the coil insulation starts to melt (see Fig. 6.38) which causes shorting of the solenoid coil copper wires due to lack of insulation between them. At complete failure, there is also considerable thermal expansion and deflection in the coil region or wire cross section (see Figs. 6.35, 6.37 and 6.38). In fact, due to melting, the coil wire can separate from the insulation, and show the presence of pores or vacant spots in and around the coil region (see section 6.2.4). The wire cross section of the (a) case solenoid valves (non-failure) shows none of the observations noted for the (c) case. Instead, in an expected manner, these samples exhibit a neatly arranged close packed helical wound coil structure [31] of a SV with a thin layer of polymer insulation clearly seen between all the copper wires. This is typical of any solenoid valve that has not shown any signs of failure.

Only 2 partial failures (type (b)) of the solenoid valves have been achieved in this work out of 22 valves tested. In all the 4 plots, these partial failures appear in between the data points of the (a) and (c) cases. The change in resistance value (see Fig. 6.26) is quite low compared to the (c) cases, likewise the peak current (Fig. 6.27) and the maximum temperature attained during each test (see Figs. 6.25, 6.27, and 6.28) are lower, and the number of cycles to failure (see Figs. 6.26 and 6.28) are higher than those achieved or shown by the (c) cases. However, similar to the (c) case samples, when the cross section of the wire region is examined under a microscope for the (b) cases, moderate thermal expansion or localized bulging out of the cross-section of wire is observed**.** A lack of insulation between the two copper wires exists, thus causing shorting. However, these regions are usually localized and less severe for the (b) case than for the (c) case. Due to

shorting only, the resistance has dropped from the original values of 3.4-3.5 ohms to 2.9 ohms in both the 2 partially failed solenoid valves. There is also disorder of the wire arrangement in both the partially (intermediate disorder) and the completely (excessive disorder) failed solenoid valves which is not present in the (a) case. Therefore, these valves are classified as partial failures due to low change in resistance, still successful solenoid actuation, and limited melting of insulation.

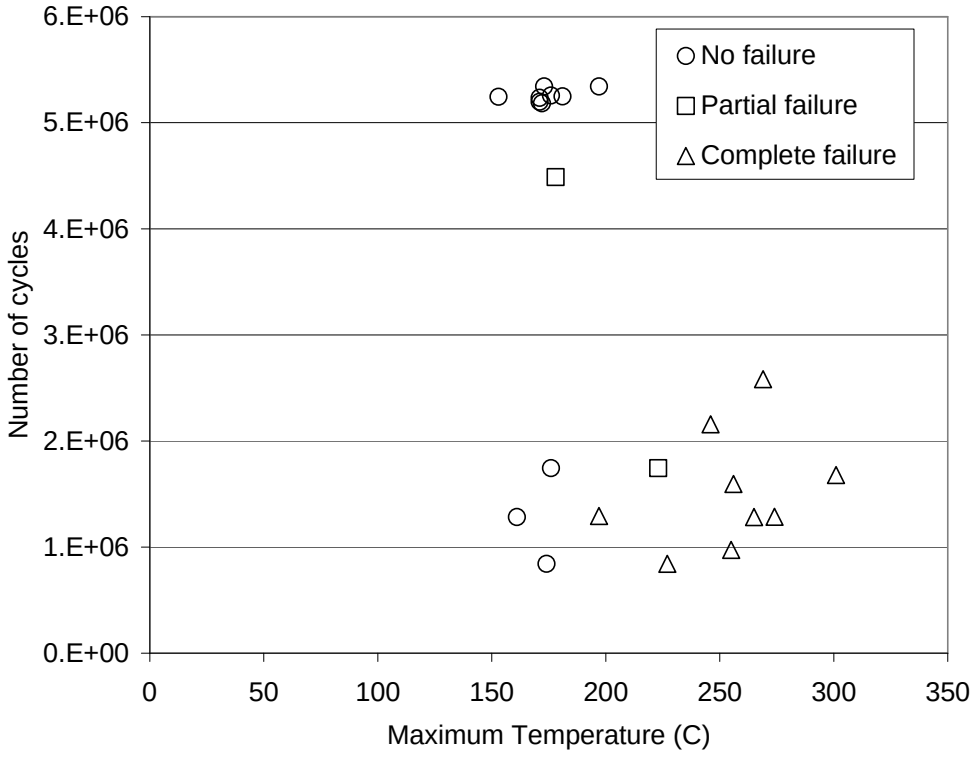

Figure 6.28: Variation of number of cycles as a function of the maximum temperature for the tested solenoid valves

Fig. 6.28 shows the variation of the number of test cycles as a function of the maximum temperature reached for all SVs. From this it shows that the higher maximum temperatures reached by the solenoid valve might be due to high peak currents. Then, these high peak currents are in turn probably a result of the large drop in resistance of the

solenoid valve from 3.4 to 3.5 ohms to the range of 1.2 to 2.5 ohms. Since these lower resistances are caused by high temperatures, there does seem to be a viscous cycle that the solenoid valve may enter once the threshold of failure is reached. Alternatively, the solenoid valves subjected to moderately high temperatures in the range 150 to 185°C run extremely well for at least 5 million cycles (that is, approximately 24 hours) with no signs of failure and therefore these tests belong to the (a) category.

From Figs. 6.25 to 6.28, for the (c) case, there are clear signs of failure and severe operating conditions. Namely, these are the very high peak currents and the corresponding rises in temperatures in the solenoid coil to a value greater than the melting point of the insulation. Together these will lead to large changes in resistance values and thus complete failure of solenoid valves. This analysis thus provides a clear indication of the failure mode and failure mechanism. This result will then assist in the prediction of life and the improvement of the reliability of solenoid valves.

6.2.4 Visual Analysis of Failure Mechanism

As mentioned earlier, based on the occurrence of failure or no failure, the solenoid valves tested in this work are classified into three types. For each of the (a), (b) and (c) cases, photographs are taken at three perspectives, namely, the macroscale external view (for outer structure of the solenoid valves), the macroscale cross-section and the microscale cross-section. The macroscale level view of the external solenoid valve and cross-section was photographed simply using a digital camera. The microscale level photographs of the cross-section were taken using a digital camera mounted on a microscope. The cross-sections of the solenoid valves were obtained by cutting open

several of the tested solenoid valves. The solenoid valves were cut using a band saw and hand saw. The surfaces of the cross-section were then ground smooth.

The following photographs (Figs. 6.29-6.39) of the (a), (b) and (c) cases show very clearly the variation of damage to the coil, insulation material between the copper wires and the plastic material that surrounds the coil structure due to the high applied currents and thus high temperatures. It can be observed that the maximum or most intense coil damage is present for the (c) case and relatively no damage imparted to the coil of the (a) case solenoid valves.

Figure 6.29: A macroscale photograph of a SV belonging to (a) case
(the solenoid valve was run for 24 hours without failure)

Figure 6.30: A macroscale photograph of a solenoid valve belonging to (b) case (partially failed but still run for 24 hours)

For the (a) and (b) cases (see Figs. 6.29 and 6.30), where both are run for 24 hours and about 5 million cycles, the outer structural appearances of the valves are similar. The presence of a brownish color is observed over most of the outer region of the valves since the outer casing of the valves is made of iron (due to iron oxidation and exposure to extreme temperatures in the range 150 to 200°C) unlike the silver color of the valves seen prior to testing. In addition, some bluish discoloration of the surfaces can also be seen due to the high temperatures that are encountered. In contrast, for the (c) case valves (see Figs. 6.31 and 6.32), along with the discoloration in the outer structure, plastic material is seen oozing or coming out of valve due to exposure to very high temperatures in the range of 200-250°C. The color of the type (c) failed solenoid valve is also bluer than the

other samples, indicating the occurrence of higher temperatures. Again, the existence of extreme temperatures in the valves is due to the applied current and the build up of Joule heat in addition to the heat in the ambient air of the thermal chamber.

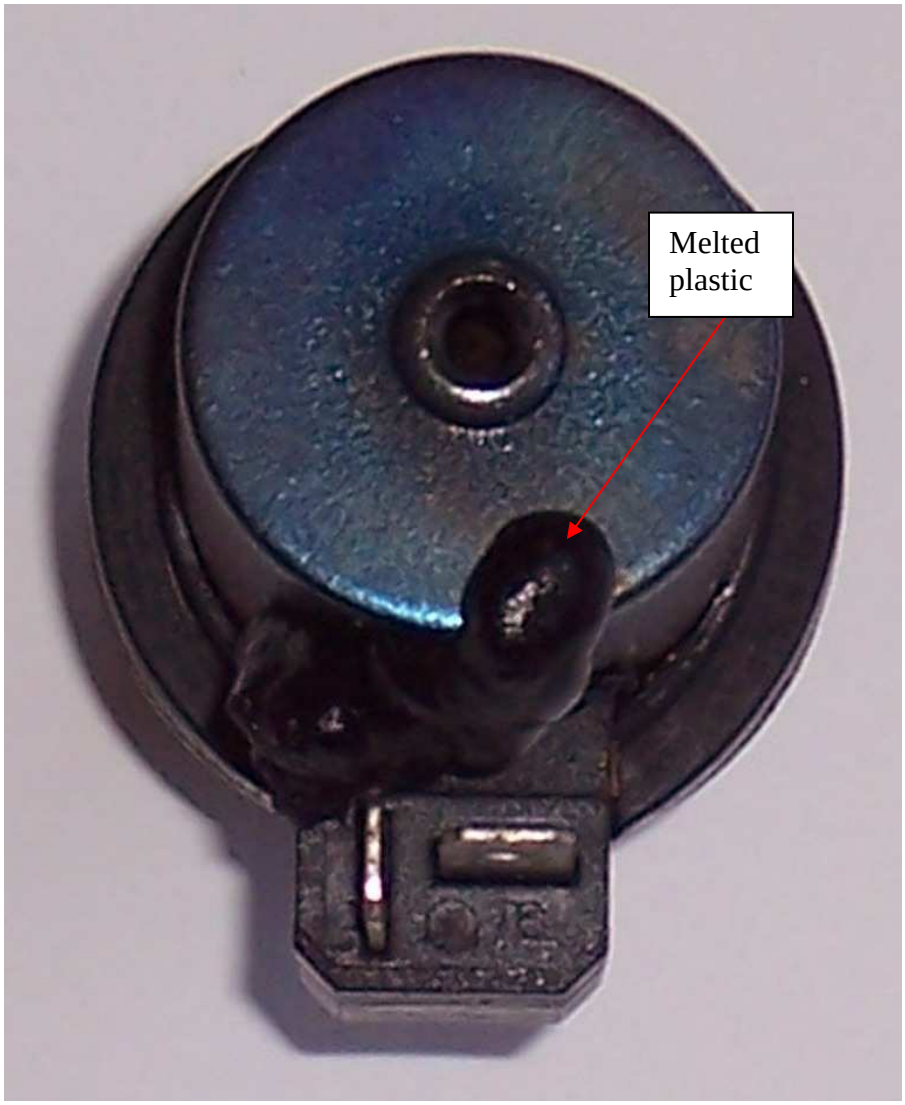

Figure 6.31: Macroscale photograph of a solenoid valve belonging to the (c) case (completely failed)

Figure 6.32: Macroscale photograph of a solenoid valve belonging to the (c) case (completely failed)

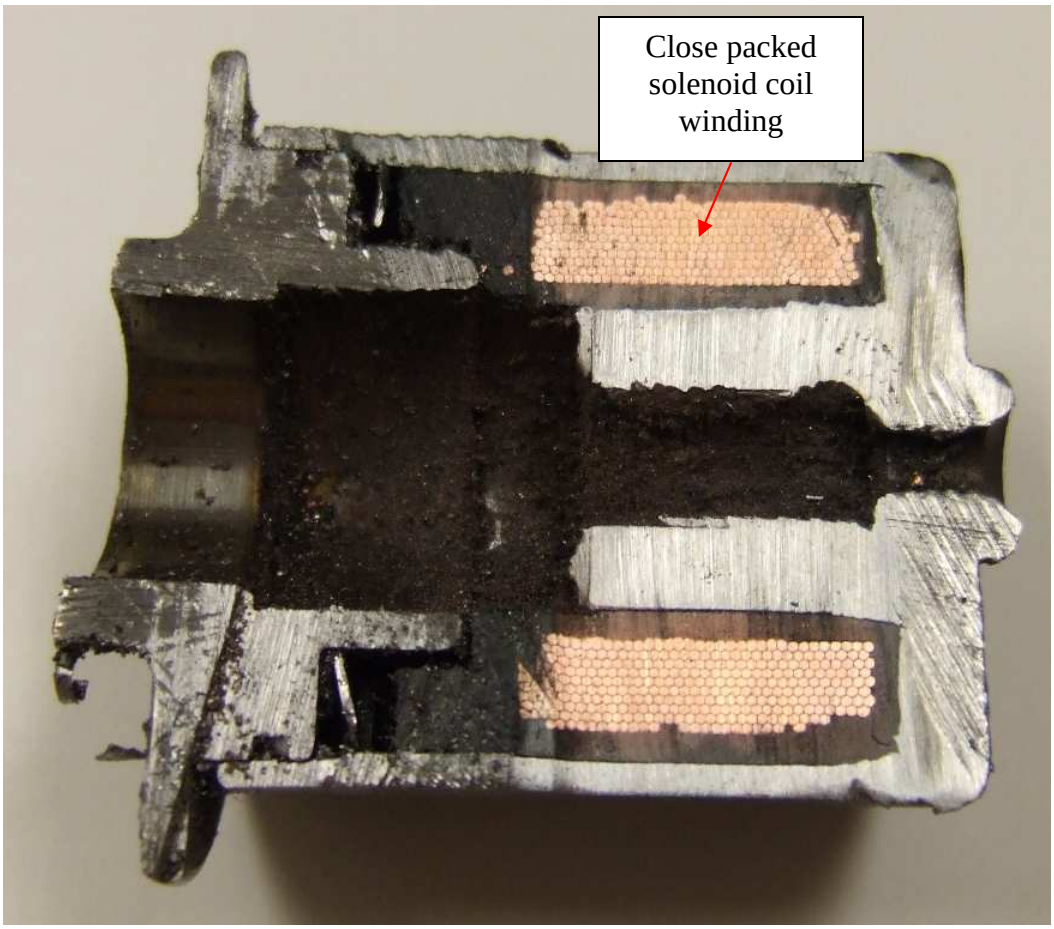

Figure 6.33: Cross section of a (a) type tested solenoid valve

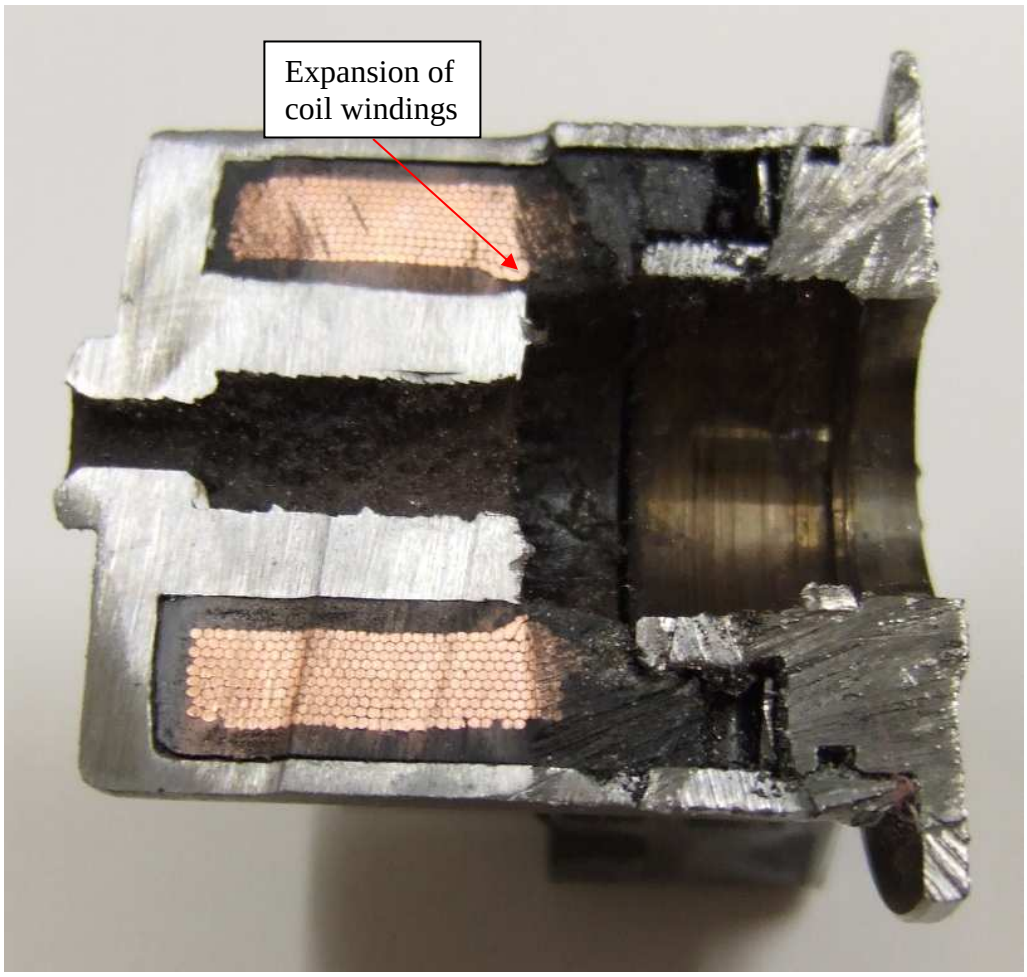

Figure 6.34: Cross section of a (b) type tested solenoid valve

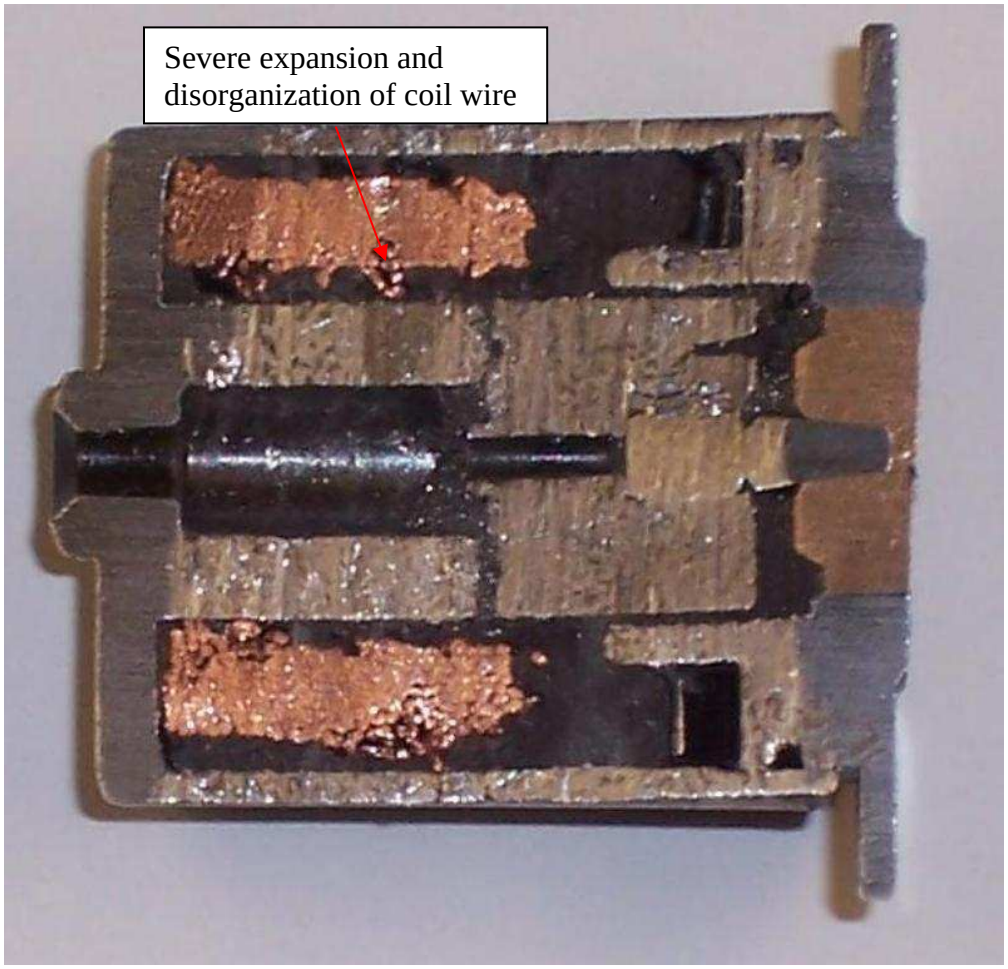

Figure 6.35: Cross section of a (c) type solenoid valve

Figures 6.33 to 6.35 show the macroscale photographs of the cross-sections of tested solenoid valves (including (a) non-failure, (b) partial failure and (c) complete failure). One can observe that the organization of the coil wire array continues to degrade from the type (a) non-failure solenoid valves to the type (c) complete failure valves. For the intermediate type (b) samples, it appears that any obstructions in the coil hexagonal packing structure is located and limited to one of the corners of the coil, as shown in Fig. 6.34. However, the type (c) solenoid valve samples show the coil being unorganized to a

good extent with wires that have even completely separated from the bulk coil into the black plastic casing material. This same black casing material was seen in the earlier photographs exiting the solenoid valve in a melted form. For complete failure, the melted plastic may have also helped to cause failure by mechanically obstructing the actuation of the valve plunger in the center axis of the solenoid valve. Some of the coil wires appear to not only have left the coil structure but are approaching the steel casing or core of the solenoid valve. This could cause further shorting of the solenoid, and perhaps even leak electrical current into any components surrounding the solenoid valve in application.

Figures 6.36 to 6.39 display the microscale photographs of the tested solenoid valve cross-sections for various levels of severity. Although all samples showed some signs of stress in the coil, the partially failed (type (b)) and completely failed (type (c)) solenoid valve cross-sections showed many more shorts between the coil wires and disorganization of the coil structure than the cross-sections of the tested but not failed samples (type (a)).

At first, considering type (c), there are a few number of vacant spots or separation between many of the copper coil wires (Figs. 6.38 and 6.39) (probably due to the melting of insulation material due to very high temperatures in the range of 200-250°C). Also, at complete failure, there is good amount of expansion or spreading out of the wires observed in the coil region (Figs. 6.38 and 6.39) whereas for the (a) case, the copper wires remain neatly arranged in a hexagonal manner (Fig. 6.36).

Now, coming to case (a), none of the features seen in (c) case can be observed and the copper windings at the end of a 24 hour test are seen to possess the same helical coil structure along with the insulation material between them, which is typical of an

operational solenoid valve. (see Fig. 6.36). In fact, this verifies the very definition of a solenoid coil or solenoid which is defined as ‘a long wire wound in a close packed helix’ [31]. However, even for the tested type (a) solenoid coils, due to plastic deformation as well as the symmetry of the coil wires, the wires appear to have been compressed together to become hexagonal in shape (originally, prior to the start of testing of type (a) SVs, they were circular). As found in the finite element model, the increase in coil temperature can cause very high compressive stresses which will press the coil wires together. This phenomenon is also seen in the other failed solenoid valves, along with more severe signs of stress in the coils.

In case (b) (see Fig 6.37), a partial failure of the SV can be recognized in that the windings at one end have undergone expansion towards the central part of solenoid valve (see Fig. 6.34). This is observed to a smaller extent than that seen in the (c) case where a large amount of expansion of the windings toward the central part of the SV can be seen in several regions of the coil (see Figs. 6.38 and 6.39). Therefore, it is observed that there is disorder of the wire winding arrangement in both the partially (intermediate disorder) and completely (excessive disorder) failed SVs which does not occur in case (a) solenoid valves. Also, there are no vacant regions in the coil region as there is no melting of the plastic material since the maximum temperature values recorded in the (b) cases is less than those in the (c) cases. However, a lack of insulation between the copper windings that causes shorting between them is noticed. It appears that, due to shorting only, the resistance has dropped from the original value of about 3.4 Ω to approximately 2.9 Ω in both of the 2 partially failed solenoid valves. Thus, due to a low change in resistance and no melting of plastic material, these valves are classified as partial failures.

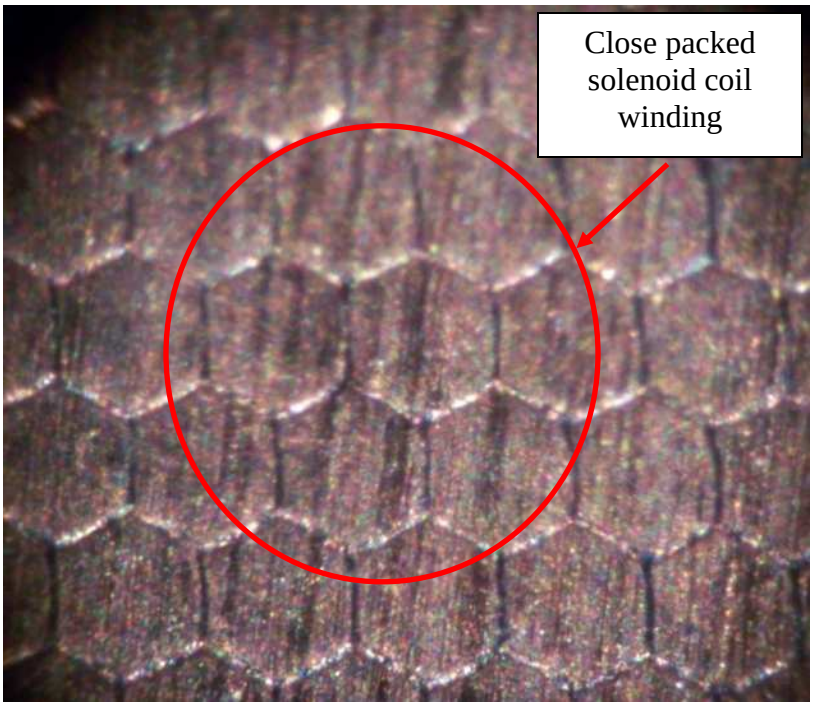

(a)

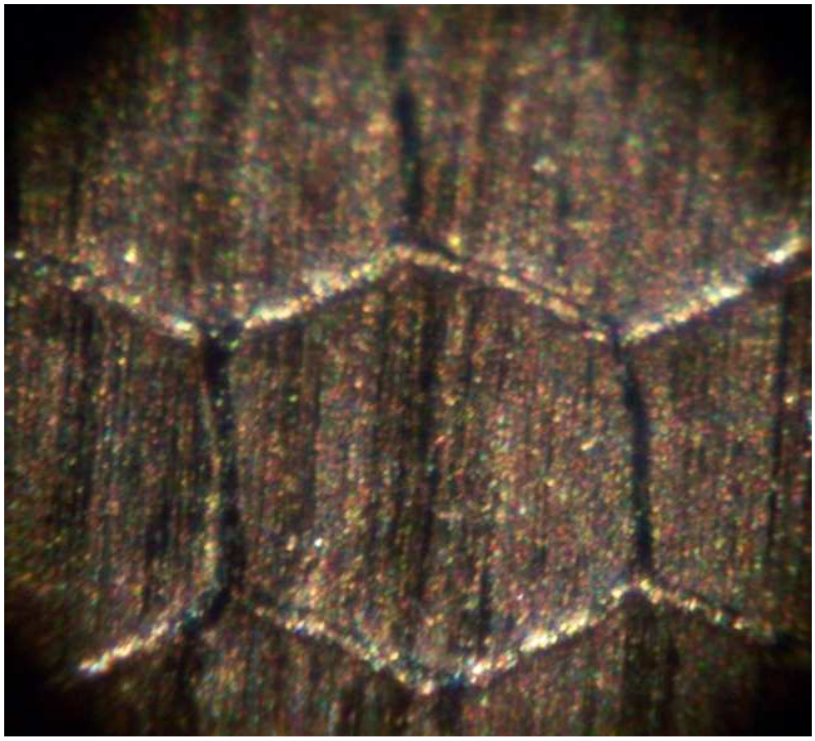

(b)

Figure 6.36: Microscale photographs of the case (a) solenoid valve cross-section

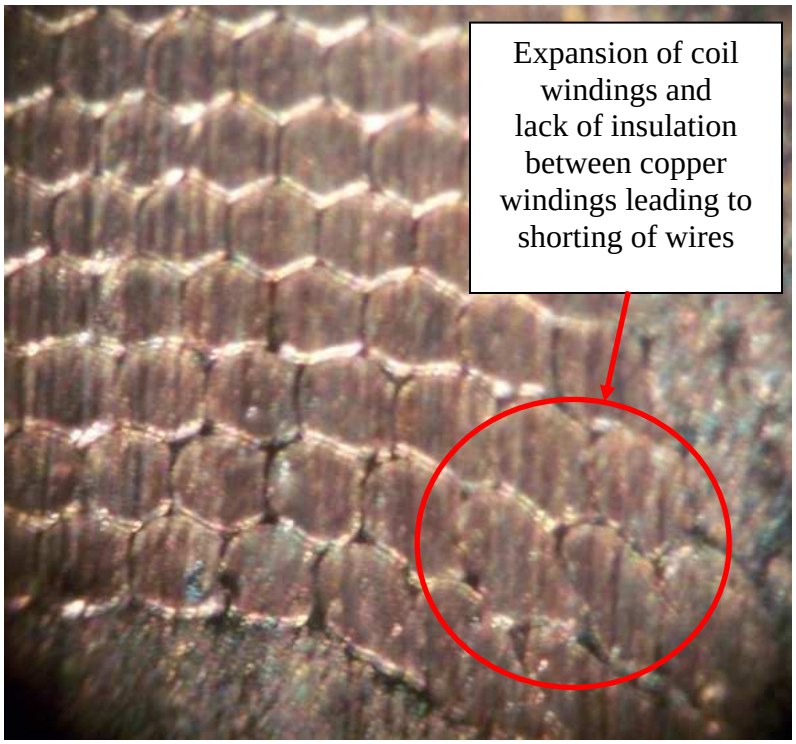

(a)

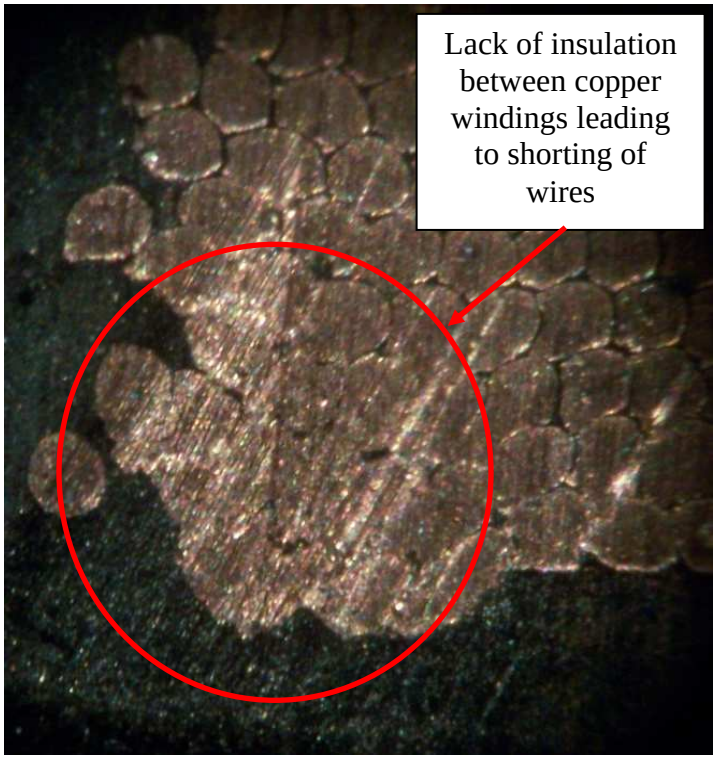

(b)

Figure 6.37: Microscale photographs of the type (b) solenoid valve cross-section

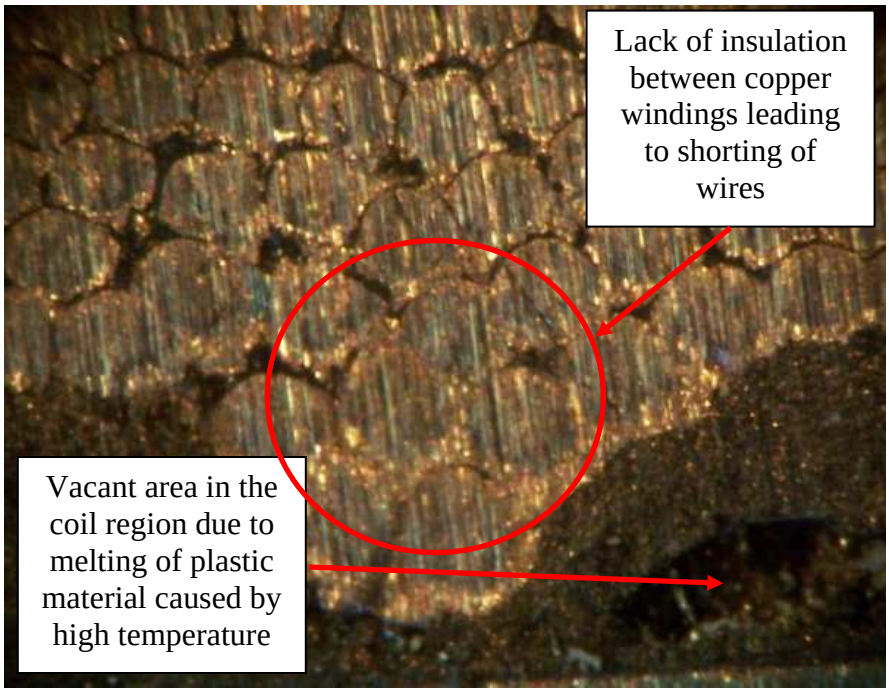

(a)

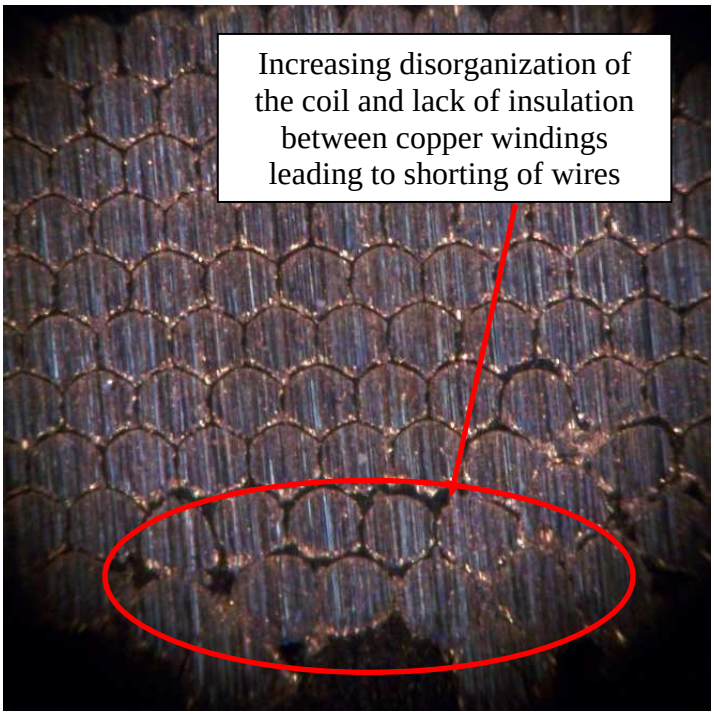

(b)

Figure 6.38: Microscale photographs of the type (c) solenoid valve cross-sections (part 1)

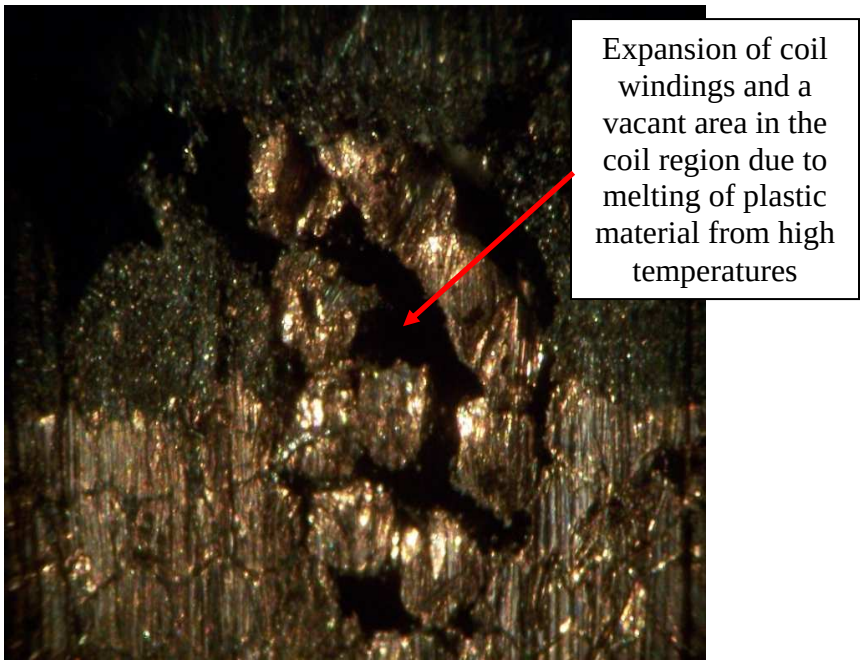

(a)

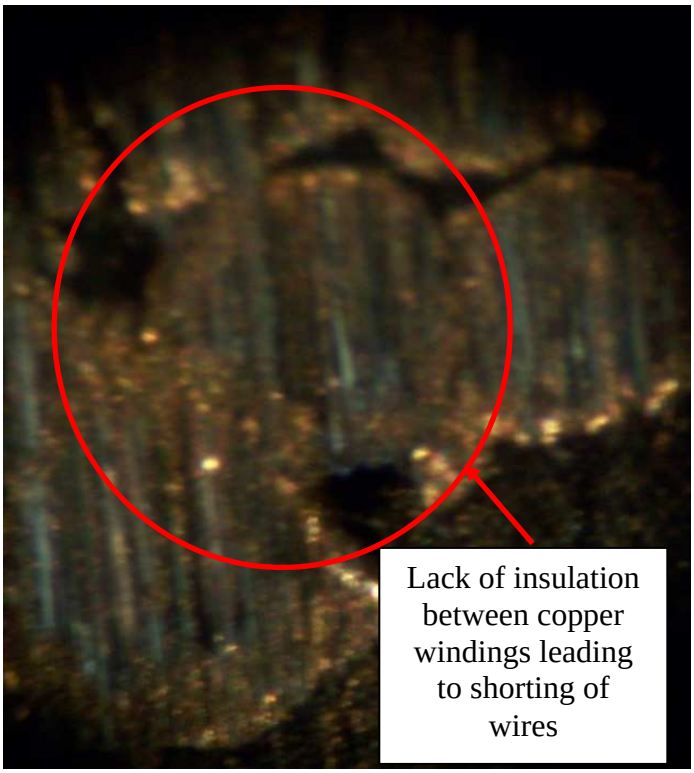

(b)

Figure 6.39: Microscale photographs of the type (c) solenoid valve cross-sections (part 2)

CHAPTER 7
CONCLUSIONS

In the current work, a literature review for the solenoid valve reliability, performance, life and failure has been documented. Based on this background search, the research on solenoid valve reliability seems relatively scarce. This is especially true for work which examines the fundamental thermo-mechanical mechanisms which cause failure of the solenoid valves.

A multiphysics finite element model of the solenoid valve is constructed that is able to make predictions of the stresses, strains and temperatures within the solenoid valve. The results suggest that under slightly elevated but realistic operating conditions very high temperatures and stresses can occur. These high compressive stresses are caused by thermal expansion of the solenoid valve components. The compressive stresses can then in combination with the high temperatures degrade and mold the insulation between the solenoid coil wires. This will result in shorting between the coil wires that will decrease the electrical resistance of the solenoid valve and also cause eventual failure. The finite element model is also used to confirm that the temperature within the coil is only a few degrees different from the temperature on the external surface of the solenoid valve that is measured experimentally.

An experimental test rig to test the solenoid valves has been fabricated and solenoid valves are tested at a constant voltage, duty cycle and actuation frequency for a fixed duration to characterize the reliability of the solenoid valve. The solenoid valves are also

placed inside a thermal chamber that is held at a constant elevated temperature that is similar to what is seen in the automotive transmission application. The influence of temperature on solenoid valve reliability and life is then observed to be very important. Additionally, during testing of a solenoid valve, valuable information such as real-time applied voltage, current flow, electrical resistance and actuation frequency of solenoid valve has been obtained.

For 100°C ambient temperature, 50% duty cycle, 16.8 V of applied voltage, and 60 Hz actuation frequency, failure was repeatedly caused for many solenoid valve test samples. It appeared that samples that reached a temperature of 200°C failed completely due to melting and degradation of the insulation between the coil wires (as predicted by the finite element model). Once the wires begin to short, the overall electrical resistance of the solenoid valve decreases. Since a constant voltage was applied to the tested solenoid valves, the applied current will then increase. They may increase the temperature further and result in very high temperatures in the solenoid valve (up to 300°C). The temperatures are so high that the metal casing and core discolors to blue and plastic within the solenoid valve melts and exits the casing. The melting plastic can also inhibit motion of the plunger. This is the observed dominant failure mechanism in the current work. Micro-scale photographs of the coil cross-section also revealed that the wire structure of a failed solenoid valve was much less organized than the tight hexagonal structure of a functioning solenoid valve. In addition, at the microscale, the shorts between the coil wires can be seen where the insulation has been moved out from between the wires.

CHAPTER 8
RECOMMENDATIONS FOR FUTURE WORK

Now that an apparent dominant failure mechanism for the solenoid valve is identified, and the cause known, this information can be used to provide suggestions for design improvements. For instance, since the failure mechanism seems to be strongly related to the maximum temperature reached in the solenoid valve, one way to reduce the chance of failure would be to reduce the temperature. This could be accomplished by increasing the convection and conduction of heat away from the solenoid valve, perhaps with the use of fins.

If the temperature cannot be reduced in a reliable manner, the insulation used between the wires could be changed to another material which can withstand higher temperatures. Since the maximum allowable operating temperature of polyamide-imide is approximately 200°C, a material that can withstand temperatures higher than this should be worth testing. Another option might be to apply thicker insulation so that it might not be squeezed out as easily.

Now that a powerful theoretical finite element model is constructed and a reliable test rig is available, these options can be easily and quickly tested at Auburn University. A comparative study between these different options and the current solenoid valve might yield substantial improvement in solenoid valve performance and reliability.

Since only one specific set of operating conditions was tested during this study, it would be advantageous to test the solenoid valves reaction to various other test

conditions not considered. For instance, the duty cycle, actuation frequency, applied voltage, and ambient temperature could all be changed in a controlled test matrix to characterize solenoid valve reliability.

BIBLIOGRAPHY

1. Sclater, N. and N.P. Chironis, Mechanisms and Mechanical Devices Sourcebook. 4th ed. 2007, New York: McGraw Hill.

2. Mercer, J.R. Reliability of solenoid valves. in Safety and Failure of Components, 1969, Brighton, England. 184: p. 89-94.

3. Baker, H., Valve operating conditions are the key reducing solenoid burnouts. Automation, 1973. 20(10): p. 68-69.

4. Rustagi, R. and R. Heilman, Achieving longer operating lives for solenoid devices. Nuclear Engineering International, 1989. 34(417): p. 53-54.

5. Tseng, C.-Y. and C.-F. Lin, A simple method for automotive switching type solenoid valve stuck fault detection. Int. J. Heavy Vehicle Systems, 2007. 14(1): p. 20-35.

6. Jeong, H.-S. and H.-E. Kim, Experimental based analysis of the pressure control characteristics of an oil hydraulic three-way on/off solenoid valve controlled by PWM signal. Journal of Dynamic Systems, Measurement and Control, Transactions of the ASME, 2002. 124(1): p. 196-205.

7. Choi, S. and D.-W. Cho, Control of wheel slip ratio using sliding mode controller with pulse width modulation. 1999. 32(4): p. 267-284.

8. Hurtig, J.K., et al. Torque regulation with the general motors ABS VI electric brake system. in Proceedings of the American Control Conference. 1994. Baltimore, MD, USA: American Automatic Control Council, Green Valley, AZ, USA.

9. Leiber, H. and A. Czinczel, Antiskid system for passenger cars with a digital electronic control unit. SAE Preprints, 1979(790458).

10. Naito, T., et al. Development of four solenoid ABS. in Current and Future Developments in ABS/TCS and Brake Technology. 1996. Detroit, MI, USA: SAE, Warrendale, PA, USA.

11. Rezeka, S.F. Modeling and sensitivity analysis of an ABS hydraulic modulator. in Proceedings of the American Control Conference. 1994. Baltimore, MD, USA: American Automatic Control Council, Green Valley, AZ, USA.

12. Goodbar, J.E. and M.D. Testerman. Design and development of a four speed powershift transmission with electronic clutch pressure modulation. in SAE Technical Paper Series. 1986. Milwaukee, WI, USA: SAE, Warrendale, PA, USA.

13. Kasuga, S., et al., Development of an electronically controlled four wheel drive system for FR vehicle with AT. JSAE Review, 1994. 15(4): p. 315-321.

14. Kolchinsky, A.E., Electrohydraulic control of transmissions. Diesel Progress Engines & Drives, 1993. 59(7).

15. Taniguchi, H. and Y. Ando, Analysis of a new automatic transmission control system for LEXUS LS400. SAE Special Publications, 1991(854): p. 57-61.

16. Wilcox, D., Will the Allison blender suit European tastes? Transport Engineer, 2004(JUE): p. 20-22.

17. Zimmermann, F., et al. Automatic dry friction clutch for passenger cars and light duty trucks. in SAE Technical Paper Series. 1986. Detroit, MI, Engl: SAE, Warrendale, PA, USA.

18. Tseng, C.-Y. and C.-F. Lin, Characterisation of solenoid valve failure for electronic diesel fuel injection system of commercial trucks. Int. J. Heavy Vehicle Systems, 2006. 13(3): p. 180-193.

19. Ferreira, J.A., F. Gomes De Almeida, and M.R. Quintas, Semi-empirical model for a hydraulic servo-solenoid valve. Proceedings of the Institution of Mechanical Engineers. Part I: Journal of Systems and Control Engineering, 2002. 216(3): p. 237-248.

20. Schultz, A. Design of valve solenoids using the method of finite elements. in Power Transmission and Motion Control. 2005. Bath, United Kingdom: John Wiley and Sons Ltd, Chichester, West Sussex, PO19 8SQ, United Kingdom.

21. Sung, D.J.T. and T.-T. Lee, Model reference adaptive control of a solenoid valve controlled hydraulic system. International Journal of Systems Science, 1987. 18(11): p. 2065-2091.

22. Szente, V. and J. Vad. Computational and experimental investigation on solenoid valve dynamics. in IEEE/ASME International Conference on Advanced Intelligent Mechatronics. 2001. Como.

23. Tao, G., H.Y. Chen, and Z.B. He, Optimal design of the magnetic field of a high-speed response solenoid valve. Journal of Materials Processing Technology, 2002. 129(1-3): p. 555-558.

24. Wang, S.-M., T. Miyano, and M. Hubbard, Electromagnetic field analysis and dynamic simulation of a two-valve solenoid actuator. IEEE Transactions on Magnetics, 1993. 29(2): p. 1741-1746.

25. Xu, M. and X. Tang. Time constant and magnetic force of an electrohydraulic seat valve solenoid. in Flucome. 1991. San Francisco, CA, USA: Publ by ASME, New York, NY, USA.

26. Li, J.-S., et al., Simulation analysis on static performance of EP solenoid valves based on ANSYS. China Railway Science, 2005. 26(5): p. 72-75.

27. Elmer, K., K. Henthorn, and P. Skellern, Self heating effects on the dynamics of a proportional control valve. Measurement & Control, 1998. 31(4): p. 101-104.

28. Churchill, S.W. and H.H.S. Chu, Correlating equations for laminar and turbulent free convection from a horizontal cylinder. Int. J. Heat Mass Transfer, 1975. 18: p. 1049 -1053.

29. Mark, J.E., Polymer Data Handbook. 1999, New York: Oxford Univ. Press.

30. Figliola, R.S. and D.E. Beasley, Theory and Design for Mechanical Measurements. 3rd ed. 2000, New York: Wiley.

31. Halliday, D., R. Resnick, and K.S. Krane, Physics. 4th ed. Vol. 2. 1992, New York: Wiley.

APPENDIX

SOLENOID VALVE TEST APPARATUS' PARTS LIST

Note that only the main components are listed.

Sl. No.	Part	Part No.	Price ($)
1.	Voltage Input module 2 channel analog input SCC-AI01, 42 V, 10 kHz	777459-20	329
	Voltage Input module 2 channel analog input SCC-AI04, 5 V, 10 kHz	777459-23	329
2.	Thermocouple input module with screw terminals SCC-TC02, 1 channel	777459-04	159
3.	Electric wires Wire guage 14 Solid building wire Length – 500 ft	54126511	79.9 each
4.	Adjustable clips (1 inch to 1-7/8 inch) - 25 pack	AJ CL -16/30-25	25
5.	Current Transformer		
6.	Thermocouples E type (-200 to 900°C)		
7.	SC5 Five-channel solenoid controller/driver		179